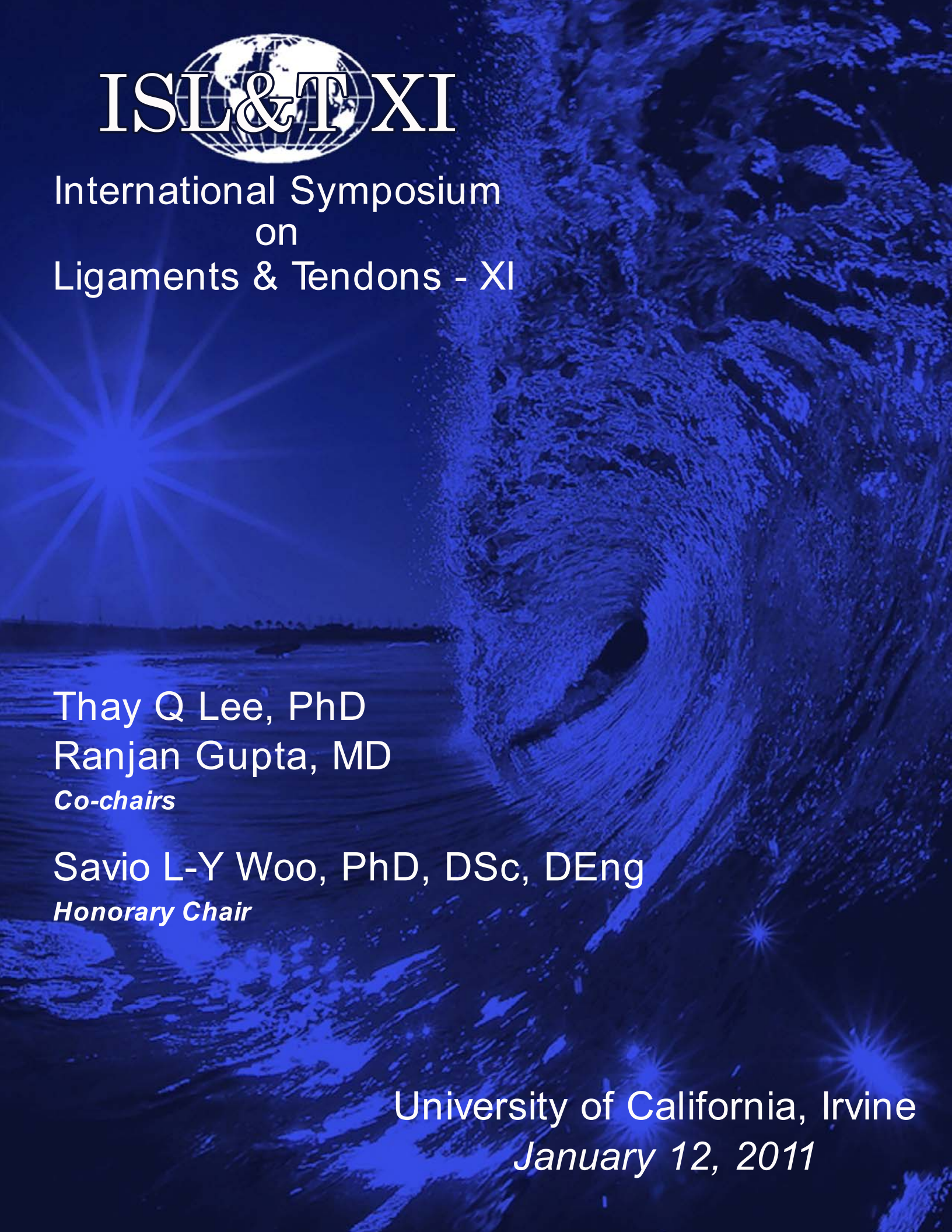
ISL&T XI
International Symposium
on
Ligaments & Tendons - XI
Thay Q Lee, PhD
Ranjan Gupta, MD
Co-chairs
Savio L-Y Woo, PhD, DSc, DEng
Honorary Chair
University of California, Irvine
January 12, 2011

Welcoming Note by Professor Savio L-Y. Woo

It is my pleasure and honor to join Professors Thay Q. Lee and Ranjan Gupta to welcome you to the University of California, Irvine for the Eleventh International Symposium on Ligaments and Tendons (ISL&T-XI)!

The first ISL&T meeting took place over a decade ago. Each year, we have been able to bring together researchers with diverse backgrounds to present and discuss new developments and important topics related to ligaments and tendons. ISL&T, also, has been a place where graduate students as well as junior and senior level biologists, engineers and clinicians exchange ideas freely, learn from one another, and establish collaborations. Last year, for the first time, we extended ISL&T outside of the US so that more young investigators from Asia could join us. The meeting in Hong Kong hosted by Professor Kai-Ming Chan was well attended by many from Asia.

Two years ago, we formed the International Advisory Committee (IAC) for ISL&T – a governing body that is consisted of experts on ligaments and tendons. The IAC has been charged to govern our organization and to lead us into the future as well as to develop strategic plans on how to move our field forward, forming a society, and creating or finding an association to a high quality international journal.

I am truly delighted that we can have a wonderful day here in Irvine, CA to be amongst good friends and colleagues. I trust that you will all enjoy the beautiful scientific program that was put together by our Program Co-Chairs, Dr. Joo Han Oh from Korea and Dr. Stavros Thomopoulos from the United States. Please participate by actively sharing your ideas and new data, as well as asking a lot of questions. I know you will want to get as much out of this meeting as possible.

Let me also congratulate all our younger colleagues who are finalists for the podium and poster awards. Also, I will be remiss if I do not call out the winners of the Woo Awards – Mr. Jeffrey Brown and Dr. Joo Han Oh and their mentors Dr. Catherine Kuo and Professor Thay Q. Lee, respectively. All of you represent the best of the best in our field! A special thanks must also be given to Dr. Al and Mrs. Beth Banes of Flexcell International for their leadership and generous support of the ISL&T awards over the years!

Finally, we are all very thankful for the most generous hospitality of Professors Thay Q. Lee and Ranjan Gupta and their great team for hosting us this year. We also want to thank all of our sponsors for their kind support so that so many young investigators could join us.

Please enjoy the day!

Savio L-Y. Woo, Ph.D., D.Sc. (Hon.), D.Eng. (Hon.)
Chair, IAC/ISL&T

ISL&T-XI Committees

Organizing Committee

Savio L-Y. Woo, PhD, DSC – Chair (Honorary)
Thay Q. Lee, PhD, Co-Chair
Ranjan Gupta, MD, Co-Chair
Michelle H. McGarry, MS
Ryan Quigley, BS
Synthia Hernandez
Marino Lampino
Diann DeCenzo, MS

International Program Committee
Co-Chairs:
Joo Han Oh, MD, PhD (Korea)
Stavros Thomopoulos, PhD (USA)

Committee:
Gregory J. Adamson, MD (USA)
Chih-Hwa Chen, MD, PhD (Taiwan)
Dawn Elliot, PhD (USA)
Braden Fleming (USA)
Hiromichi Fujie, PhD (Japan)
Wei-Hsiu Hsu, MD (Taiwan)
Joseph P. Iannotti, MD, PhD (USA)
Jon Karlsson, MD (Sweden)
Catherine K. Kuo, PhD (USA)
Mike Lavagnino PhD (USA)
Yeon Soo Lee, PhD (Korea)
Orr Limpisvasti, MD (USA)
Helen Lu, PhD (USA)
Pauline P. Y. Lui, PhD (Hong Kong)
Nicola Maffulli, MD (England)
Fabrizio Margheritini, MD (Italy)
Masataka Sakane, MD (Japan)
James E. Tibone, MD (USA)
Harukazu Tohyama, MD, PhD (Japan)
Michael Torry, PhD (USA)
Rene Verdonk, MD (Belgium)
Kazunori Yasuda, MD, PhD (Japan)

International Advisory Board
Chair:
Savio L-Y. Woo, PhD, DSc (USA)

Committee:
Thomas P. Andriacchi, PhD (USA)
Steve Arnoczky, DVM (USA)
Albert Banes, PhD (USA)
David Butler, MD (USA)
K.M. Chan, MD, PhD (Hong Kong)
Chih-Hwa Chen, MD, PhD (Taiwan)
Giuliano Cerulli, MD (Italy)
Mahmut Doral, MD (Turkey)
Toru Fukubayashi, MD, PhD (Japan)
James Goh, PhD (Singapore)
Sinan Karaoglu, MD (Turkey)
Catherine Kuo, PhD (USA)
Thay Q. Lee, PhD (USA)
Guoan Li, PhD (USA)
Nicola Maffulli, MD (England)
Christos Papageorgiou, MD (Greece)
Per Renstrom, MD (Sweden)
J. Richard Steadman, MD (USA)
Lou Soslowsky, PhD (USA)
Ray Vanderby, PhD (USA)
Jennifer Wayne, PhD (USA)
Kazunori Yasuda, MD, PhD (Japan)

ISL&T-XI Sponsors

ISL&T-XI would like to acknowledge the support of our sponsors.

ASIAM Institute

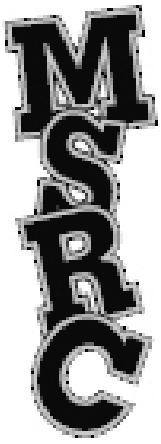

Musculoskeletal Research Center

Pfizer Inc

ISL&T Awards

The ISL&T has established a number of awards to honor and stimulate high quality scientific research in ligaments and tendons. The winners are chosen by members of the program committee based on the quality of the abstract and presentation as well as the overall merit of the study.

I. Best Paper Presentation to a Graduate Student
Award: USD$200 and Certificate

- **Eligibility** Open to current graduate students. Applicant must be the first author of the abstract and be present at the ISL&T meeting to accept the award. Advisor's verification of eligibility is required.
- **Application** Upon submission of the abstract by the regular submission deadline applicant must indicate his/her intention to be considered for the award.
- **Selection Criteria** Applicant's abstract submitted for the ISL&T will be reviewed by the program committee through the evaluation process based on scientific merit and research quality.
- **Selection Process** The Program Committee will select the best paper during the international meeting. The final announcement will be made at the banquet.
- **Acknowledgements** Sponsored by Flexcell International Corporation.

II. Best Paper Presentation to a Research Fellow
Award: USD$200 and Certificate

- **Eligibility** Open to clinical fellows or post-doctoral fellows. Applicant must be the first author of the abstract and be present at the ISL&T meeting to accept the award.
- **Application** Upon submission of the abstract by the regular submission deadline, applicant must indicate his/her intention to be considered for the award.
- **Selection Criteria** Applicant's abstract submitted for the ISL&T will be reviewed by the program committee through the regular evaluation process based on scientific merit and research quality.
- **Selection Process** The Program Committee will select the best paper during the international meeting. The final announcement will be made at the banquet.
- **Acknowledgements** Sponsored by Flexcell International Corporation.

III. Best Poster Presentation
Award: USD$200 and Certificate

- **Eligibility** Open to all participants of poster presentation. Applicant must be the first author of the abstract and be present at the ISL&T meeting to accept the award.

- **Application** Upon submission of the abstract by the regular submission deadline, applicant must indicate his/her intention to be considered for the award.

- **Selection Criteria** Applicant's abstract submitted for the ISL&T will be reviewed by the program committee through the regular evaluation process based on scientific merit and research quality.

- **Selection Process** The Program Committee will select the best poster during the international meeting. The final announcement will be made at the banquet.

- **Acknowledgements** Sponsored by Flexcell International Corporation.

IV. Savio L-Y. Woo Young Researcher Award
Award: Up to USD$1000 and Certificate

To celebrate the tenth anniversary, the ISL&T established a new award in honor of Professor Savio L-Y. Woo

- **Purpose** Professor Savio L-Y. Woo founded the International Symposium on Ligaments and Tendons (ISL&T) to promote awareness of the field, the exchange of information and collaboration nationally and internationally. The ISL&T has been a venue for lively discussion of current topics in connective tissue research and clinical applications. In addition to his leadership and significant scientific contributions to our field, Professor Woo has been an internationally recognized intellectual ambassador for training, mentoring and for aspiring students in the field of biomedical engineering and orthopaedic surgery. We are honored to present the Savio L-Y. Woo Young Researcher Award to individuals who perform the best research studies in three major areas, biomechanical, biological and clinical and have submitted their work to the ISL&T meeting. The Woo Award is the highest honor given by the IS&T and is intended to provide partial support towards the applicant's research or for travel expenses to attend the ISL&T meeting. Up to four awards may be given in each year.

- **Woo Award Committee**
  Albert Banes, PhD – Chair, Award Committee
  Thay Q. Lee, PhD – Chair, ISL&T-XI
  Jennifer Wayne, PhD
  Steven Arnoczky, DVM
  Nicola Maffulli, MD

- **Eligibility** Open to graduate students and postdoctoral fellows. Applicant must be the first author of the abstract and be present at the ISL&T meeting to accept the award. Advisor's verification of eligibility is required.

- **Award Categories** Upon the decision of the Woo Award Committee, one or more awards can be given to highly qualified candidates in each of the following three categories
  Biomechanical: Experimental studies involving biomechanics of ligaments and tendons, new methods for measurement of biomechanical properties, or computational analyses
  Biological: Basic science studies to characterize the cellular behavior of ligaments and tendons, as well as the extracellular matrix
  Clinical: Studies which compare existing surgical procedures or propose a novel alternative

- **Application** Upon submission of the abstract by the regular submission deadline, applicant must indicate his/her intention to be considered for the award.

- **Selection Criteria** Abstracts will be first reviewed by the program committee through the regular evaluation process. Based on scientific merit and research quality, a number of highly meritorious abstracts will be selected and the first author will be invited to submit 3-page extended abstracts.

- **Selection Process** The Woo award committee will conduct a thorough review of the extended abstracts and select the winners based on the clear motivation and relevance, quality experimental methods and scientific reasoning, appropriate conclusion as well as high impact of the study.

- **Past Award Recipients**
  2010, Inaugural Year ISLT-X in Hong Kong
  Biological Research – X. Chen, Z. Yin, J. Chen, W. Shen, H-W. Ouyang, TENDON-LINEAGE DIFFERENTIATION OF HUMAN EMBRYONIC STEM CELLS
  (From Zhejiang University School of Medicine, Zhejiang, China)
  Clinical Research - S. Chaudhry, H.R.C. Screen, R.C. Woledge, D.Bader1, D. Morrissey, ECCENTRIC & CONCENTRIC CALF MUSCLE LOADING: AN IN VIVO STUDY OF FORCE & EMG
  (From Queen Mary University of London, London, UK)

- **ISL&T-XI Award Recipients**
  Biomechanical (p15) JH Oh, MH McGarry, JU Tilan, YJ Chen, KC Chung, TQ Lee
  BIOMECHANICAL EFFECTS OF LATISSIMUS DORSI TENDON TRANSFER IN IRREPARABLE MASSIVE ROTATOR CUFF TEAR (From Orthopaedic Biomechanics Laboratory, VA Long Beach Healthcare System and University of California, Irvine)
  Biological Research (p19) JP Brown, RM Lind, and CK Kuo
  SPINAL LIGAMENT TISSUE DEVELOPMENT IN VIVO AND CELL RESPONSE TO GROWTH FACTORS IN VITRO (From Tufts University, Medford, MA)

- **Acknowledgements** Sponsored by Flexcell International Corp. and the Asian♦American Institute for Research and Education (ASIAM).

Instructions to Presenters

Podium Presenters

Podium presentations are 6 minutes in length with discussion time allocated after several presentations.

Please upload and check your presentation at least 15 minutes prior to your session begins.

Poster Presenters

Please hang your poster between 7:30 and 8:15 am and remove promptly following the meeting.

Please be available during the two breaks for poster discussions.

PROGRAM

7:30 – 8:15 am Registration/Check-In and Continental Breakfast

8:15 am Welcome
Savio L-Y. Woo, PhD, DSc, Deng and Ranjan Gupta, MD

Podium Session 1: Tendon

Session Chairs: Michael Lavagnino, DVM and Joo Han Oh, MD, PhD

8:30 am **Keynote Lecture**
Joe Iannotti, MD, PhD "Is There a Role for Augmentation Grafts in Rotator Cuff Repair?"

8:45 am *p22* Functional Ultra Sound Elastography (FUSE) of Achilles Tendon: A Novel Reliable Mechanical and Clinical Outcome Tool
J Alsousou#, L Li, M Thompson, E McNally, K Willett, A Noble*

8:51 am *p23* Ultrasound Echo Intensity in in vivo Tendon Exhibits Load Dependent Behavior
KE Frisch#, R Vanderby, DG Thelen*

8:57 am *p24* Ultrasonic Characterization of Tendon Viscoelasticity
SE Duenwald-Kuehl#, H Kobayashi, R Lakes, R Vanderby, Jr*

9:03 am *p25* The Optimization of a Collagen Gel Patch with Bone Marrow Stromal Cells for Tendon Repair
*M Hayashi#, CF Zhao, K-N An, YL Sun, Y Morizaki, PC Amadio**

9:09 am *p26* Intratendinous Substance P Increases with Exercise in an in vivo Model of Tendinopathy: Peptidergic Elevation Preceding Tendinosis-like Tissue Changes
L Backman, G Andersson, Gl Wennstig, S Forsgren, P Danielson#*

9:15 – 9:30 am **Discussion**

9:30 am *p27* Intensive Mechanical Loading Contains the Risk of Developing Tendinopathy
J Zhang, JH-C Wang#*

9:36 am *p28* Gene Expression Profile after a Single Loading Episode during Rat Tendon Healing
P Eliasson#, T Andersson, P Aspenberg*

9:42 am *p29* Rehabilitative Mechanical Conditioning Regime for Tendon/Ligament Tissue Regeneration
*TKH Teh#, S-L Toh, JCH Goh**

9:48 am *p30* Investigation of Tendon Progenitor Cells in Healing Tendons and its Relationship with Neovascularization
*SC Fu, YC Cheuk#, TY Mok, WH Cheng, LK Hung, KM Chan**

9:54 am *p31* Canonical Correlation between the Neovascularization and Mechanical Restoration in Tendon Healing
TY Mok#, SC Fu, LK Hung, YC Cheuk, PPY Lui, KM Chan*

10:00 – 10:15 am Discussion

10:15 – 10:45 am Break/Posters

Podium Session 2: Rotator Cuff

Session Chairs: Orr Limpisvasti, MD and Sang-Jin Shin, MD, PhD

10:45 am Keynote Lecture
James E. Tibone, MD "Rotator Cuff Repair – From the Lab to the OR"

11:00 am *p32* Margin Convergence to Bone for Reconstruction of the Anterior Attachment of the Rotator Cable in Massive Rotator Cuff Tears
ML Nguyen#, BJ Jun, RJ Quigley, SE Galle, MH McGarry, R Gupta, SS Burkhart, TQ Lee*

11:06 am *p33* Platelet-Rich Plasma Augmentation for Arthroscopic Rotator Cuff Repair: A Randomised Controlled Trial
UG Longo#, R Castricini, MD Benedetto, N Panfoli, P Pirani, R Zini, N Maffulli, V Denaro*

11:12 am *p34* The Influence of Subscapularis Partial Tears; Are We Neglecting Them?
*JC Yoo#, MH McGarry, BJ Jun, J Scott, TQ Lee**

11:18 am *p35* Biomechanical Comparison of Single-Row, Double-Row, and Transosseous-Equivalent Repair Techniques after Healing in an Animal Rotator Cuff Tear Model
RJ *Quigley #, A Gupta, JH Oh, KC Chung, MH McGarry, R Gupta, JE Tibone, TQ Lee**

11:24 am *p36* Biomechanical Effects of Latissimus Dorsi Tendon Transfer in Irreparable Massive Rotator Cuff Tear
*JH Oh#, MH McGarry, J Tilan, YJ Chen, KC Chung, TQ Lee**

11:30 – 11:45 am Discussion

11:45 am – 12:45 pm Lunch Break

Podium Session 3: Knee ACL

Session Chairs: Braden Fleming, PhD and Masataka Sakane, MD, PhD

12:45 pm **Keynote Lecture**
Guoan Li, PhD "Current ACL Reconstruction"

1:00 pm *p37* Calcium Phosphate-Hybridized Tendon Graft to Reduce Knee Laxity and Bone Tunnel Enlargement 1 Year after ACL Reconstruction
M Sakane#, H Mutsuzaki, A Kanamori, K Ikeda, N Ochiai*

1:06 pm *p38* Differences in the Proteome of the Male and Female Anterior Cruciate Ligament
*D Little#, JW Thompson, LG Dubois, DS Ruch, F Guilak**

1:12 pm *p39* A New Hypothesis for ACL Injury Mechanisms based on Video Analysis using Model-based Image-matching Technique
H Koga#, R Bahr, G Myklebust, L Engebretsen, T Muneta, I Sekiya, T Krosshaug*

1:18 pm *p40* Tunnel Placement in Failed Anterior Cruciate Ligament Reconstruction: An Imaging Analysis
P Lodhia, A Hosseini, SK Van de Velde, AL Williams, PD Asnis, B Zarins, TJ Gill, G Li#*

1:24 – 1:40 pm **Discussion**

1:40 pm *p41* Effect of Graft Tensioning on Mechanical Restoration in a Rat Model of Anterior Cruciate Ligament Reconstruction using Free Tendon Graft
*SC Fu, WH Cheng#, YC Cheuk, TY Mok, SH Yung, CG Rolf, KM Chan**

1:46 pm *p42* Mechanical Augmentation using Sutures to Stimulate Healing of the ACL in the Goat Model
*MB Fisher#, KE Kim, HJ Jung, PJ McMahon, SL-Y Woo**

1:52 pm *p43* Non-Linear Mechanics of Tissue Engineered Ligament, Anterior Cruciate Ligament and Patellar Tendon
*J Ma#, MJ Smietana, EM Wojtys, LM Larkin, EM Arruda**

1:58 pm *p44* Effect of ACL Reconstruction on Primary and Secondary Restraints in the Porcine Knee for 6-DOF Motions
DV Boguszewski#, JT Shearn, C T Wagner, DL Butler*

2:04 pm *p45* A Novel Robotic System Capable of Simulating Physiological Knee Motions Using a High-Speed Displacement/Force Control
H Fujie, H Yagi, Y Matsuda#*

2:10 – 2:25 pm **Discussion**

2:25 – 2:45 pm Break/Posters

Podium Session 4: Tissue Engineering

Session Chairs: Catherine Kuo, PhD and Pauline Lui, PhD

2:45 pm **Keynote Lecture**
David Butler, PhD "Reverse Tissue Engineering: Focusing on Clinical Problems and Preclinical Strategies in Device Development"

3:00 pm
p46
Novel Aligned Collagen-Carbon Nanotube Fiber for Tendon Repair
XG Cheng#, S Desai*

3:06 pm
p47
Tenomodulin Regulation in Equine Bioartificial Tendons in vitro
*AN Banes, J Qi, M Tsuzaki, JM Dmochowski#, M Schramme, A Nixon, R Smith, N Yeung, R Sumanasinghe, AJ Banes**

3:12 pm
p48
TGFβ-mediated Mechanical Strain Modulation of Metalloproteinases in Human Tenocytes
ER Jones#, GC Jones, GP Riley*

3:18 pm
p49
Effects of Small Intestine Submucosa (SIS) Hydrogel on the Proliferation and Matrix Production of ACL Fibroblasts
*KE Kim#, R Liang, G Yang, SL-Y Woo**

3:24 – 3:40 pm **Discussion**

3:40 pm
p50
Human MSCs Produce Collagenous Extracellular Matrix in Matrix Metalloproteinase-degradable Hydrogels
*DM Doroski#, JS Temenoff**

3:46 pm
p51
Effects of Cell Freezing and Thawing on the Mechanical Properties of a Stem Cell-based Self-assembled Tissue (scSAT)
*R Emura#, K Oya, H Sudama, K Shimomura, N Nakamura, H Fujie**

3:52 pm
p52
Effects of MSC Cell Source and Media Supplementation of ALP Expression
AP Breidenbach#, JA Turner, NA Dyment, DL Butler*

3:58 – 4:13 pm **Discussion**

Podium Session 5: Ligament

Session Chair: Martha Murray, MD and Nicola Mafulli, PhD

4:15 pm	**Keynote Lecture** ***Hiromichi Fujie, PhD "A Novel Robotic System and ACL Force-induced Ridge Formation"***
4:30 pm *p53*	Intramedullary and Extramedullary Free-tissue Graft Reconstruction of the Acromioclavicular Joint Complex *GJ Adamson#, TQ Lee**
4:36 pm *p54*	Quantitative Analysis of the Hip Capsular Ligaments and their Footprints for Anatomic Reconstruction *JM Telleria#, DP Lindsey, NJ Giori, MR Safran**
4:42 pm *p55*	Spinal Ligament Tissue Development in vivo and Cell Response to Growth Factors in vitro *JP Brown#, RM Lind, CK Kuo**
4:48 pm *p56*	A Novel Method to Quantify the Anatomy of the Anterior Cruciate Ligament: An Experimental Study in Goats *DT Nguyen*#; M van de Giessen; JP van den Wijngaard; P van Horssen; GJ Streekstra; JA Spaan; C Niek van Dijk; L Blankevoort*
4:54 pm *p57*	Effect of Cycle-Dependent Damage on Normal and Healing Ligaments *KA Fitzpatrick*#, SJ Bailey, GM Thornton*

5:00 – 5:15 pm	**Discussion**
5:15 pm	**Closing Remarks**
5:30 – 6:30 pm	**Reception and cocktail hour (cash bar)**
6:30 – 9:30 pm	**Dinner (walking distance from student center)** **Chakra Cuisine** **4143 Campus Dr.** **Irvine, CA 92612** **Bus will return to downtown Long Beach following dinner**

Posters

SAVIO L-Y. WOO YOUNG RESEARCHER AWARD WINNER

Biomechanics

Biomechanical Effects of Latissimus Dorsi Tendon Transfer in Irreparable Massive Rotator Cuff Tear

+*Oh JH, *McGarry MH, *Tilan JU, *Chen YJ, *Chung KC, *Lee TQ
+Department of Orthopedic Surgery, Seoul National University College of Medicine, Seoul, Korea
*Orthopaedic Biomechanics Laboratory, VA Long Beach Healthcare System and University of California, Irvine

INTRODUCTION

The treatment of massive rotator cuff tear remains a challenge as options must address each patient's desired activity level as well as the severity of the rotator cuff pathology. Latissimus dorsi tendon transfer, introduced by Gerber et al in 1988[1], is one of the surgical options available for irreparable massive rotator cuff tears. While several authors reported favorable outcomes of this salvage procedure, clinical outcomes as a whole remain unpredictable and vary among patients[2,3] . Warner et al[4] reported that late rupture of transferred latissimus dorsi tendon and poor function were due to the relatively small size of latissimus dorsi and suggested autogenous iliotibial band augmentation for improved outcomes. Few cadaveric studies have been reported in the literature regarding the biomechanical influence of latissimus dorsi transfer using a massive rotator cuff tear model. Therefore, the purpose of this study was to determine the biomechanical influence of latissimus dorsi transfer using a cadaveric model with a massive posterosuperior rotator cuff tear. We hypothesized that latissimus dorsi tendon transfer for repair of massive cuff tear would closely approximate normal joint kinematics while increasing glenohumeral joint contact pressure in relation to the intact rotator cuff.

METHODS

Specimen Preparation: Eight fresh-frozen cadaveric shoulders were used (mean age: 56.5 years, range: 45-65 years). All soft tissues were excised except for the joint capsule, rotator cuff muscles, deltoid (DEL), pectoralis major (PEC) and latissimus dorsi (LAT). Suture loops were fashioned at the insertion of each muscle: 1 for teres minor (TM), 2 each for supraspinatus (SSP) and infraspinatus (ISP), and 3 each for the remaining muscles in order to anatomically load the shoulder joint based on muscle fiber orientation and multiple lines of pull. The entire LAT was preserved for the subsequent latissimus dorsi tendon transfer procedure. A custom testing device which permits axial rotation and abduction of the shoulder was used. The scapula was fixed in the anatomical resting position with 20º of anterior tilt (Fig. 1).

Massive Irreparable Rotator Cuff Tear Model & Latissimus Dorsi Tendon Transfer (LDT) Procedure: Massive rotator cuff tear was induced via complete transection of both the SSP and ISP tendons just proximal to the greater tuberosity. The massive rotator cuff tear was then repaired by latissimus dorsi tendon transfer as described by Gerber et al[1]. The LAT tenotomy was performed as close to its insertion as possible and was transferred to the superior-posterior humeral head ensuring coverage of the entire SSP and ISP footprints. The lateral edge of the tendon was secured to the greater tuberosity using three transosseous sutures with #2 FiberWire (Arthrex, Naples, Florida). A total of 3 simple sutures were used to secure the medial LAT tendon edge to the remaining cuff muscles, and 2 simple sutures were used to attach the LAT tendon to the superior edge of subscapularis (SSC) tendon (Fig. 2).

Fig. 1 Custom testing system

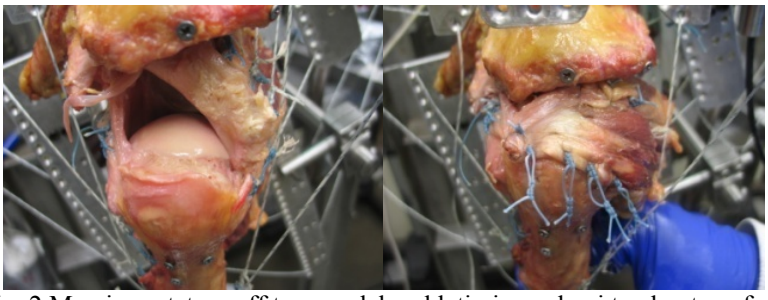

Fig. 2 Massive rotator cuff tear model and latissimus dorsi tendon transfer

Muscle Loading Conditions: The amount of muscle loading was determined based on the physiologic muscle cross-sectional area: SSP 10N, SSC 24N, ISP/TM 24N, DEL 48N, PEC 24N, and LAT 24N. The increased loading conditions for LAT (LDT 2X, 48N) were incorporated into our study to simulate increased tendon tension caused by limited muscle excursion which can occur after LDT.
Testing Positions: Testing was performed in the scapular plane (30° anterior to the coronal plane) with 0°, 30°, and 60° shoulder abduction with a 2:1 ratio of glenohumeral to scapular abduction.
Glenohumeral (GH) Joint Contact Characteristics: Contact area and force were measured throughout the rotational range of motion (ROM) at each abduction angle using Tek·Scan Pressure Measurement System (Tekscan Inc, South Boston, MA) with pressure sensors inserted into the joint through the rotator interval. Contact pressure and peak pressure were also recorded and calculated.
Testing Procedure, Dependent Variables and Statistics: Prior to testing at each step, all muscles were loaded and the specimen was "pre-conditioned" for 10 cycles from maximum internal (Max IR) to external rotation (Max ER) to minimize the viscoelastic effect of soft tissues. 1) Resting position of the humeral head, defined as the amount of humeral head rotation when the specimen was loaded without torque, was measured. 2) Max IR and Max ER were measured with 2.3 Nm of applied humeral shaft axial torque. 3) Contact data within GH joint was assessed throughout the rotational ROM from Max IR to Max ER. 4) The position of the humeral head apex (HHA) with respect to the glenoid was calculated using a MicroScribe 3DLX (Immersion Corporation, San Jose, CA) at each abduction angle from Max IR to Max ER in 30º increments. These procedures were performed for the conditions of intact cuff, irreparable RCT, LDT, and LDT 2X. All measurements were performed twice to demonstrate reproducibility, and the averages were used for data analysis. A repeated-measure ANOVA with a Tukey post hoc test was used to determine any significant differences.

RESULTS
***Humeral head rotation due to muscle loading*:** The average humeral head rotation due to muscle loading across all abduction angles with the intact rotator cuff condition was 7.1 ± 4.8º of internal rotation. Six specimens maintained 0º of rotation, while two specimens internally rotated an average of 28.5± 4.3º. With massive rotator cuff tear, the humeral head rotated internally 42.1 ± 3.6º due to muscle loading. After the latissimus dorsi transfer was performed all specimens maintained 0º of rotation and did not internally rotate.
Rotational range of motion: Maximum internal rotation significantly increased following massive rotator cuff tear at each abduction angle ($p<0.05$). Latissimus dorsi transfer significantly decreased maximum internal rotation compared to massive cuff tear at all abduction angles ($p<0.05$). At 30º and 60º shoulder abduction, latissimus dorsi transfer also significantly decreased maximum internal rotation compared to intact ($p<0.05$). Furthermore at 30º and 60º of abduction, increased muscle loading following latissimus dorsi transfer significantly decreased maximum internal rotation compared to latissimus dorsi transfer with normal muscle loading ($p<0.05$, Fig. 3). There were no significant differences in maximum external rotation.
Path of Humeral Head Apex: At maximum internal rotation, the massive cuff tear condition's humeral head apex (HHA) shifted anteriorly, superiorly and laterally at 0º abduction ($p<0.05$). The latissimus dorsi transfer shifted the humeral head inferior-medially at 0º abduction essentially restoring the normal humeral head kinematics ($p<0.05$, Fig 4). However, in 30º and 60º of glenohumeral abduction, both latissimus dorsi transfer conditions significantly shifted the humeral head anteriorly, inferiorly and medially ($p < 0.05$).
Contact Characteristics: Compared to the intact condition, glenohumeral contact area was decreased by massive rotator cuff tear, but was restored by latissimus dorsi transfer, especially at 0º and 30º abduction angles (Fig. 5). Latissimus dorsi transfer with increased muscle loading showed a pattern of increased contact pressure and peak pressure (Fig. 6) during the mid-range of motion, especially at 30º and 60º abduction angles.

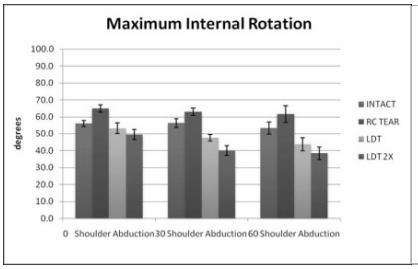

Fig. 3 Maximum internal rotation.

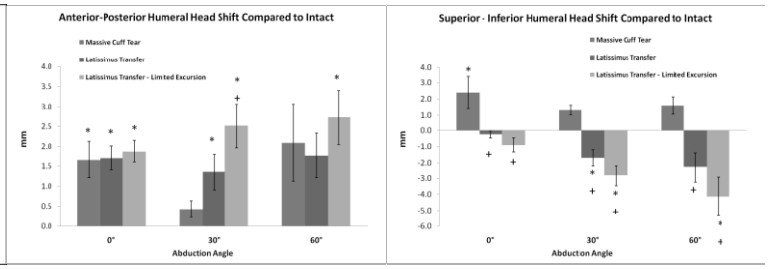

Fig. 4 Path of humeral head apex.

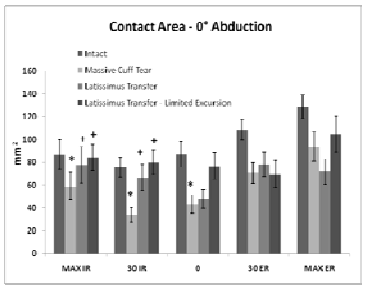

Fig. 5 Contact area at 0º abduction.

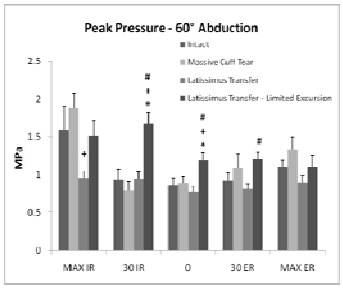

Fig. 6 Peak contact pressure at 60º abduction.

DISCUSSION

To our knowledge, this study is the first cadaveric biomechanical analysis of the latissimus dorsi tendon transfer in irreparable massive rotator cuff tear evaluating glenohumeral kinematics throughout the rotational range of motion at varying abduction angles with anatomically based muscle loading. Based on the findings of the present study, patients with massive rotator cuff tears electing for the latissimus dorsi tendon transfer may benefit from the restoration of normal biomechanics. It should be noted that due to the limited muscle excursion of the latissimus dorsi tendon, the increased muscle tension as a result of performing a tendon transfer may lead to an over-compensation phenomenon which increases contact pressure and may further deteriorate the normal kinematics of the shoulder joint. To the authors' knowledge, no study has reported the biomechanical change after latissimus dorsi tendon transfer and no study has compared the biomechanical variables between normal, massive cuff tear and latissimus dorsi tendon transfer conditions.

We defined the rotational balance of humeral head as the amount of humeral head rotation when the specimen was fully loaded and zero torque was applied. In intact cuff conditions, the humeral head was well balanced between the internal and external rotators of the shoulder. However, the humeral head rotated internally due to the loss of the active external rotators in the massive tear condition. Internal rotators, that is, subscapularis, pectoralis major and latissimus dorsi muscles were much stronger than the remaining external rotator muscle, teres minor. This rotational imbalance in massive cuff tear could be restored by latissimus dorsi tendon transfer to the posterosuperior footprint of humeral head. Patients with massive cuff tear may compensate for this rotational muscle imbalance with over-firing of the remaining external rotators such as teres minor or the posterior deltoid muscle. These muscles may be subject to fatigue and should be considered for strengthening exercises if surgery is not indicated.

The results of the rotational range of motion assessment showed that the abnormally increased maximum internal rotation seen in massive cuff tear was reversed as a result of latissimus dorsi tendon transfer. However, increased shoulder abduction angle, especially with increased muscle tension (latissimus dorsi transfer-limited excursion condition), may further decrease maximum internal rotation possibly much lower than the intact state. Insufficiently short latissimus dorsi tendon failing to cover the whole footprint and resultant higher tension after latissimus dorsi tendon transfer can limit the rotational range of motion. In this situation, a teres major tendon transfer should be considered. Moreover if the latissimus dorsi tendon can be transferred without excessive tension, the patient's shoulder may not be forced into an abducted position and may not suffer further loss of rotational range of motion, especially maximal internal rotation.

The current data confirmed abnormal shift of humeral head apex with massive rotator cuff tear; superior and lateral displacement of humeral head apex at the maximum internal rotation position. Furthermore, we found that the latissimus dorsi tendon transfer procedure improved the abnormal humeral head apex kinematics seen in massive rotator cuff tear. The data also suggested that the transferred latissimus dorsi tendon may act as a humeral

head depressor and compressor at maximum internal rotation. However, increased shoulder abduction angle and increased tendon tension may result in over-compensation and abnormal displacement of humeral head apex as it moves through the rotational range of motion pathway. The pattern of increased contact pressure and peak pressure in the glenohumeral joint during the rotational pathway observed in both latissimus dorsi tendon transfer conditions (LDT and LDT 2X) may also suggest negative effects of latissimus dorsi tendon transfer, specifically in patients exhibiting shorter tendon lengths. Increased glenohumeral contact pressure along with the abnormal humeral head kinematics caused by massive rotator cuff tear and by latissimus dorsi tendon transfer may contribute to patients' pain and long-term consequences such as osteoarthritis. Considering that most patients who meet criteria for latissimus dorsi tendon transfer are relatively young, complicated osteoarthritis of the shoulder may be prevented by acknowledging the characteristics of altered glenohumeral kinematics.

In conclusion, based on our data, the latissimus dorsi tendon transfer can be beneficial as it can reverse the abnormal biomechanics caused by massive rotator cuff tear; restoring the rotational balance of the humeral head, range of motion, and path of humeral head apex. However, the increased abduction angle and muscle tension due to potentially limited muscle excursion observed with latissimus dorsi tendon transfer can lead to an over-compensation that can further deteriorate normal kinematics of the shoulder; limiting rotational range of motion, causing abnormal displacement of the humeral head, and increasing glenohumeral joint pressure. Therefore, the authors believe that the clinical assessment of latissimus dorsi tendon length is critical for a successful procedure.

REFERENCES

1. Gerber C, Vinh TS, Hertel R, Hess CW. Latissimus dorsi transfer for the treatment of massive tears of the rotator cuff. A preliminary report. Clin Orthop Relat Res. 1988;232:51-61.
2. Iannotti JP, Hennigan S, Herzog R, Kella S, Kelley M, Leggin B, Williams GR. Latissimus dorsi tendon transfer for irreparable posterosuperior rotator cuff tears. Factors affecting outcome. J Bone Joint Surg Am. 2006;88:342-8.
3. Warner JJ, Parsons IM 4th. Latissimus dorsi tendon transfer: a comparative analysis of primary and salvage reconstruction of massive, irreparable rotator cuff tears. J Shoulder Elbow Surg. 2001;10:514-21.
4. Warner JP. Management of Massive Irreparable Rotator Cuff Tears: The Role of Tendon Transfer. J Bone Joint Surg Am. 2000. 82:878-87.

SAVIO L-Y. WOO YOUNG RESEARCHER AWARD WINNER

Biological Research

SPINAL LIGAMENT TISSUE DEVELOPMENT IN VIVO AND CELL RESPONSE TO GROWTH FACTORS IN VITRO

J.P. Brown, R.M. Lind, and C.K. Kuo
Tufts University, Medford, MA

INTRODUCTION

Spinal ligaments are critical for joint stabilization between vertebrae. These tissues are susceptible to ossification, age-related hypertrophy, and iatrogenic damage during spine surgery, all of which have been associated with pain and aberrant function[1,2,3]. Pathological spinal ligaments are surgically removed, and like ligaments that have been collaterally injured during spine surgery, are left to heal via scarring. Scarring is known to negatively affect ligament mechanical properties and function[4] and has been implicated in failed back surgery syndrome[5]. Moreover, cutting spinal ligaments reduces spine stability[6]. Tissue engineering is a promising means to provide replacement ligaments and thus mitigate the negative consequences of current spinal ligament pathologies and surgical outcomes. Our long term goal is to engineer functional spinal ligaments for replacement. However, much is unknown, ranging from *in vivo* development to spinal ligament cell behavior *in vitro*. In this work, we report on our studies to characterize the *in vivo* embryonic development of a spinal ligament and the use of soluble cues to regulate gene expression of axial tendon/ligament (T/L) cells *in vitro* as a function of developmental stage.

METHODS

Immunohistochemistry and Histology. Mice that have been engineered with a transgenic green fluorescent protein (GFP) reporter for scleraxis (Scx)[7], a kind gift of R. Schweitzer, were harvested on embryonic days (E) 15 and 18, and postnatal days (P) 7, 35, and 15 months. Spine tissues were dissected out, fixed in methacarn, decalcified in 6% isotonic trichloroacetic acid, and routinely embedded in paraffin. Spines were sectioned at 6 μm for histology (Verhoeff van Gieson stain; VVG) and immunohistochemisty (antibodies against tropoelastin, fibrillin-1 and fibulin-4) and visualized.

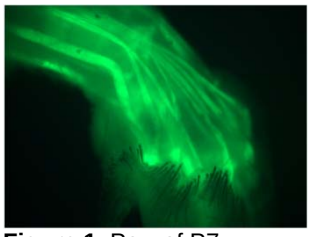

Figure 1. Paw of P7 ScxGFP mouse.

In Vitro Cell Study. Trunks and limbs from ScxGFP embryos and mice at E12, E15, E17 and P7 were digested and sorted via fluorescence activated cell sorting (FACS) on the basis of GFP expression to harvest Scx-expressing axial and limb T/L cells, respectively (Fig. 1). Cells were cultured in medium with 1% FBS +/- 1 ng/mL TGFβ2. Cells were imaged for GFP expression and harvested for RNA isolation and gene expression analysis.

RESULTS

Embryonic and postnatal mouse spines were sectioned and characterized for the presence of mature elastic fibers (VVG stain) and active elastogenesis (immunostaining of tropoelastin, fibrillin-1 and fibulin-4). In this work, we focused on the ligamentum flavum (LF) of the spine. *In vivo*, embryonic LF appeared highly cellular with a randomly oriented matrix. Collagen (pink) and elastic fibers (black) of the

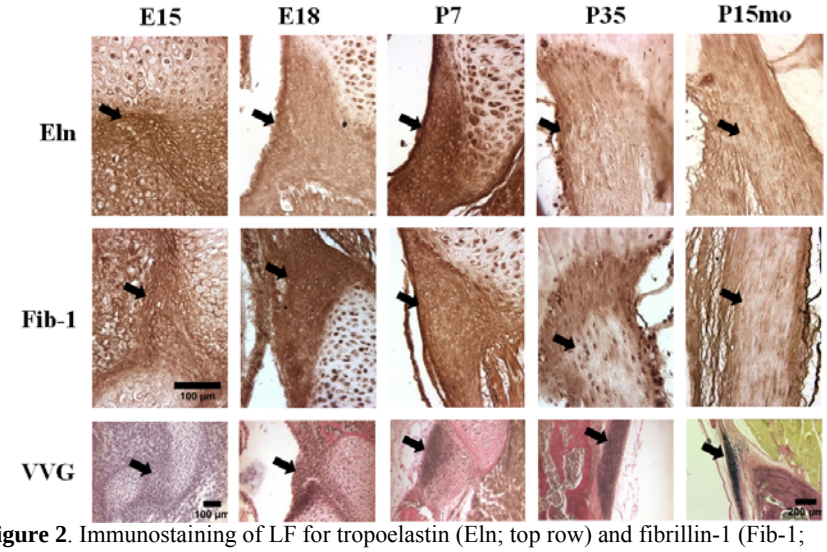

Figure 2. Immunostaining of LF for tropoelastin (Eln; top row) and fibrillin-1 (Fib-1; center row). VVG staining of LF (bottom row). Unless otherwise noted, scale bar is 100 um.

LF were identified by VVG staining (Fig. 2 bottom row). Elastic fibers became discernable by P7 and were thin and disorganized. At P35, and through 15 months of age, fibers were thick and aligned cephalocaudally. The emergence of elastic fibers at P7 coincided with the peak of elastogenic activity as demonstrated by immunohistochemical

staining of tropoelastin (Fig. 2 top row). Staining intensity of fibulin-4, a chaperone for the conversion of immature tropoelastin to mature elastic fibers, also peaked at P7 (not shown). For the microfibril component fibrillin-1, staining intensity peaked at E18 (Fig. 2 center row).

Table 1. Scx expression as a function of culture medium for different cell types; "-" indicates no Scx expression; number of "+" indicates strength of Scx expression.

ScxGFP Response to TGFβ2		
Cell Type	**No TGFβ2**	**1 ng/mL TGFβ2**
E12 Limb	+	+
E12 Trunk	+	+
E15 Limb	-	+++
E15 Trunk	++	++
E17 Limb	-	+
E17 Trunk	-	+
P7 Limb	+	++++
P7 Trunk	+	+++

T/L cells were harvested from the limbs and trunks of mice at E12, E15, E17 and P7 and cultured for 3 days with or without TGFβ2. Cells were imaged for the transgenic GFP reporter to assess Scx expression (Table 1). On the basis of GFP intensity, axial and limb E12 cells showed moderate Scx expression regardless of the presence of TGFβ2 (Fig. 3). Axial E15 cells showed a moderately high level of Scx expression, in contrast to weak expression by limb cells (not shown). When treated with TGFβ2, axial E15 cells seemed to maintain the same level of Scx expression as under control conditions (no growth factor). However, Scx expression of limb cells increased significantly in the presence of TGFβ2. E17 axial and limb cells showed low Scx expression in control medium (not shown). When treated with TGFβ2, both axial and limb cells increased the level of Scx expression. This enhancement of Scx expression in response to TGFβ2 on both axial and limb cells was also observed in P7 cells (Fig. 4).

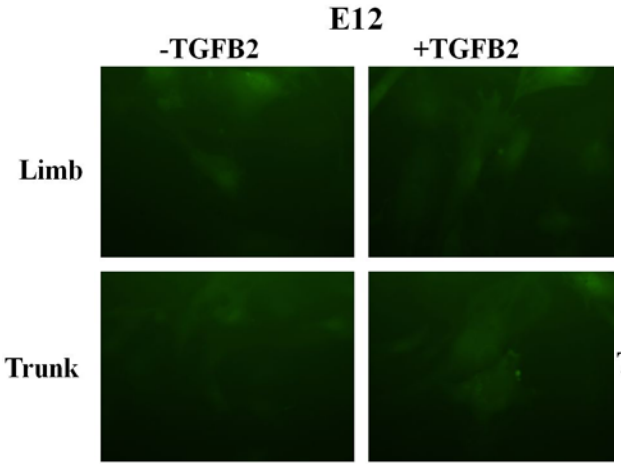

Figure 3. E12 limb and trunk T/L cells after 3 days of culture +/- TGFβ2.

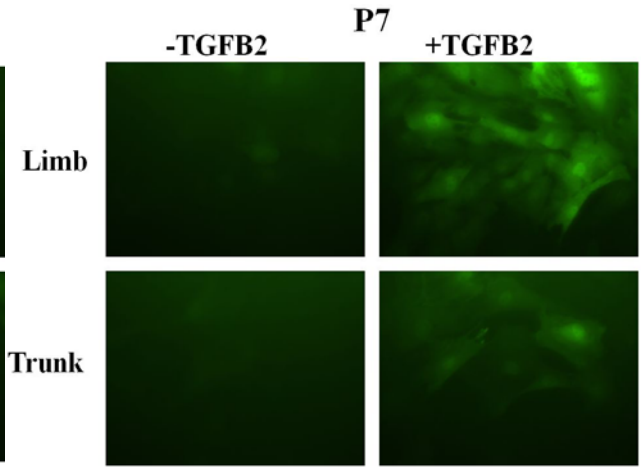

Figure 4. P7 limb and trunk T/L cells after 3 days of culture +/- TGFβ2.

DISCUSSION

Spinal ligaments are critical for spine stability. They are involved in various pathological conditions that are associated with pain and dysfunction, and suffer iatrogenic damage during routine spine surgery from which they are unable to heal normally. Thus, we are interested in a long term goal of engineering functional spinal ligaments. A specific property of spinal ligaments that we are interested in is their relatively high elastin content. The posterior longitudinal ligament, for example, is composed of 7.5% elastin[8], and the ligamentum flavum is approximately 50% elastin in a variety of species[9], including human[10]. The development of elastic fibers (elastogenesis,) in such tissues as the lung[11] and aorta[12] has been extensively characterized; however, similar characterization of elastogenesis of spinal ligaments has yet to be pursued.

Elastogenesis of the LF appears to follow a progression similar to that previously reported for other tissues[11,12]. During elastogenesis of aorta and lung, fibrillin-1 is the first to be expressed[12] and acts as a scaffold for tropoelastin alignment[13]. Fibulin-4 is required for elastic fiber formation[14] and is thought to chaperone tropoelastin crosslinking

and its alignment onto microfibrils[13]. In this study we characterized the distribution of elastin and other key proteins involved in elastogenesis of the LF during embryonic development and through postnatal stages. Specifically, we showed a spatiotemporal correlation between the production of these proteins and the appearance of elastic fibers.

In vitro, the ability of TGFβ2 to enhance Scx expression varied between E15 axial and limb T/L cells. TGFβ2 has been shown to be critical for tendon and ligament development during embryogenesis[15] and to upregulate scleraxis in mouse embryonic fibroblasts *in vitro*. Our results demonstrate a differential regulation of cells *in vitro* as a function of both developmental stage and anatomical location. In our work, E12 was the only developmental stage in which neither limb nor axial cells changed Scx expression in response to the growth factor. Interestingly, in a previous study, Scx expression at E11.5 was normal in both the limb buds and the somites of TGFβ2$^{-/-}$ mice [15]; at E12.5, however, Scx expression in the somites was significantly reduced and expression was partially downregulated in the limbs, suggesting a phenotypic change in cells circa E12. However, the study did not continue to characterize the somites or spinal tendons and ligaments throughout development.

Taken together, our *in vivo* characterization study has provided insight into elastogenesis of spinal ligaments during development embryonically and postnatally, while our *in vitro* studies suggest axial T/L (including spinal ligament) cells are differentially regulated by soluble factors as compared to limb T/L cells. Continuing studies will analyze elastogenic and tissue-specific gene expression regulation in spinal ligament cells as a function of anatomical location and in response to soluble factors.

REFERENCES

1. Okuda et al, Spine 2004. 2. Schrader et al, Eur Spine J 1999. 3. Genevay et al, Best Prac Res Clin Rheum 2010. 4. Frank et al, Am J Sports Med 1983. 5. Nicholetti et al, Surg Neurol 2005. 6. Gillespie et al, Spine 2004. 7. Pryce et al, Develop Dynam 2007. 8. Nakagawa et al, Spine 1994. 9. Ponseti I, Iowa Orthopaedic J 1995. 10. Nachemson et al J Biomechanics 1968. 11. Mariani et al, Am J Respir Cell Mol Biol 2002. 12. Kelleher et al, Cur Top Dev Bio 2004. 13. Wagenseil et al, Birth Def Res 2007. 14. McLaughlin et al, Mol Cel Biol 2006. 15. Pryce et al, Development 2009.

Functional Ultra Sound Elastography (FUSE) of Achilles tendon: a novel reliable mechanical and clinical outcome tool

Joseph Alsousou, Larry Li, Mark Thompson, Eugene McNally, Keith Willett and Alison Noble

University of Oxford
Nuffield Department of Orthopaedic Rheumatology and Musculoskeletal Sciences
Oxford, UK

Purpose: Functional ultrasound Elastography (FUSE) of Tendo-Achilles is an ultrasound technique developed by our team utilizing controlled, measurable movement of the foot to non-invasively evaluate TA elastic and load-deformation properties. The study purpose is to assess Achilles tendons, paratenon and bursa mechanical properties in healthy volunteers and patients to establish a clinical outcome tool for TA treatment.

Methods: We studied 40 Achilles tendons in healthy volunteers using our novel Elastography method, which we developed in the university of Oxford. US scan device (Z.one, Zonare Medical System Inc., USA, 8.5 MHz) with and without the oxford isometric dynamic foot and Ankle mover were used. Tendon insertion, midportion and musculotendinous junction were examined during lateral movement and axial compression/decompression modes. B mode and elasticity images were derived from the raw ultrasound radio frequency data. The anatomical structures mechanical properties were evaluated by a semi-quantitative score of different colours representing stiff tissue (blue) to more soft tissue (green, yellow, red).

Results: The Achilles tendons showed mainly a hard structured pattern on sonoelastography. Compression/decompression modes are best used to demonstrate axial softening, while longitudinal displacement is best used to asses load transfer. The average strain along the tendon was 2% (range 0-6%). The overall correlation (κ) between real-time sonoelastography and ultrasound findings was < 0.3. However, the correlation (κ) between FUSE UEI and US findings was 1.0.

Conclusion: Our findings show that the novel FUSE method seems to be a sensitive method for assessment of TA mechanical properties. Elasticity and stiffness measurement may offer an invaluable tool to guide TA rupture and tendonopathy treatment and rehabilitation protocol.

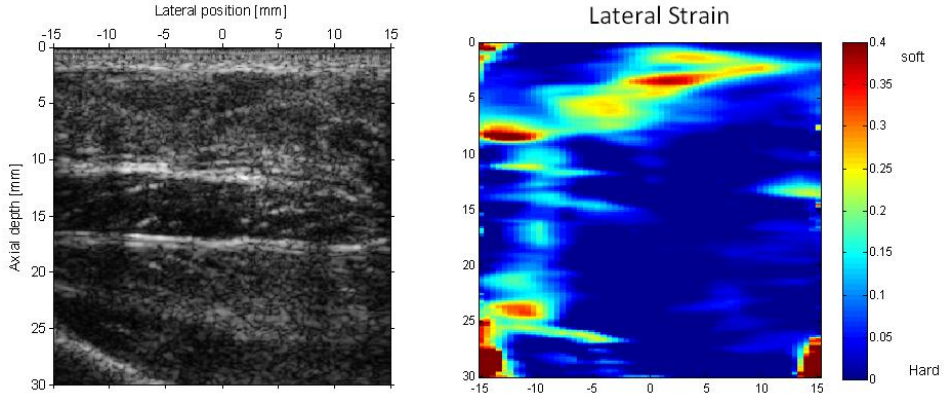

ULTRASOUND ECHO INTENSITY IN *IN VIVO* TENDON EXHIBITS LOAD DEPENDENT BEHAVIOR

K.E. Frisch, R. Vanderby Jr., D.G. Thelen
University of Wisconsin-Madison

INTRODUCTION

Few noninvasive methods exist to quantify *in vivo* tendon mechanics. A new method developed in our lab, called acoustoelastography, (AE) uses a higher order wave propagation theory to assess tissue strain and stiffness from cine ultrasound images (1,2). Consistent with AE theory, we previously showed that echo intensity varies cyclically with a load for *ex vivo* tendon (3). If similar effects can be observed when tissues are imaged *in vivo,* AE techniques could potentially be used to map stiffness distributions in normal, diseased and injured tissues. The goal of this study was to assess whether AE effects are evident when *in vivo* tendon is subjected to varying loads.

METHODS

The relationship between echo intensity and load was investigated in the tibialis anterior (TA) tendon for three subjects. Subjects were seated and wore a stiff-soled shoe that was attached to a fixed load cell. They first performed a maximum voluntary contraction (MVC) of the ankle dorsiflexors. Subjects were then asked to maintain voluntary contraction at one of six specified pre-loads (from 0% to 50%MVC) while cine (74Hz) ultrasound images were collected of the distal TA tendon. For each pre-load, the TA was then electrically stimulated inducing a twitch contraction that was observable in the images and force record. Each of the 6 pre-loads was repeated 3 times. Acoustoelastic techniques were used to quantify the magnitude of the echo signal prior to and after stimulation. Tendon motion during the twitch was accounted for using digital image correlation techniques. The twitch-induced change in echo intensity was assessed from the onset of the twitch to the generation of peak twitch force.

RESULTS

For all three subjects, the normalized average echo intensity during the voluntary contraction increased linearly with pre-load (Fig. 1). The average change in tendon echo intensity during the twitch exhibited temporal patterns that were remarkably similar to that seen in the twitch contraction force (Fig. 2). The echo intensity increased rapidly after stimulation onset and then decayed more slowly, in correspondence with twitch contraction and relaxation characteristics. When the change in twitch echo intensity was plotted against pre-load, a systematic decrease in echo intensity was observed (Fig. 3).

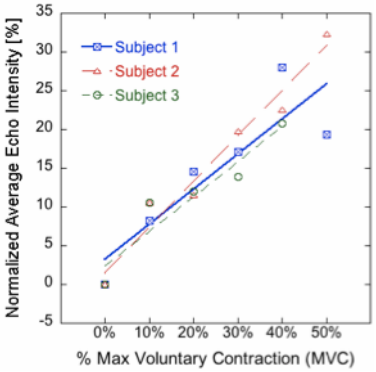

Figure 1: Normalized echo intensity from tendon increased linearly with contraction level.

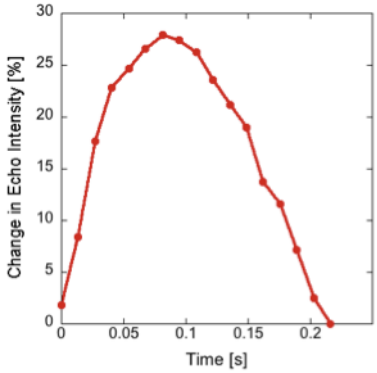

Figure 2: The change in tendon echo intensity in response to stimulation of a twitch contraction.

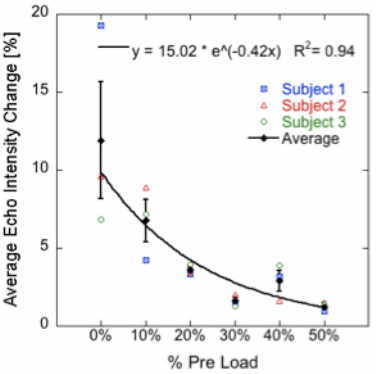

Figure 3: The average change in echo intensity during a twitch decreases with increasing preload in a systematic manner.

DISCUSSION

The load dependent nature of the echo intensity may represent a strain-stiffening effect. Since echo intensity is related to stiffness (1,2) and tendon is a strain-stiffening tissue, echo intensity would be expected to increase with tendon load as seen in Fig. 1. The change in echo intensity during a twitch decreased as the amount of pre-load increased. This could represent two effects. First, the magnitude of an induced twitch force decreases with pre-load due to a decrement in the number of motor units being recruited via the stimulation. Secondly, echo intensity is related to tissue stiffness, which increases with load in tendon. The large change in echo intensity at low loads may represent the lower slope of the toe region of the tendon stress-strain, while the smaller change at larger pre-loads may correspond to the more linear portion of the typical tendon stress-strain curve.

We conclude that these data demonstrate that acoustoelastic affects are evident *in vivo* when tendon is subjected to varying loads.

ACKNOWLEDGEMENTS

Joe Farron, NIH AR05620, NIH EB08548.

REFERENCES: 1. Kobayashi and Vanderby J Appl Phys 2005. 2. Kobayashi and Vanderby J Acoust Soc Am 2007. 3. Duenwald et al. J Biomech, in press.

ULTRASONIC CHARACTERIZATION OF TENDON VISCOELASTICITY

S.E. Duenwald-Kuehl, H. Kobayashi, R. Lakes, and R. Vanderby, Jr.
University of Wisconsin-Madison

INTRODUCTION

Customary methods of viscoelastic testing involve the use of animal models or cadaveric tissues and extraction from the body for testing in a mechanical test system, precluding direct study of viscoelasticity *in vivo*. The first step in such *in vivo* testing is developing a method by which time-dependent load and strain information can be gathered noninvasively. Acoustoelastic theory predicts that the acoustic properties of a material are altered as it is deformed[1] and has been applied to derive the acoustoelastic relationship between reflected A-mode ultrasonic wave amplitude and mechanical behavior in pseudo-elastic, incompressible materials by Kobayashi and Vanderby.[2] This phenomenon is also manifested in B-mode ultrasound, as tensioning tendons increases the intensity of reflected ultrasound echo, leading to a brighter image. This study examines whether the relationship between ultrasonic echo intensity from B-mode images is manifested in time-dependent echo intensity changes during viscoelastic testing.

METHODS

Porcine flexor tendons (n=16) were preconditioned using a sinusoidal wave to 2% strain in a mechanical test system (MTS Bionix, Minneapolis, MN). Tendons were split into groups with half undergoing creep tests and half undergoing relaxation tests. Six tendons were subjected to creep testing at 25 and 50N for 100s followed by a 100s recorded period of recovery from load (at preload) while B-mode cine ultrasound was recorded using a GE 12L-RS Linear Array Transducer at 12MHz and GE LOGIQ*e* ultrasound (General Electric, Fairfield, Connecticut). Two tendons were subjected to creep testing at 6.25N, 12.5N, 18.75N, 25N, and 37.5N to determine load-dependent viscoelastic changes in echo intensity. Six tendons underwent relaxation testing at 2 and 6% strain followed by recorded recovery from strain (at half the original strain) while B-mode cine ultrasound was recorded. Two tendons underwent relaxation tests at 2, 4, and 6% strain to determine strain-dependent viscoelastic changes in echo intensity.

In order to measure changes in average echo intensity (average grayscale brightness in the B-mode ultrasound image) of the tendons over the entire area between the grips over time, a region-based optical flow matching technique was used to track the movement of "speckles" (patterned echo reflections caused by tissue heterogeneity) during viscoelastic testing. A summed-squared difference metric based on region-based optical flow tracking was used to estimate the movement of speckles between consecutive frames of cine ultrasound. Echo intensity changes were compared to strain (during creep) and load (during relaxation) data collected by the mechanical test system.

RESULTS

Echo intensity changed in a time-dependent fashion during both creep and relaxation testing, and changed in the opposite direction during recovery. The changes in echo intensity during creep and recovery were greater at larger load (Fig 1) and strain (Fig 2) levels, respectively.

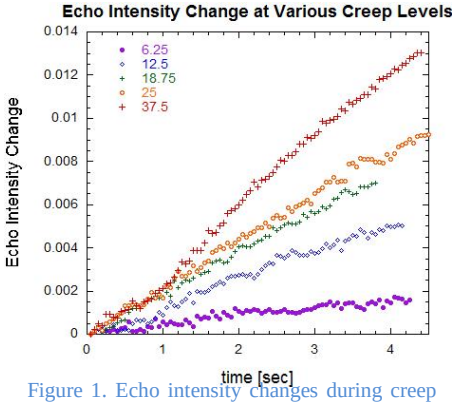

Figure 1. Echo intensity changes during creep at various load levels

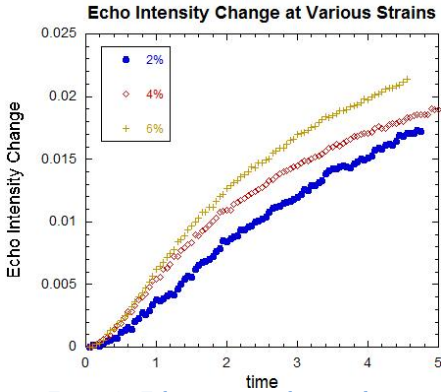

Figure 2. Echo intensity changes during stress relaxation at various strain levels

DISCUSSION

In order to better assess, understand, and study treatments for tendon injuries, it would be valuable to be able to quantify mechanical properties, including viscoelastic properties, noninvasively. The current study showed the time-dependent echo intensity changes that occur when B-mode cine ultrasound is collected simultaneously with viscoelastic testing. Echo intensity changes increase as load/strain increases, following previous mechanical data results. Thus, it is possible to noninvasively detect ultrasound signals that correlate with viscoelastic changes in tendon. This allows for *in vivo* characterization of viscoelastic changes in live tissue, and holds potential as a future scientific and diagnostic tool.

ACKNOWLEDGEMENTS

This work was funded in part by NSF 0553016 and NIH EB008548-01A1.

REFERENCES:

1. Hughes DS and Kelly JL. Phys Rev 1953; 1145-1149. 2. Kobayashi H and Vanderby R. J Acoust Soc Am 2007; 121(2):879-887.

The Optimization of a Collagen Gel Patch with Bone Marrow Stromal Cells for Tendon repair

M. Hayashi, C.F. Zhao, K.N. An, Y.L. Sun, Y. Morizaki and P.C. Amadio
Mayo Clinic Biomechanics Laboratory Rochester, Minnesota, USA

INTRODUCTION

Tissue engineering offers the possibility of replacing damaged tendon with a functional structure.[1] Recent studies have demonstrated that gel patch with bone marrow stromal cells (BMSCs) that was placed between lacerated tendon ends accelerated tendon healing using extra vivo model.[2] However, the quality of the BMSC patch is very determined by how the patch is manufactured, in which many factors are involved. Considering the future clinical application, this patch should be easy to make with a standard protocol within a desired time, matched size of the tendon cross-sectional area, easy to handle during surgery, and maintained at the position after surgery. The purpose of this study is to optimize the size of the gel patch for easier handling during tendon repair and to maintain the cells in the patch to maximize its effect.

METHODS

BMSC Harvest and Culture: The bone marrow was harvested from mixed-breed dogs. After centrifugation, the bone marrow cells were cultured in minimal essential medium (MEM, Gibco), 10% fetal bovine serum (FBS), and 1% antibiotics at 37°C with 5% CO_2. The adherent cells were defined as BMSCs. *Preparation of Cell-Seeded Collagen Gel Patch:* PureCol bovine dermal collagen (Inamed. Co) was prepared following the company's instructions. The original method: after mixing the same volume of collagen stock solution and cell suspension, the collagen solution with cells was incubated in each well at 37°C in a 5% CO_2 for 24 h. The modified method: after mixing the same volume of collagen stock solution and MEM with 20% FBS, the collagen solution was incubated at 37°C for 1 h. After gelation, the cell suspension was added on the gel and incubated at 37°C in a 5% CO_2 for 24 h. Two well sizes (24 well and 48 well plate) and three BMSC concentrations (0.1, 0.5, and 1.0×10^6 cells/ml) were studied with a collagen concentration of 0.5 mg/ml and both methods respectively. In order to evaluate the effect of the detachment, the edge of the gel was detached in each method. *Cellular labeling:* BMSCs were stained with DiI (Invitrogen) following the company's instructions. *Quantification of Gel Contraction ratio:* The cell-seeded gel was photographed at each time point with the same distance and zoom (Fig. 1). The digital images of the surface were calculated using ImageJ software. *Statistics:* The percentage of gel contraction area was analyzed using two-way ANOVA.

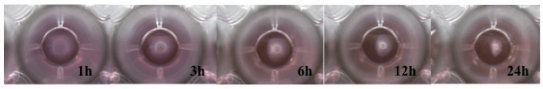

Figure 1. Contraction of BMSC-seeded collagen gel

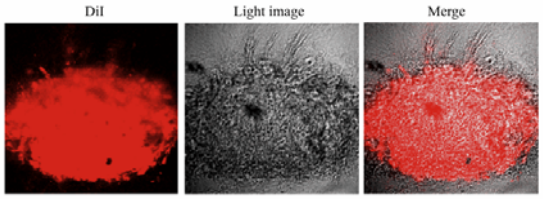

Figure 2. BMSCs in the collagen gel

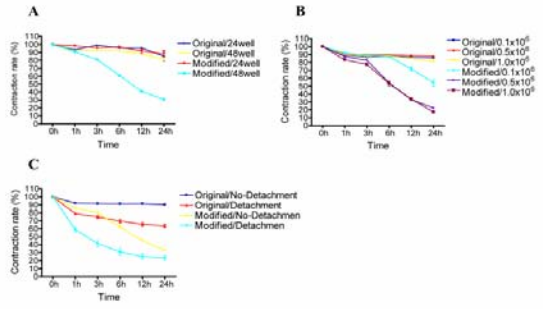

Figure 3. Time-dependent change of contraction rate

RESULTS

BMSCs were still alive after contraction (Fig. 2). The higher contraction rate of collagen gel was observed with the modified method and 48 well plate (Fig. 3A). In the original method the gel contractions were small, even with the various cell concentrations. In the modified method the contraction rates for the gel with concentrations of 0.5×10^6 and 1.0×10^6 cells/ml were significantly ($P<0.01$) higher than that of the concentration of 0.1×10^6 cells/ml at 24h (Fig. 3B). The detached gels contracted faster than non-detached gels in both methods (Fig. 3C).

DISCUSSION

The contraction rate of the cell-seeded patch is an important parameter affecting preparation time. In this study, we observed that our modified method had a positive effect on the contraction rate of BMSC-seeded collagen lattices. In the original method, most of the cells precipitate and attach to the well surface during contraction, even if using a non-coated plate. This may inhibit contraction of collagen gel. The cells stay around the superficial layer of collagen gel and contribute to contraction more efficiently when using our modified method. This result will be useful in advanced studies which focus on in vivo procedures.

ACKNOWLEDGEMENTS

This study was supported by grants from NIH (NIAMS AR44391) and Mayo Foundation.

REFERENCES: 1. Butler DL et al. JOR. 2008. 2. Zhao C et al. Med Eng Phys. 2009.

INTRATENDINOUS SUBSTANCE P INCREASES WITH EXERCISE IN AN *IN VIVO* MODEL OF TENDINOPATHY : PEPTIDERGIC ELEVATION PRECEDING TENDINOSIS-LIKE TISSUE CHANGES

L. Backman (1,2), G. Andersson (1), G. Wennstig (1), S. Forsgren (1), and P. Danielson (1) ✉
Dept of Integrative Medical Biology, Anatomy (1), and Dept of Surgical and Perioperative Sciences, Sports Medicine (2), Umeå University, Umeå, Sweden

INTRODUCTION

Tendinopathy is characterized by tissue changes ('tendinosis') like cellular proliferation and angiogenesis. It is, however, unclear why tendinosis occurs. To study the events leading to these tissue changes, we have established an *in vivo* animal (rabbit) model for tendon overuse.

A new hypothesis suggesting the involvement of locally produced neurochemical mediators in the pathology of tendinosis has recently emerged. This hypothesis is based on findings of a non-neuronal production of, traditionally neuronal, signal substances by the tendon cells (often collectively named 'tenocytes') of human Achilles tendon tissue; findings mainly seen in tissue from patients with tendinopathy. Particularly interesting is the finding of such an endogenous production of the neuropeptide substance P (SP). Studies have also confirmed that tenocytes and blood vessels of the tendon express the preferred receptor for SP, the neurokinin-1 receptor (NK-1 R), in both man and rabbit, making these structures susceptible to SP-stimulation. However, the exact role of SP in tendinosis is unclear. It is not known whether there is a significant increase of the local SP-production in tendinosis tissue, nor if such an increase precedes the tissue changes or if it is just a mere side-effect of the latter. Therefore, in this study, the endogenous production of SP at different stages of exercise in our animal model was measured. Furthermore, the study aimed at investigating the source of the locally produced SP.

METHODS

A total number of 24 New Zealand white rabbits were used (4 groups, 6 animals/group). Animals were subjected to our established protocol of electrical stimulation and passive flexion–extension of the right triceps surae muscle every second day for 1, 3 or 6 weeks. One group was subjected to no training at all (untrained controls). ELISA was performed on specimens from both the experimental (exercised), side and the contralateral (unexercised) side to measure the levels of SP. Immunohistochemistry (IHC) and *in situ* hybridisation (ISH) were performed to investigate the location of SP in the tissue. Kruskal-Wallis test (K-W), followed by pair-wise Mann-Whitney U test (M-W U), with Bonferoni correction, was performed on the data obtained from the ELISA.

Fig. 1: *Intratendinous SP-concentration*

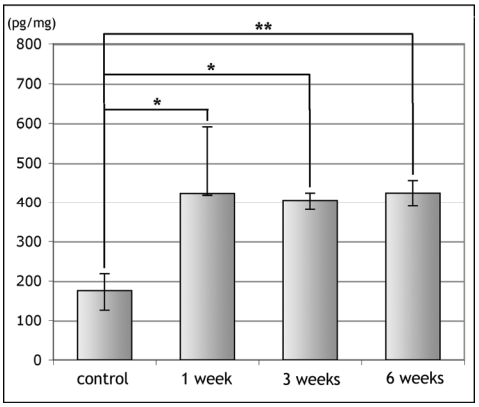

RESULTS

ELISA revealed significantly increased levels of endogenously produced SP in the Achilles tendon from the exercised limb in all the experimental groups as compared to the control group (see **Fig. 1**; K-W: $p=0.01$; M-W U: *: $p<0.05$, **: $p<0.01$). In the unexercised limb, the levels were also increased in all experimental groups, although this was not significant (K-W: $p=0.14$). IHC illustrated reactions of SP mainly in blood vessel walls, both in arteries and venoles. ISH confirmed presence of SP mRNA in these cells.

DISCUSSION

It is here shown that the endogenous production of SP in tendon tissue is elevated already after 1 week of exercise in the current animal model. That is interesting, considering the fact that we have previously shown that the tendinosis-like tissue changes in the rabbit Achilles tendon (hypercellularity and vascular proliferation, same as for human tendinosis) occur only after a minimum of 3 weeks of exercise. This would indicate that increased intratendinous SP-production precedes tendinosis; making theories on the involvement of SP in the early stages of tendinosis pathophysiology more plausible, especially if one bear in mind that SP is known to have proliferative effects on fibroblast and also to promote angiogenesis. The study furthermore indicates that the main source of the local SP-production might be cells of the blood vessel walls, although other sources cannot be excluded.

In an earlier study we demonstrated that tendinosis-like tissue changes also occur in the contralateral (unexercised) Achilles tendon to the same degree as on the exercised side in this model. The present study shows, although not significant, that SP-production is also increased on the contralateral side in the experimental groups, suggesting the involvement of central neuronal mechanisms.

In summary, this study confirms observations from research on man that there is a production of SP in the Achilles tendon, and furthermore verifies that this production is significantly increased when the tissue undergoes development of tendinosis; the SP elevation preceding the tendinosis-like tissue changes.

✉ patrik.danielson@anatomy.umu.se

INTENSIVE MECHANICAL LOADING CONTAINS THE RISK OF DEVELOPING TENDINOPATHY

Jianying Zhang, James H-C. Wang[#]

MechanoBiology Laboratory, Departments of Orthopaedic Surgery and Bioengineering
University of Pittsburgh, Pittsburgh, PA, [#]wanghc@pitt.edu

INTRODUCTION

Mechanical loading has been considered to play a major role in the development of tendinopathy, which is characterized by the presence of lipid deposition, increased amounts of proteoglycans, and calcified tissue in the affected tendon [1,2]. These histopathological findings suggest that tendon cells may be able to undergo aberrant differentiation such that non-tendinous tissues are formed in the tendons in response to excessive mechanical loading placed on them. Therefore, this study aims to test the hypothesis that moderate mechanical loading produces anabolic responses from the tendon in terms of increasing expression of tendon-related genes, whereas excessive mechanical loading induces expression of genes related to non-tendinous tissues. To test this hypothesis, we used mouse treadmill running as an experimental model.

MATERIALS AND METHODS

A total of 18 C57BL/6J female mice (2.5 months old) were divided into three groups: moderate treadmill running group (MTR), intensive treadmill running group (ITR), and cage control group, with 6 mice in each group. In the first week, all 12 mice in both the MTR and ITR groups received training for treadmill running at 13 m/min, 15 min/days, and 5 days/week. Following this training period, mice in the MTR group ran at the same speed for 50 min/day, 5 days/week, and 3 weeks total. On the other hand, mice in the ITR group ran at the same speed for 3 hr/day, 4 hr/day, and 5 hr/day for 5 days in the second, third, and fourth weeks, respectively. The control group remained in cages with free movement during treadmill running experiments. After the end of treadmill running, mice were sacrificed, and their patellar tendon (PT) and Achilles tendon (AT) tissue samples were harvested for gene expression analysis using real time qRT-PCR. A *t*-test was used for statistical analysis, with $p < 0.05$ being considered significantly different.

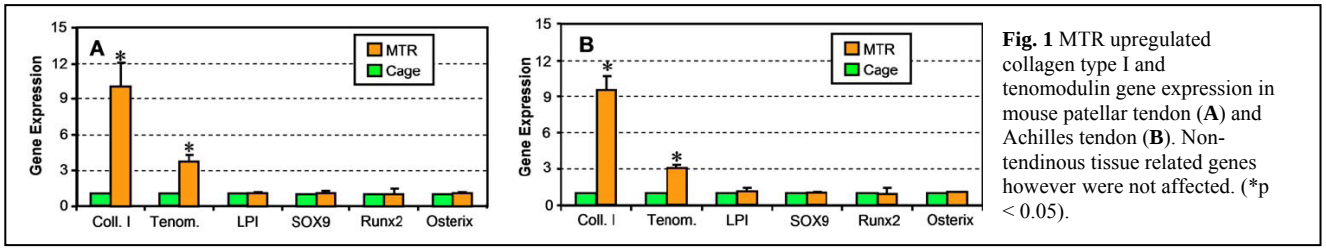

Fig. 1 MTR upregulated collagen type I and tenomodulin gene expression in mouse patellar tendon (**A**) and Achilles tendon (**B**). Non-tendinous tissue related genes however were not affected. (*p < 0.05).

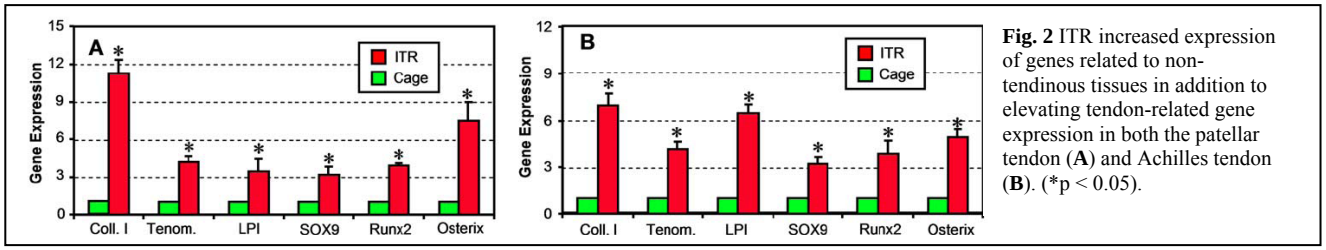

Fig. 2 ITR increased expression of genes related to non-tendinous tissues in addition to elevating tendon-related gene expression in both the patellar tendon (**A**) and Achilles tendon (**B**). (*p < 0.05).

RESULTS

We found that for both PTs and ATs in the MTR group, tendon-related genes, including collagen type I (Coll. I) and tenomodulin (Tenom.) were markedly upregulated, but genes related to non-tendinous tissues, LPL (fatty tissue), SOX9 (cartilage), and Runx2 and osterix (bony tissue), were not affected (**Fig. 1**). However, in the ITR group, all genes related to non-tendinous tissues in both PTs and ATs were highly expressed in addition to high levels of tendon-related gene expression (**Fig. 2**).

RESULTS

The results of this study support our working hypothesis. They show that while moderate mechanical loading on tendons may be beneficial in terms of upregulating collagen type I and tenomodulin gene expression, intensive mechanical loading could be detrimental as it induces expression of non-tendinous tissue related genes. The highly expressed genes correspond to the tissue phenotypes found in tendinopathic tendons [1, 2]. Therefore, long term, intensive mechanical loading may eventually lead to degenerative changes (lipids, proteoglycan accumulation, and calcification) in the tendon tissue. Moreover, we suspect that tendon stem cells (TSCs) [3] are responsible for the upregulation of non-tendinous tissue related gene expression, as TSCs are known to express genes related to non-tenocytes in vitro [4].

References: [1] Kannus and Jozsa, 1991;[2] Tallon et al., 2001; [3] Zhang and Wang, 2010; [4] Zhang and Wang, 2010.

Acknowledgement: This work was supported in part by NIH AR049921 and AR049921S2 (JHW).

GENE EXPRESSION PROFILE AFTER A SINGLE LOADING EPISODE DURING RAT TENDON HEALING

[1]P. Eliasson; [1] T. Andersson; [1]P. Aspenberg
+[1]University of Linköping, Linköping, Sweden

INTRODUCTION

Short daily loading episodes can improve tendon healing in rats[1]. An additional loading episode 8 hours later the same day does not further improve healing. This indicates that the response to loading lasts for several hours. We have also seen that one single loading episode for 30 minutes is sufficient to improve tendon mechanical properties 7 days later. This prompted us to further investigate how long the induced changes in gene expression lasts after a single loading episode. Since there are no clear-cut candidate genes, we selected a hypothesis generating approach, with a gene expression microarray to study gene expression 3, 12, 24 and 48 hours after a single loading episode.

MATERIALS AND METHODS

The Achilles tendon was transected and left to heal in thirty Sprague-Dawley rats ~200 g[1]. The day after surgery, all rats were subjected to hindlimb unloading by tail suspension and divided into 7 groups: 2 groups were unloaded without exercise for 5 or 7 days (C1 and C2), and 4 groups were subjected to 30 min of exercise on a treadmill, day 5, but were otherwise tail-suspended. These animals were euthanized 3, 12, 24 and 48 hours after the exercise. Tendon calluses were harvested and snap-frozen in liquid nitrogen. RNA was extracted and the yield and integrity was analyzed. The three best samples in each group were analyzed with rat microarrays (Gene 1.0 ST array system, Affymetrix inc, Santa Clara, USA). We first analyzed if there was any statistical difference between the control groups from different days (C1 and C2). If there was no difference between the two groups, the gene expression data were pooled together and were considered as one control group (C). Each time-point was thereafter analyzed compared to control (C) and the results were analyzed as fold-change compared to this group. All comparisons were also tested by Student's t-test, and the genes were characterized both by fold-change and p-value. The experiment was approved by the regional animal ethics committee.

RESULTS

The main response in gene regulation was seen 3 hours after the loading episode. At this time-point, 157 genes were regulated by mechanical loading with at least a twofold change and $p \leq 0.05$, 88 genes were up-regulated and 69 down-regulated. With a fold-change (FC) of ±1.5 and $p \leq 0.001$, there were 512 regulated genes (Figure 1). 12 hours after the loading episode, 42 genes were regulated with at least a twofold change and $p < 0.05$. However, at this time-point most changes consisted of down-regulation (39 of 42 genes). There were 93 genes with a fold-change of ± 1.5 and $p \leq 0.001$, all down-regulated. Virtually no gene response was seen after 24 and 48 hours.

Many of the genes regulated at 3 hours were involved in inflammation or apoptosis; these were mainly up-regulated (Table1). Also transcription factors were mainly up-regulated at this time-point. Genes involved in cell proliferation and cell differentiation were both up- and down-regulated. Some of the interesting up-regulated genes were iNOS (FC 3.2), argininosuccinate synthetase 1 (FC 3.3), PGE-2 synthase (FC 1.9), inhibin beta-A (FC 3.0), fos-like antigen 1 (FC 3.2) and IL-1 receptor antagonist (FC 3.1). Some down-regulated genes were TGF-β3 (FC 2.5), aggrecan (FC 2.5), keratocan (FC 2.4) and glutamate receptor AMPA 1 (FC 2.7).

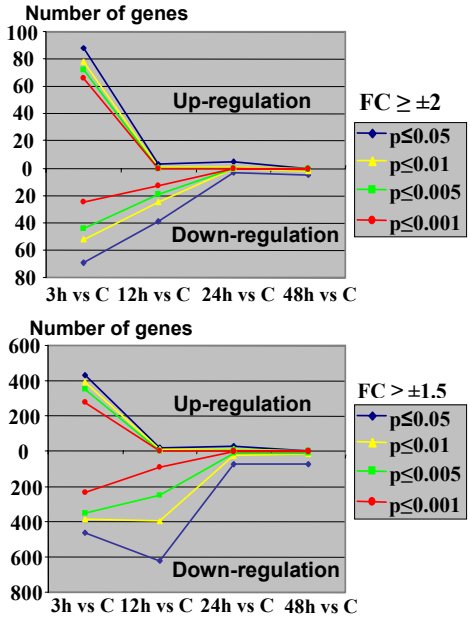

Figure 1. Number of genes expressed at each time-point. Top: Fold-change ≥ 2. Bottom: Fold-change ≥ 1.5. The colors represent p-values ranging from 0.05 to 0.001.

DISCUSSION

The number of regulated genes peaked 3 hours after the loading episode. However there were still many genes down-regulated after 12 hours. There was hardly any response left after 24 hours. This suggests that there is a need to refresh the loading stimulus every day. Our detailed analysis of individual genes is not ready, but we note that iNOS and related genes are highly mechanosensitive in this system, also MMPs, Wnt signaling and TGF-beta superfamily seems to be somewhat mechanosensitive. One of the few genes that showed a lasting change over 24 h was keratocan, which is a small leucine-rich proteoglycan that binds to fibrillar collagen and regulates the collagenous matrix[2]. This protein is normally expressed in fibro-cartilaginous regions and was here down-regulated by loading. Interestingly, some genes that are up-regulated in tendinosis (eg glutamate signaling, aggrecan) seem to be down-regulated, during healing, by mechanical loading.

1. Andersson et al. 2009
2. Rees et al. 2009

Table 1. Number of regulated genes in different functional groups with at least a twofold change. Up-regulated: ↑ . Down-regulated: ↓

	3h		12h		24h		48h	
FC ≥ +/-2; p ≤ 0.05	↑	↓	↑	↓	↑	↓	↑	↓
Cell proliferation	6	7	0	3	0	1	0	0
Cell differentiation	6	7	0	3	0	1	0	0
Extra-cellular matrix	2	1	0	4	0	0	0	0
Inflammation	11	1	0	1	0	1	0	0
Apoptosis	11	5	0	4	0	1	0	0
Transcription	7	3	0	4	0	1	0	1

REHABILITATIVE MECHANICAL CONDITIONING REGIME FOR TENDON/LIGAMENT TISSUE REGENERATION

Thomas K.H. Teh, Siew-Lok Toh, James C.H. Goh
Division of Bioengineering and Department of Orthopaedic Surgery, National University of Singapore, Singapore

INTRODUCTION

Bioreactors have been widely used in tissue engineering applications, often with the aim to provide a closer resemblance of the *in vivo* environment *ex vivo*. When it comes to tissue engineering the tendon/ligament, its essential function is to provide mechanical stimulus to modulate the cell physiology and increase overall biosynthetic activity in the 3D constructs for effective tissue regeneration *in vitro* [1]. The common approach has been to provide leveled physiological loading to condition cell-seeded constructs [2-4]. However, this may be sub-optimal as the stimulation intensity may not be relevant or suitable throughout the different phases of the constructs' development. The aim of this study is thus to design a novel rehabilitative mechanical conditioning regime to enhance the dynamic culture process. It is hypothesized that the rehabilitative stimulation process will accelerate the differentiation process of mesenchymal stem cells (MSCs) seeded constructs to realize functional tissue engineered tendons/ligaments within a shorter duration *in vitro*.

METHODS

Rabbit MSCs derived from bone marrow (P3) were seeded onto the sterilized aligned hybrid silk fibroin (AL) scaffolds, which consisted of aligned electrospun silk fibroin integrated with knitted silk. The seeded constructs were cultured in varying conditions ranging from static (control) to dynamic cultures of different regimes ("continuous low", "continuous high" and "rehab") with continuous or sequential provision of varied levels of stimulation intensities, based on variation of cyclic frequency and cycle numbers. Specifically, the "rehab" group was stimulated with static, low intensity and high intensity stimulation conditions progressively. Multi-dimensional strains of both the tensile (5%) and rotational (90° clockwise) types were provided by a standalone bioreactor setup over the 28 days culture period for the dynamically cultured groups. Each group of cultured AL scaffolds were assessed through the experimental period for viability and cell proliferation (Alamar Blue™ assay, n=5), collagen deposition (Sircol™ collagen assay, n=3), tenogenic gene expression (real-time qRT-PCR, n=3), extracellular matrix (ECM) morphology and protein distribution (Masson's trichrome staining and immunohistochemical staining, n=3), ligament-specific protein synthesis (Western blot, n=3) and biomechanical properties (tensile tests, n=5).

RESULTS

The "rehab" group had 62% and 10% more viable cells on day 28 compared to the "continuous high" group and "static" control respectively. Consistent proliferation was found for the "static" and "continuous low" groups till day 21, and "rehab" group till day 14. Consistent increase in collagen deposition was found for both the "continuous low" and "rehab" groups over the culture duration, with the "rehab" group stimulated significantly more collagen deposition than "continuous high" (220% more), "continuous low" (73% more) and "static (217% more) on day 28. By day 28, all targeted tendon/ligament-specific genes were significantly expressed in the "rehab" group compared to the other groups, with aligned ECM depositions and tendon/ligament-like microstructural "crimped" collagenous structures observed in the "rehab" groups. The ECM components, as determined by immunohistochemical staining and Western blot analyses, were predominantly collagen I, with significantly more tendon/ligament-specific proteins produced in the "rehab" group relative to the "static" control by day 28. This increased ECM deposition was translated to mechanically superior constructs obtained using the "rehab" dynamic conditioning regime for culture, whereby constructs had a maximum load of 238.08 ± 19.29 N and stiffness of 44.44 ± 2.84 N/mm.

DISCUSSION

By comparing the different conditioning regimes, it was apparent that the rehabilitative approach was promising over the leveled stimulation regimes in providing dynamic conditions for regenerating tendon/ligament tissue. The rehabilitative stimulation regime allowed the freshly seeded MSCs to acclimatize to mechanical cues of a low intensity prior to higher intensity of stimulation for differentiation to occur. Consequently, proliferation was found for the earlier stages of the stimulation period, which transcended towards the differentiative phase in an accelerated manner after 14 days. Differentiation was marked by the increased collagen deposition, up-regulation of ligament-specific genes and deposition of the corresponding ECM components. This was especially so for tenascin-C and tenomodulin, which were consistently up-regulated to trigger collagen fiber build-up and thickening, leading to overall tissue maturation. Although the collagen fibers produced were not as compact and dense as the native tissue within this 28 days duration, the rehabilitative stimulation regime was shown to provide dynamic cues for collagen fiber formation and maturation in a manner that was more effective than leveled stimulation regimes.

REFERENCES: 1. Butler et al. J Biomech Eng 2000. 2. Altman et al. J Biomech Eng 2002. 3. Chen et al. Tissue Eng 2006. 4. Joshi and Webb JOR 2008.

INVESTIGATION OF TENDON PROGENITOR CELLS IN HEALING TENDONS AND ITS RELATIONSHIP WITH NEOVASCULARIZATION

Fu SC[1,2], Cheuk YC[1,2], Mok TY[1,2], Cheng WH[1,2], Hung LK[1,2], Chan KM[1,2]
[1]The Chinese University of Hong Kong, Hong Kong SAR, China, [2]The Hong Kong Jockey Club Sports Medicine and Health Sciences Centre, Hong Kong SAR, China

INTRODUCTION

We previously showed that cultured healing tendon cells exhibited different cellular activities as compared to cultured tendon fibroblast from intact tendon[1] but the origin of healing tendon cells is still unclear. Multipotent tendon progenitor cells (TPC) are recently characterized and their role in tendon healing was implicated[2-3], though there is no direct evidence of involvement of TPC in natural healing of tendon injuries. Although the *in situ* location of TPC is still unknown, perivascular mesenchymal cells might be a possible source[4]. As neovacularization is important for tendon healing, it is interesting to know (1) if TPC was also present in the wound at early tendon healing phases of cell recruitment, and (2) whether there is any association between neovascularization and quantity of TPC present in the wound. In this study, presence of TPC will be checked using CFU analysis and multi-differentiation assays, and neovascularization will be examined using 3-D Doppler ultrasonagraphy.

METHODS

A well established central one-third patellar window injury rat model was used. A 1x4mm window wound was created in rats unilaterally (n=8). At day 7 post-injury, rats were put for 3-D Doppler ultrasound imaging (Visualsonics) at the injured knee. Rats were then euthanized and the wound tissues from both injured and untraumatized knee were excised and digested in 0.3% collagenase I for 2.5hr. Cells released were plated at low density (50 cells/cm^2) in 35mm petri dishes. Cells cultured for 8 days were fixed for Crystal Violet staining. CFU number and colony size from intact and healing tendon was counted using image analysis software (MediaCybernetics). Cells in other dishes on day 8 of culture were switched to osteogenic, chondrogenic and adipogenic medium for 14 days. Osteogenesis, chondrogenesis, and adipogenesis of the cells were confirmed by Alizarin Red staining, Alcian Blue staining, and Oil Red staining respectively. Results of differentiation assay were compared between untraumatized and injured legs. Neovascularization was measured as increase in percentage volumetric vascular flow (% vascularity) within the tendon wound and the whole patellar tendon. Pearson's correlation was employed to correlate % vascularity with total cells and total CFU number from injured knees. Statistical significance was set at $p<0.05$.

RESULTS

As shown by CFU assays, the percentage of tendon progenitor cells (TPC) in total released cells from healing tendons was significantly decreased as compared to intact tendons ($p=0.017$), but the average colony size was similar ($p=0.917$). CFU from intact tendon were positively stained with Alizarin Red staining, Alcian Blue staining, and Oil Red staining after incubation with osteogenic, chondrogenic and adipogenic medium, indicating a tri-lineage multipotency. TPC from healing tendons only responded to osteogenic medium and did not exhibit chondrogenic and adipogenic activities. We found that percentage vascularity in the wound at day 7 post injury was positively correlated to total cells ($r=0.750$, $p=0.032$) and total TPC ($r=0.772$, $p=0.025$), while percentage vascularity in whole tendon was correlated to percentage TPC in total released cells ($r=0.731$, $p=0.039$).

DISCUSSION

Our study showed that TPC were also present in healing tendons, but the percentage of TPC was decreased as compared to that in intact tendon, probably due to increased recruitment of non-TPC cells during tendon healing. TPC from healing tendons also exhibited a lower multipotency as compared to intact tendon TPC, it may support the view that TPC originally resident inside tendon may be activated to mediate tendon healing with a loss of multipotency. A positive correlation between neovascularization and amount of TPC in the wound may suggest the involvement of vasculature in providing progenitor cells for healing. The increased availability of TPC may also help to explain the beneficial effects of neovascularization to tendon healing.

REFERENCES: 1. Fu SC, et al. (2008) J Orthop Res. **2.** Bi Y, et al. (2007) Nat Med 13(10):1219-27. **3.** Rui YF, et al. (2010) Tissue Eng Part A 16(5):1549-58. **4.** Tempfer H, et al. (2009) Histochem Cell Biol 131(6):733-41.

CANONICAL CORRELATION BETWEEN THE NEOVASCULARIZATION AND MECHANICAL RESTORATION IN TENDON HEALING

Mok TY[1,2], Fu SC[1,2], Hung LK[1,2], Cheuk YC[1,2], Lui PPY[1,2], Chan KM[1,2]
[1]The Chinese University of Hong Kong, Hong Kong SAR, China, [2]The Hong Kong Jockey Club Sports Medicine and Health Sciences Centre, Hong Kong SAR, China

INTRODUCTION

Neovascularization is commonly known to play an important role in tendon healing, but some studies have reported a negative mechanical outcome with sustained high vascularization. Our previous study reported the use of 3-dimensional Doppler ultrasound imaging to examine the temporal change of vascularity in natural tendon healing. Two peaks of increased vascularity at day 7 and 28 post injury was noticed in the whole injured tendon, but the contribution of these vascular changes to the mechanical outcome is unknown. In current study, the relationship between the mechanical properties of the healing tendon at day 42 post-injury and the temporal changes in vascularization was analyzed by canonical correlation analysis.

METHODS

Fifteen Sprague-Dawley rats were recruited in this study. Central-third donor site injury was operated on the patellar tendon of the right knee. 3D Doppler ultrasound imaging was performed at pre-injury, and 7, 14, 28, and 42 days post-injury. Neovascularization was measured in % vascularity within the wound (fig.1A-D). The animals were euthanized at day 42 and samples were harvested for biomechanical testing (fig.1E). Ultimate tensile stress, strain and Elastic's modulus were calculated. Canonical correlation analysis will be performed between the vascularity % at all time points and the final mechanical properties at a significant level of p=0.05.

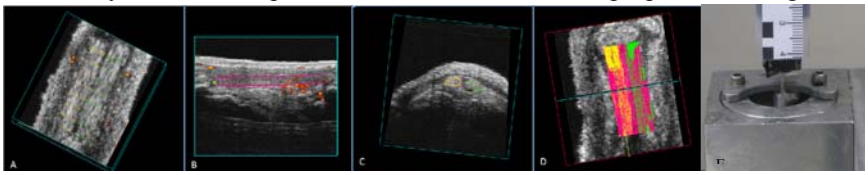

Figure 1. Vascularity % was calculated by selecting the volume of interest by drawing contours along the tendon (A-D). Biomechanical testing was performed by fixing both the patellar and tibial end, and the tendon was pulled along the direction of the force until breakage (E).

RESULTS

We found that mechanical restoration at day 42 post-injury exhibited a significant canonical correlation with the vascularity in the wound (R= 0.945 for the first root of canonical variate). The elastic modulus comprised the highest canonical factor loadings (0.989) to the first root in the mechanical test data, while neovascularization at day 7 exhibited highest canonical factor loading (0.963) in the vascularity data. 47 % (mechanical test data) and 22 % (vascularity data) of variance was explained by the first root of canonical variate. The second root of canonical variate (R = 0.772) was primarily correlated to ultimate stress (-0.830) and vascularity at day 42 (-0.707).

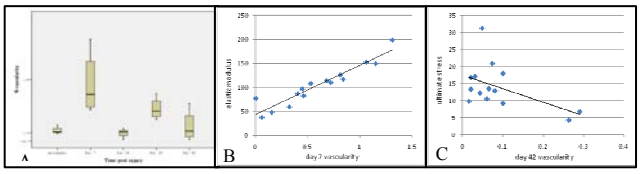

Figure 2. When the temporal change of vascularity was calculated (A), only vascular % at day 7 post-injury exerts a positive relationship with the elastic modulus (B), while there is a trend of negative association between the vascularity % at day 42 and the ultimate stress (C).

DISCUSSION

Our results showed that neovascularization at early healing phase (day 7) was associated with better mechanical restoration at a longer time point (day 42) as revealed by the first root of canonical variate. This relationship may be attributed to beneficial effects brought by neovascularization during inflammatory phase. Zhang et al., (2003) reported that VEGF injection increased neovascularization and improved tendon healing at early healing stage, but the beneficial effect was not observed at late healing. In contrast, our study suggested that neovascularization at early inflammatory phase may have a profound effect on final mechanical restoration. It is possible that the beneficial effect of natural neovascularization may not be completely mimicked by the VEGF-induced changes. On the other hand, sustained level of vascularization is reported to be harmful to tendon healing. In our study of normal tendon healing, only a few samples exhibited a sustained vascularization at day 42 post-injury, and a negative correlation with mechanical restoration was observed. This relationship may be attributed to the disruption of tendon matrix by the presence of increased vasculature. Our findings support the view that a timely neovascularization and subsequent vascular regression is necessary for better healing outcomes.

REFERENCE: 1. Zhang et al. Plast Reconstr Surg 2003.

Margin Convergence to Bone for Reconstruction of the Anterior Attachment of the Rotator Cable in Massive Rotator Cuff Tears

[1]Nguyen, ML; [1]Jun, BJ; [1]Quigley, RJ; [1]Galle, SE; [1]McGarry, MH; [1]Gupta, R; [2]Burkhart, SS; +[1]Lee, TQ
[1]*Orthopaedic Biomechanics Laboratory, VA Healthcare System and UC Irvine, Long Beach, CA*
[2]*The San Antonio Orthopaedic Group, San Antonio, TX*
tqlee@uci.edu

INTRODUCTION:

The rotator cable is a thickened band of the coracohumeral ligament that runs from its anterior attachment just posterior to the bicipital groove to its posterior attachment at inferior border of the infraspinatus. Being a stronger, thicker tissue it acts as a stress shield for the thinner, weaker rotator crescent tissue. The importance of the anterior attachment of the rotator cable has previously been shown to be associated with rotator cuff tears involving the anterior attachment and the ensuing fatty degeneration[1]. Margin convergence to bone is a surgical technique that uses a suture anchor to perform both footprint restoration and side-to-side repair. To our knowledge, no study has been performed to assess the biomechanical properties of restoring the anterior attachment of the rotator cable. Therefore the objective of this study was to compare the biomechanical characteristics of a massive rotator cuff tear repaired with a posterior transosseous-equivalent repair and an anterior repair using either two soft tissue margin convergence sutures or margin convergence to bone reconstructing the anterior cable attachment.

METHODS:

Eight matched-pair cadaveric shoulders were dissected leaving the rotator cuff muscle insertions and the rotator interval tissue intact. The supraspinatus and infraspinatus were secured in a custom curved cryo-clamp specifically designed to accommodate both the supraspinatus and infraspinatus tendons with the proximal humerus in 30º of glenohumeral abduction (Figure 1). The subscapularis was secured in a separate clamp and a constant 10N load was applied. The supraspinatus and infraspinatus were clamped before creating the tear in order to simulate a retracted, immobile tear. A massive tear was created by creating a triangle with its points at (1) the anterolateral border of the supraspinatus, (2) the anterior margin of the supraspinatus 75% of the length from the musculotendinous junction to the tendon edge, and (3) a point 1.5 times the width of the supraspinatus posterior to the bicipital groove (Figure 2). Once the triangle was marked, it was sharply excised. The posterior aspect of the tear was repaired using a transosseous-equivalent suture bridge technique. In the soft tissue margin convergence group, two margin convergence sutures were placed between the supraspinatus and the rotator interval. In the margin convergence to bone group, a double-loaded suture anchor was inserted at the anterior attachment of the rotator cable. Margin convergence to bone was then performed between the supraspinatus and the rotator interval. By clamping the supraspinatus and infraspinatus before creating and repairing the tear, non-uniform distribution of tension across the repair was achieved. Each specimen was tested using an Instron material testing machine for biomechanical characteristics and a video digitizing system for gap formation and footprint strain. Each specimen underwent a preload of 10N for 10 seconds followed by cyclic loading from 10N to 180N at a rate of 1mm/s for 30 cycles followed by load to failure. A paired-t test was used for statistical analysis.

RESULTS:

Margin convergence to bone significantly decreased gap formation at cycle 1, cycle 30 and yield load across the entire footprint ($p < 0.05$). In both constructs, the anterior gap was significantly greater than the posterior gap at cycle 1, cycle 30, yield load, and ultimate load ($p < 0.05$). There was no difference in footprint strain between the two groups. Margin convergence to bone significantly decreased hysteresis during the first cycle and increased yield load as well as stiffness ($p < 0.05$).

DISCUSSION:

Using margin convergence to bone to reconstruct the anterior attachment of the rotator cable improved the structural integrity of the repair by decreasing hysteresis, increasing yield load, increasing stiff ness, and decreasing gap formation not just anteriorly, but throughout the entire footprint. The anterior attachment of the rotator cable serves as an anchor to further reduce the tension from the rest of the rotator cuff repair. These results reinforce the concept that the rotator cable acts as a stress shield across the entire footprint.

.

REFERENCES:

1. Kim et al., JBJS 2010, 92(4). 829-39.

Figure 1. Experimental Setup

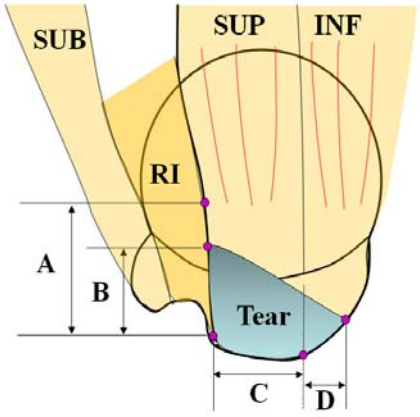

Figure 2. Tear Creation

Platelet-rich plasma augmentation for arthroscopic rotator cuff repair: a randomised controlled trial

Umile Giuseppe Longo MD 1, Roberto Castricini MD 2, Massimo De Benedetto MD 2,
Nicola Panfoli MD 3, Piergiorgio Pirani MD 2, Raul Zini MD 2,
Nicola Maffulli MD, MS, PhD, FRCS(Orth) 4, Vincenzo Denaro MD 1

1 Department of Orthopaedic and Trauma Surgery, Campus Bio-Medico University, Via Alvaro del Portillo, 200, 00128 Trigoria, Rome, Italy
2 Department of Orthopaedic and Trauma Surgery, Villa Maria Cecilia Hospital, Cotignola-Ravenna, Italy
3 Department of Orthopaedic and Trauma Surgery. Ospedale Civile, Viale della Vittoria. Jesi, Italy
4 Centre for Sports and Exercise Medicine, Barts and The London School of Medicine and Dentistry, Mile End Hospital, 275 Bancroft Road, London E1 4DG, England

INTRODUCTION
Following reinsertion on the humerus the rotator cuff (RC) has limited ability to heal [3-6]. Growth factors augmentation has been proposed to be able to enhance healing in such procedure. The purpose of this randomised controlled trial is to assess the efficacy and safety of the addition of growth factor augmentation during rotator cuff repair
METHODS
Eighty-eight patients with a rotator cuff tear were randomly assigned by a computer-generated sequence to receive arthroscopic rotator cuff repair without (n=45) or with (n=43) augmentation with autologous platelet-rich fibrin matrix (PRFM). The primary endpoint was the post-operative difference in the Constant score [1] between the 2 groups. The secondary endpoint was the integrity of the repaired rotator cuff, as evaluated by MRI. Analysis was on an intention to treat basis
RESULTS
All the patients completed follow-up at 16 months. There was no statistically significant difference in total Constant Score when comparing the results of arthroscopic repair of the 2 groups (95% confidence interval [CI], -3.43 - 3.9) (P=0.44). There was no statistically significant difference in MRI tendon score when comparing arthroscopic repair with or without PFRM (P=0.07).
DISCUSSION
Our study does not support the use of autologous PRFM for augmentation of a double row repair of a small or medium RC tear to improve the healing of the RC. Our results are applicable to small and medium RC tears: it is possible that PRFM may be beneficial for large and massive RC tears [2,7]. Also, given the heterogeneity of PRFM preparation products available on the market, it is possible that other preparations may be more effective.
ACKNOWLEDGEMENTS
None
REFERENCES:
1. Constant CR, Murley AH. A clinical method of functional assessment of the shoulder. Clin Orthop Relat Res 1987: 160-164.
2. de Vos RJ, Weir A, van Schie HT, Bierma-Zeinstra SM, Verhaar JA, Weinans H, Tol JL. Platelet-rich plasma injection for chronic Achilles tendinopathy: a randomized controlled trial. Jama 2010; 303: 144-149.
3. DeOrio JK, Cofield RH. Results of a second attempt at surgical repair of a failed initial rotator-cuff repair. J Bone Joint Surg Am 1984; 66: 563-567.
4. Longo UG, Franceschi F, Ruzzini L, Rabitti C, Morini S, Maffulli N, Denaro V. Histopathology of the supraspinatus tendon in rotator cuff tears. Am J Sports Med 2008; 36: 533-538.
5. Longo UG, Franceschi F, Ruzzini L, Rabitti C, Morini S, Maffulli N, Forriol F, Denaro V. Light microscopic histology of supraspinatus tendon ruptures. Knee Surg Sports Traumatol Arthrosc 2007; 15: 1390-1394.
6. Longo UG, Lamberti A, Maffulli N, Denaro V. Tendon augmentation grafts: a systematic review. Br Med Bull 2010: Jan 4. [Epub ahead of print] DOI:10.1093/bmb/ldp1051.
7. Randelli PS, Arrigoni P, Cabitza P, Volpi P, Maffulli N. Autologous platelet rich plasma for arthroscopic rotator cuff repair. A pilot stud
.

The Influence of Subscapularis Partial Tears; Are We Neglecting Them?

+§*Jae Chul Yoo, MD, *Michelle H McGarry, MS, *Bong Jae Jun, PhD, Jonathan Scott, *Thay Q Lee, PhD

*Orthopaedic Biomechanics Laboratory,
VA Long Beach Healthcare System and University of California, Irvine, CA, USA
+§Department of Orthopedic Surgery, Sungkyunkwan University College of Medicine,
Samsung Medical Center, Seoul, Korea
shoulderyoo@gmail.com

Introduction: Due to the advent of arthroscopy, more partial subscapularis tendon tear is being recognized with or without supraspinatus/infraspinatus tendon tear. The guidelines for the treatment of these partial subscapularis tear to date has been anecdotal at best. Therefore, the purpose of this study was 1) to evaluate the changes in the kinematics of glenohumeral joint with increasing partial tears of subscapularis upper portion tendon and added supraspinatus tendon tear and2) to evaluate the effects of repairing only the supraspinatus tendon tear and leaving the subscapularis partial tear alone and then repairing both tendon tear. The first hypothesis was that there will be changes in the kinematics even with 1/4 tear of the subscapularis tendon tear and second, the complete repair of both tendon will better restore the kinematics and ROM compared to supraspinatus tendon tear alone.

Methods:
Six cadaveric shoulders were used (mean age of 59 years, range 44-78). All soft tissues were removed except the glenohumeral joint capsule, insertion of rotator cuff muscles. Suture loops were made at the insertion of each muscle: 1 for teres minor (TM), 2 for supraspinatus (SSP) and 3 for infraspinatus (ISP), and 4 for subscapularis muscles in order to load anatomically based on fiber orientation and multiple lines of action. The line of pull for subscapularis muscle and infraspinatus/teres minor had 4 lines based on the previous studies and our MRI study showing mean 4 distinct tendons within subscapularis. (Fig.1) A Custom shoulder testing system was used.
Six conditions were tested. Three progressive stages of rotator cuff tears (RCT) were created based on footprint anatomy of subscapularis. Subscapularis tendon insertion approximately has 3/4 tendinous insertion on the lesser tuberosity whereas 1/4 has muscular insertion directly to the humerus. So we considered 1/3 of the subscapularis tendon tear on the lesser tuberosity equal to 1/4 tear of the entire subscapularis insertion. Test I was the glenohumeral (GH) kinematics of intact specimens. Test II was a tear of the 1/4 upper tendinous portion complete tear of subscapularis tendon. Test III was a tear of the 1/2 of the subscapularis insertion. Test IV was an anterosuperior tear of 1/2 subscapularis tendon tear and entire supraspinatus (SS) tendon tear. Test V was repair of only the SS using classic transosseous equivalent method of repair. Finally Test VI, repair of the subscapularis using double-loaded suture anchor making two simple sutures.

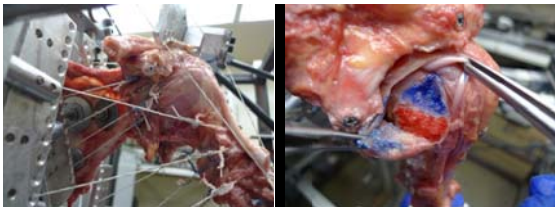

Figure 1. 4 line of muscle pull for subscapularis 2. Partial tear 1/4 (blue) and 1/2(red) of subscapularis, complete-thickness.

The amount of muscle loading was determined based on the physiological muscle cross-sectional area: supraspinatus 20N, subscapularis 30N, infraspinatus/teres minor 30N. Only the rotator cuff muscles loading were performed based on prior pilot study. So load was divided 7.5 N each (adding 30 N) for each line of pull (Fig. 1)
Testing was performed in the scapular plane (30° anterior to the coronal plane) with 0°, 30°, and 60° shoulder abduction with a 2:1 ratio of glenohumeral to scapular abduction.
The maximum internal rotation (Max IR) and external rotation (Max ER) were measured with 3.4 Nm of torque using a torque wrench. The position of the humeral head apex (HHA) with respect to the glenoid was measured using a Microscribe 3DLX at each abduction angle for 5 position; Max IR, IR 30°, Neutral, ER 30° and Max ER. A repeated measure ANOVA with a Tukey post hoc test was used with a significance level of 0.05.

Results:
Rotational Range of Motion (ROM): Max ER increased as the tear size increased, statistical significance was seen after 1/2 tear of subscapularis tear ($p<0.05$). The two repair conditions did not restore to the level of its individual intact ROM with statistical significance ($p<0.05$). Max IR showed a slightly increase with 1/2 subscapularis tear and combined supraspinatus tendon tear, but there were no statistical significance. Total range of motion increased in same pattern with max ER ($p<0.05$). Both repair conditions did not also restore to its previous conditions ($p<0.05$).
.
Path of Humeral Head Apex: The overall humeral head Apex (HHA) shifted posterior, superior, and medial in midrange 30º IR to 30º ER rotation in all abduction angle. At max ER showed maximum shift of the apex in all 3 axis and abduction angles. At max ER the difference became evident after 1/2 tear of subscapularis partial tear, especially in superior-inferior axis in all abduction angle ($p<0.05$). Increase in abduction angle caused humeral head shift less in magnitude. No definite increase in superior-inferior HHA shift occurred even with increase in supraspinatus tear (Fig 2.).

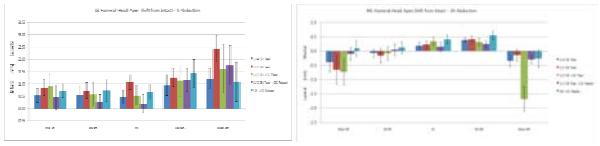

Figure 2.1) Superior-Inferior shift at 0 degree abduction, 2) Medial-Lateral shift at 30 abduction

The effect of added supraspinatus tendon tear had more effect on the medial-lateral shift than any other plane at max ER. (Fig. 2) The repair did not restore the kinematics or the ROM to the intact state.

Discussion
Our study showed that isolated 1/4 and 1/2 tear of subscapularis tendon tear did not change the glenohumeral kinematics, and as expected added supraspinatus tendon tear (anterosuperior tear) shifted the humeral head to maximum displacement in both end point of the rotation. However even with 1/4 tear of subscapularis partial tear showed increased in maximum external rotation. The two different repairs (supraspinatus tendon tear alone or with added subscapularis tendon partial tear) did not restore the GH kinematics or the ROM prior to the level of intact tendon. In addition, there were no significant differences in kinematics and ROM between the complete repair groups versus supraspinatus tendon repair group.

Reference

Klapper & Jobe. AJSM, 1992: 307; 307-310
Ide et al. Arthroscopy, 2008: 24 (7); 749-753
Halder A & Ahn KN. JOR, 2000: 18; 829-834
Kedgley et al. Clin Biomech, 2007: 22; 1068-1073
Su WR & Budoff JE. Arthroscopy, 2009: 25; 282-289

Acknowledgments
VA Rehab R&D and Medical Research
Arthrex® (Naples, FL) for donating the anchors

Biomechanical Comparison of Single-Row, Double-Row, and Transosseous-Equivalent Repair Techniques After Healing in an Animal Rotator Cuff Tear Model

+[1]Quigley R J; [1]Gupta A; [1]Oh J H; [1]Chung K C; [1]McGarry M H; [1]Gupta R; [1,2]Tibone J E; [1]Lee T Q
+[1]Orthopaedic Biomechanics Laboratory, Long Beach VA Healthcare System and University of CA, Irvine, CA
[2]Department of Orthopaedic Surgery, University of Southern California, Los Angeles, CA
tqlee@med.va.gov

INTRODUCTION

Recent studies investigating rotator cuff repairs have shown that the double-row (DR) and transosseous-equivalent (TOE) techniques provides improved contact area and pressure between the rotator cuff tendon and footprint compared to single-row (SR)[1]. However, no study to date has shown a direct correlation between increased contact area and pressure and improved healing. Based on previous studies that demonstrate the unique similarities between the rabbit subscapularis muscle and the human supraspinatus, this study aimed to use an established rabbit subscapularis chronic rotator cuff tear model[2] and biomechanically compare the SR, DR, and TOE techniques after healing. We hypothesized that repair with TOE and DR will show improved biomechanical properties over SR after healing.

METHODS

Twenty one New Zealand White Rabbits were used with seven rabbits in each repair group: SR, DR, or TOE. A two-stage surgical procedure was performed with the rabbits under anesthesia. First, surgical resection of the left subscapularis tendon was performed followed by a 6 week recovery period to allow for muscle atrophy and fatty infiltration seen in chronic rotator cuff tears. Repair was then performed using either the SR, DR, or TOE technique. During both surgical procedures, the contralateral shoulder was exposed and noted to be free of subscapularis pathology. Rabbits were then allowed to recover for 12 weeks to allow for healing, after which they were euthanized. Repaired and control humeri with attached subscapularis were then dissected out, potted, and loaded cyclically from 5 to 50 N for 10 cycles and then loaded to failure at a rate of 10 mm/min using an Instron materials testing machine. Strain on both the superior and inferior part of the tendon was measured using Video Digitizing System and Winanalyze software.

RESULTS

2 rabbits from the SR and TOE groups and 1 from the DR were excluded as the tendons were unrepairable due to tendon retraction. Results are shown as a ratio of the repaired values to its control values. Non-paired t-tests were used to compare groups with significance set at $p<0.05$.

The parameters evaluated were hysteresis, initial stiffness, linear stiffness, displacement, load, and energy absorbed (Figure 1). TOE repair showed a greater biomechanical characteristics than DR which in turn had a better biomechanical characteristics than SR in terms of displacement, yield load, energy absorbed to yield load, and ultimate load ($p<0.05$). TOE and DR were equivalent to each other but greater than SR in terms of energy absorbed to ultimate load. All other parameters were not statistically significant.

Strain was evaluated on both the superior and inferior part of the tendon at the 1st cycle, 10th cycle, yield load, and ultimate load (Figure 2). Tendons that underwent TOE repair demonstrated higher strain in the inferior tendon than SR at both the yield and ultimate load ($p<0.03$). There were no statistically significant differences in strain between repairs in the superior part of tendon.

DISCUSSION

After the creation of a chronic tear followed by repair and healing, the TOE technique demonstrated the strongest biomechanical construct followed by DR with SR being the weakest. These results suggest that the improved biomechanical profile of TOE and DR shown in previous studies does in fact translate to better healing characteristics.

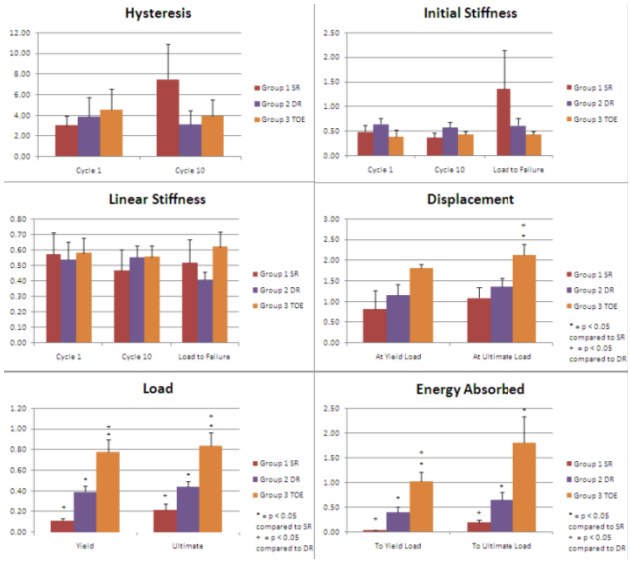

Figure 1: Graphs showing hysteresis, initial stiffness, linear stiffness, displacement, load, and energy absorbed to failure across single-row, double-row and transosseous-equivalent repairs.

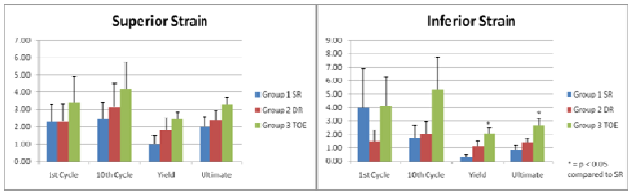

Figure 2: Graphs showing superior and inferior strain across single-row, double-row and transosseous equivalent repairs.

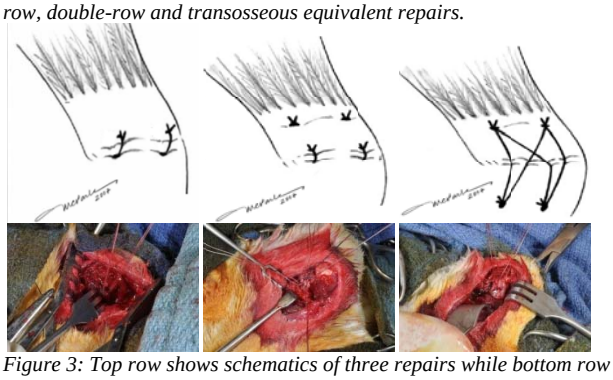

Figure 3: Top row shows schematics of three repairs while bottom row shows surgical images of the repairs. From left to right, single row, double row, and transosseous equivalent repair (photo shown before anchoring of lateral row of TOE).

REFERENCES

1) Park MC, et al., *2007*, 16(4):461-8.
2) Grumet RC, et al. *Acta Orthopaedica*, *2009*,80(1),97 -103.

ACKNOWLEDGEMENTS

VA Rehab R&D and Medical Research
DePuy Mitek (Raynham, MA)

Biomechanical Effects of Latissimus Dorsi Tendon Transfer in Irreparable Massive Rotator Cuff Tear

A human cadaveric study using anatomy based muscle loading testing apparatus

Joo Han Oh[*†], MD, PhD, Michelle H. McGarry[†], MS, Justin Tilan[†], MS,
Yu-Jen Chen[†], PhD, Kyung Chil Chung[†], MD, PhD, Thay Q. Lee[†], PhD
[†]*Orthopaedic Biomechanics Laboratory[†], VA Healthcare System and UC Irvine, Long Beach, CA*
**Department of Orthopedic Surgery, Seoul National University College of Medicine, Korea*

INTRODUCTION: The treatment of massive rotator cuff tear (RCT) remains a challenge, and latissimus dorsi tendon transfer (LDT), introduced by Gerber et al in 1988, is one of the surgical options available for irreparable massive RCT. While several authors reported favorable outcomes of this salvage procedure, clinical outcomes as a whole remain unpredictable and vary among patients. To date, there have been few biomechanical studies regarding LDT; therefore, the purpose of this study was to determine the biomechanical effects of LDT in a cadaveric model of massive irreparable posterosuperior RCT.

METHODS: Eight cadaveric shoulders were used with a custom testing system (Figure 1). Irreparable RCT was created by resection of the entire supraspinatus (SSP) and infraspinatus (ISP) tendons. LDT was performed as described by Gerber et al (Clin Orthop Relat Res. 1988;232:51-61). The amount of muscle loading was determined based on the physiological muscle cross-sectional area ratios (SSP 10N; subscapularis, ISP/teres minor, pectoralis major, latissimus dorsi (LAT) 24N each; deltoid 48N). An increased load condition for the LAT (LDT2X, 48N) was incorporated to simulate increased muscle tension after LDT due to limited excursion of the LAT. All procedures were performed for the intact cuff, RCT, LDT, and LDT2X conditions in the scapular plane with 0, 30, and 60° shoulder abduction. Resting position of the humeral head (the amount of humeral rotation due to muscle loading) followed by maximum internal (MaxIR) and external rotation (MaxER) with 2.3 Nm of torque were measured. The position of humeral head apex (HHA) with respect to the glenoid was calculated using a MicroScribe 3DLX from MaxIR to MaxER in 30º increments. Contact area, force, pressure and peak pressure were measured using Tek·Scan Pressure Measurement System.

RESULTS: The humeral rotation due to muscle loading was 7º internally for the intact cuff, and 40º internally for the RCT group; this increased internal rotation due to muscle loading with massive tear was corrected following LDT. MaxIR and total range of motion (ROM) significantly increased following RCT. LDT and LDT2X significantly decreased Max IR and total ROM compared to RCT at every abduction angle (all $p<0.05$). LDT/LDT2X significantly decreased MaxIR and total ROM in 30º and 60º abduction when compared to intact ($p<0.05$), and LDT2X showed a significant decrease in both when compared to LDT ($p<0.05$). At MaxIR, HHA shifted supero-laterally at every abduction angle in the RCT condition compared to intact, and LDT/LDT2X significantly reversed these displacements ($p<0.05$). However, LDT2X over-compensated the correction in HHA kinematics and resulted in significant infero-medial displacement at MaxIR compared to intact cuff, especially at 30º and 60º abduction ($p<0.05$)**.** Contact area decreased following RCT, but was restored by LDT/LDT2X, especially in 0º and 30º abduction. LDT/LDT2X showed increased contact pressure and peak pressure during the mid-range of rotation, especially in 60º abduction.

DISCUSSION: The findings from this study suggest that the LDT can be beneficial as it reverses the abnormal biomechanics resulting from massive RCT, restore the rotational balance of the humeral head, rotational range of motion, and HHA kinematics and contact characteristics. However, the increased muscle tension due to the possibility of limiting muscle excursion after LDT, especially at higher abduction angles can lead to an overcompensation that may further deteriorate normal kinematics of the shoulder, limit Max IR, cause abnormal displacement of the HHA, and increase GH joint pressure. Therefore, the clinical assessment of LAT tendon length is critical for a successful LDT.

ACKNOWLEDGEMENTS
VA Rehab R&D and Medical Research
California Orthopaedic Research Institute

REFERENCES: 1. Gerber C et al. Clin Orthop Relat Res, 232:51-61, 1988. 2 Iannotti JP et al. J Bone Joint Surg Am. 88:342-8, 2006. 3. Warner JJ et al. J Shoulder Elbow Surg. 10:514-21, 2001.

CALCIUM PHOSPHATE-HYBRIDIZED TENDON GRAFT TO REDUCE KNEE LAXITY AND BONE TUNNEL ENLARGEMENT 1 YEAR AFTER ACL RECONSTRUCTION

Masataka Sakane[1], Hirotaka Mutsuzaki[2], Akihiro Kanamori[1], Kotaro Ikeda[3] and Naoyuki Ochiai[1]

[1] Department of Orthopaedic Surgery, Institute of Clinical Medicine, Graduate School of Comprehensive Human Sciences, University of Tsukuba, Tsukuba, Japan

[2] Department of Orthopaedic Surgery, Ibaraki Prefectural University of Health Sciences, Ami, Japan

[3] Department of Orthopaedic Surgery, Ichihara hospital, Tsukuba, Japan

INTRODUCTION

A calcium phosphate (CaP)-hybridized tendon graft using an alternate soaking process during anterior cruciate ligament (ACL) reconstruction improved tendon-bone attachment in the early postoperative period in animal studies (1-3). After approval of ethical committee, we performed a randomized clinical study using the CaP-hybridized method with conventional graft preparation for primary ACL reconstruction. The purpose of this study was to clarify the effect of the CaP-hybridized tendon graft 1 year after human ACL reconstruction.

MATERIALS AND METHODS

Patients selected at random were performed primary ACL reconstruction using a single-bundle hamstring autograft with/without CaP hybridization preparation (CaP group: n = 20, untreated group: n = 20). We analyzed anterior-posterior (A-P) knee laxity using a KT1000 knee arthrometer (side to side difference) before and one-year after ACL reconstruction. Bone tunnel enlargement ratio in tibia and femur were determined using computed tomography in both groups. Student' T test was utilized for statistical analysis.

RESULTS

Average knee laxity in the CaP group (0.3 ± 1.6 mm) was significantly smaller than in the untreated group (2.0 ± 1.3 mm) ($p = 0.0003$). Bone tunnel enlargement ratio (anterior-posterior direction) using the CaP-hybridized tendon graft (15.8 ± 12.9%) was smaller than that of untreated group (27.9 ± 17.3%) in the femoral side ($p = 0.0087$). There was no significant difference in tibial tunnel enlargement rate in both groups.

DISCUSSION

Acceptable clinical results were obtained at 1 year in both groups. However, using the CaP hybridized tendon graft, the A-P knee laxity was reduced and femoral bone-tunnel enlargement was smaller compared with conventional technique. Relationship among tunnel enlargement, knee laxity, and clinical results are still controversial. We believe that increasing bone tunnel enlargement gives negative impact to long-term clinical success. The CaP hybridized tendon graft can lead to promote relatively early and firm bone-graft anchoring to reduce knee laxity associated with bone tunnel enlargement, especially in the femoral side.

REFERENCES

(1) Mutsuzaki H, Sakane M, et al. J Biomed Mater Res A 2004;70A:319-327.

(2) Mutsuzaki H, Sakane M, et al. Biomaterials 2005;26:1027-1034.

(3) Mutsuzaki H, Sakane M, et al. Biomed Mater 2009;4:045013.

Differences in the Proteome of the Male and Female Anterior Cruciate Ligament

D. Little[1], J.W. Thompson[3], L.G. Dubois[3], D.S. Ruch[1] and F. Guilak[1,2]
[1]Department of Orthopaedic Surgery, [2]Department of Biomedical Engineering,
[3]Duke Institute for Genome Sciences and Policy, Duke University Medical Center, Durham, NC.

INTRODUCTION

The incidence of anterior cruciate ligament (ACL) injury is greater among female athletes than males, and a number of sex-dependent risk factors have been identified.[1-3] The female ACL has lower collagen fibril area fraction and large fibril diameters compared to male, and failure load and failure stress are correlated to collagen fibril area fraction.[4] A variant of COL5A1 has been associated with an increased risk of ACL injury in female, but not male athletes.[5] However there has been no comprehensive analysis of the composition of male and female ACL to determine if underlying differences may suggest other reasons for the differences in injury rate. The objective of this study was to quantitate the proteome of the human ACL for differences between the male and female ACL.

METHODS

The entire anterior cruciate ligament was harvested from 3 male and 3 female cadavers with no history of knee injury or disease (male ages 68-69, female ages 53-63). Each sample was rinsed in 50mM ammonium bicarbonate, minced, lyophilized and pulverized in liquid nitrogen. For each sample, approximately 250mg of tissue was washed at elevated temperature with 0.25% Rapigest, then digested in-situ with 0.25% Rapigest/Trypsin overnight at 37^{o}C. Protein concentration was normalized across the 6 samples using a BCA assay. Yeast alcohol dehydrogenase digest was spiked in at a concentration of 25fmol/μg as an internal standard. Approximately 3 μg of ACL digest from each sample was subjected to LC/LC-MS/MS, using a reversed-phase first dimension fractionation into 8 fractions at pH 10, followed by 60 minute pH 2 reversed-phase separation with direct analysis on a Synapt HDMS system. Label-free quantitative analysis was performed in Rosetta Elucidator v3.3, with protein identifications generated from database searching with Mascot v2.2 and PLGS v2.4 RC7. Aggregate peptide annotation after database searching was performed using the PeptideProphet algorithm, at a false discovery rate of 1%. Statistically significant proteomic changes between male and female samples where determined using a Students T-test (α=0.05). Power analysis based on data sets with similar inter-group coefficient of variation estimates that n=3/group can reliably detect a 1.5-fold difference. The Database for Annotation, Visualization and Integrated Discovery 6.7 (NIAID, NIH) was used for functional annotation of protein lists with gene ontology and function.[6]

RESULTS

All data was aligned based on accurate mass and retention time in Elucidator, which allowed for quantitation of 261 proteins, with 1933 peptides, across the set of male and female ACL samples. A number of previously reported and novel extracellular matrix constituents of ACL, or of tendon and ligament in general, were identified. Of the 261 proteins, 127 proteins are associated with the extracellular region, 124 proteins with signaling function, 120 are glycoproteins, 27 proteins are implicated in extracellular matrix organization, 22 proteins are associated with glycosaminoglycan binding and 18 proteins contain epidermal growth factor-like domains. Quantitation of the proteome identified proteins that were enriched in either male or female ACL. In female ACL, 7 proteins were enriched at least 1.5-fold compared to male ($p \leq 0.05$). Of these, 3 proteins from the extracellular region were enriched including epidermal growth factor (4.5-fold enriched), matrix metalloproteinase-3 (1.8-fold enriched), and alpha-3 defensin (3.0-fold enriched). In male ACL, 33 proteins were enriched at least 1.5-fold compared to female ($p \leq 0.05$). Of these, 21 proteins were enriched from the extracellular region, including tenascin X (1.8-fold enriched), tenascin C (2.4-fold enriched), thrombospondin-4 (1.7-fold enriched), proteoglycan 4 (2.2-fold enriched) and myocilin (5.1-fold enriched). Of the collagen superfamily, type XII (1.7-fold), XIV (2.0-fold) and XXVII (2.7-fold) were the only members enriched in male compared to female ACL.

DISCUSSION

These data demonstrate that the composition of the ACL is more complex than can be identified by traditional biochemical, histological and gene expression techniques alone. These compositional differences are potentially related to important structural, and presumably functional, differences between male and female ACL that warrant further investigation to determine their role in injury mechanism.

ACKNOWLEDGMENTS

Supported by an unrestricted fellowship grant from Synthes (DL, DSR), NIH grants AR48852, AG15768, AR50245 (FG) and Duke University's CTSA grant UL1 RR024128-01 (JWT, LGD, DL).

REFERENCES: 1. Waldén et al. Knee Surg Sports Traumatol Arthrosc 2010. **2.** Elliot et al. Sports Med 2010. **3.** Brophy et al. Sports Med Arthrosc 2010. **4.** Hashemi et al. J Orthop Res 2008. **5.** Posthumus et al. Am J Sports Med 2009. **6.** Huang et al. Nature Protocols 2009.

A NEW HYPOTHESIS FOR ACL INJURY MECHANISMS BASED ON VIDEO ANALYSIS USING MODEL-BASED IMAGE-MATCHING TECHNIQUE

[1, 2]Koga, H; [1]Bahr, R; [1]Myklebust, G; [1]Engebretsen, L; [2]Muneta, T; [2]Sekiya, I; [1]Krosshaug, T
[1]Oslo Sports Trauma Research Center, Oslo, Norway, [2]Tokyo Medical and Dental University, Tokyo, Japan

INTRODUCTION

The mechanism for non-contact ACL injury is a matter of controversy and several theories have been proposed. A precise description of the injury mechanism is critical to be able to target intervention programs to prevent ACL injuries. Video analysis of injury tapes is the only method available to extract biomechanical information on the mechanism. The objective of this study was to describe knee joint kinematics in actual ACL injury situations using a model-based image-matching technique (MBIM) we have developed.

METHODS

Eleven video sequences with at least two views of ACL injuries from women's handball (n=7), basketball (n=3) and men's soccer (n=1) were analyzed using MBIM based on the animation program Poser. Computer models of the background were modeled and matched to the video image. A skeleton model with 57 degrees of freedom was adapted individually to each of the injured players and matched frame by frame, providing an estimate of the time course of knee joint kinematics (rotational degrees) and ground reaction forces for the injury sequence. In addition, in the soccer case where the videos were taken by high-definition, high-speed cameras, translational degrees of knee joint kinematics were also analyzed.

RESULTS

Mean knee flexion angle was 23° (range, 11 to 30) at initial contact (IC) and had increased by 24° (95% CI, 19 to 29, $p<0.001$) 40 ms later. Valgus angle was neutral, 0° (range, -2 to 3) at IC, but had increased by 12° (95% CI, 10 to 13, $p<0.001$) 40 ms later. The knee was externally rotated 5° (range, -5 to 12) at IC, but abruptly rotated internally by 8° (95% CI, 2 to 14, $p=0.017$) during the first 40 ms. From 40 ms to 300 ms after IC, however, we observed an external rotation of 17° (95% CI, 13 to 22, $p<0.001$) (Fig. 1). In the soccer case, anterior tibial translation (ATT) started at 20 ms after IC, and by 40 ms, 13 mm of ATT had occurred. The ATT plateaued by 150 ms, and then shifted back to a reduced position between 200 ms and 240 ms after IC. Peak vertical ground reaction force was 3.2 times body weight (95% CI, 2.7 to 3.7), and occurred at 40 ms (range, 0 to 83) after IC.

DISCUSSION

Based on when the sudden changes in joint angular motion and the peak vertical ground reaction force occurred, we assumed that the ACL injury occurred about 40 ms after IC. Knee kinematics was remarkably consistent. Valgus loading seems to be an important factor, because all players had immediate valgus motion within 40 ms after IC. Moreover, the knee rotated internally during the first 40 ms, and then an external rotation was observed, which seemed to have occurred after the ACL was torn. ATT reached 13 mm at 40 ms after IC, which is beyond the maximum ATT in intact knees. Based on these results together with previous studies, we proposed a new hypothesis for ACL injury mechanisms that valgus loading and lateral compression generate internal rotatory motion and anterior translation of tibia, due to the joint geometry, resulting in ACL rupture (Fig. 2).

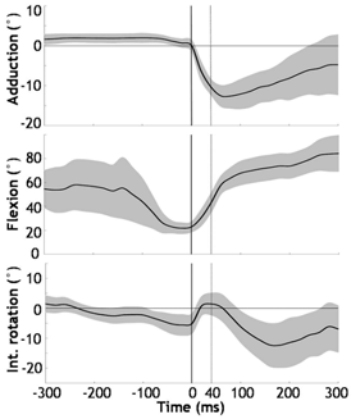

Fig.1 Knee joint kinematics.

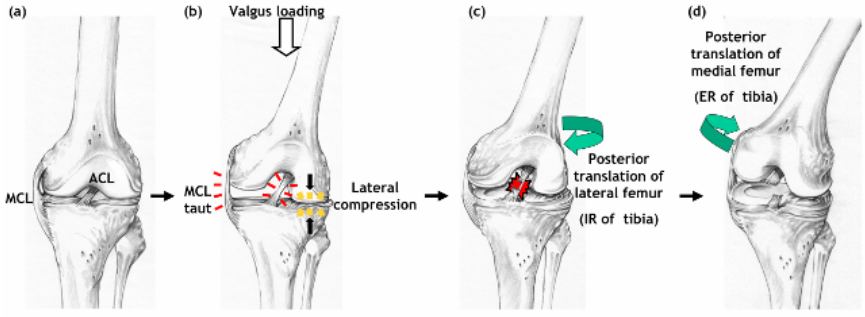

Fig.2 Our hypothesis for non-contact ACL injury mechanism.

ACKNOWLEDGEMENTS

The Oslo Sports Trauma Research Center has been established at the Norwegian School of Sport Sciences through grants from the Royal Norwegian Ministry of Culture, the South-Eastern Norway Regional Health Authority, the International Olympic Committee, the Norwegian Olympic Committee and Confederation of Sport, and Norsk Tipping AS.

REFERENCES: 1. Krosshaug et al. J Biomech 2005. 2. Krosshaug et al. Scand J Med Sci Sports 2007.

TUNNEL PLACEMENT IN FAILED ANTERIOR CRUCIATE LIGAMENT RECONSTRUCTION: AN IMAGING ANALYSIS

P. Lodhia[a, b], A. Hosseini[a], S.K. Van de Velde[a], A.L. Williams[a], P.D. Asnis[a], B. Zarins[a], T.J. Gill[a] and G. Li[a]
[a] Orthopaedic Bioengineering Lab, Massachusetts General Hospital, Boston, Massachusetts, USA
[b] University of British Columbia, Vancouver, British Columbia, Canada

INTRODUCTION

ACL reconstruction is one of the most common procedures performed in orthopedics. Clinical failure rate has been reported between 3.6% and 15%. At the time of revision ACL reconstruction, 22% to 79% of failures are thought to be due to technical errors, with the most common error being incorrect tunnel positions.

The purpose of this study was to retrospectively evaluate the femoral and tibial tunnel positions, and the intraarticular graft orientation of the primary ACL reconstruction in patients who had undergone revision ACL reconstruction. We hypothesized that this patient cohort had a nonanatomical tunnel position and graft orientation.

METHODS

Twenty six patients (seventeen male and nine female, with a mean age of 31.8 ± 9.5 years; range, 16.2 to 51.9 years) who had undergone a revision ACL reconstruction and had magnetic resonance imaging (MRI) scans of their injured knee after primary but before revision ACL reconstruction were included in this study. We excluded patients with more than one revision ACL reconstruction, multiligament deficient knees, or a mechanical malalignment in addition to ACL deficiency. The clinical magnetic resonance (MR) images prior to revision but after primary ACL reconstruction were analyzed. MRI-based three-dimensional (3D) models were created along with an anatomic coordinate system. The bone tunnels on the femur and tibia were outlined and cylinders were fit through their contours. Based on these cylinders, the intraarticular graft orientation was measured as angles in axial, sagittal, and coronal planes. The graft positions were measured on the tibial plateau as a percentage from anterior to posterior and medial to lateral; the graft positions on the femur were measured using the quadrant method, relative to the femoral notch. [1, 2]

RESULTS

The mean axial, sagittal, and coronal angles were 37.3° ± 21.0°, 69.6° ± 13.4°, and 75.9° ± 7.5°, respectively. These angles were significantly different when compared to previously published native anteromedial and posterolateral ACL bundle angles by our group.[2] The mean tibial tunnel position was 47.3% ± 8.5% in the anterior-to-posterior direction and 46.6% ± 3.7% in the medial-to-lateral direction. The mean femoral tunnel position was 41.8% ± 9.8% measured from the posterior edge of the medial wall of the lateral femoral condyle parallel to Blumensaat line, and 12.5% ± 18.2% measured perpendicular to the Blumensaat line. (**Fig. 1**)

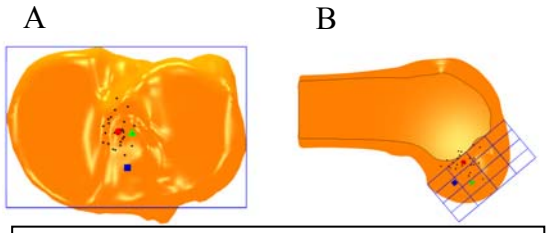

Fig. 1 Graft position on the left knee. **A**. Axial view of the tibial plateau with anterior to the bottom and medial to the left of the figure. **B**. Sagittal view of the medial aspect of the lateral femoral condyle with anterior to the top and proximal to the left of the figure. Black circles, individual failed ACL graft positions; red circle, mean failed ACL graft position; blue square, native anteromedial bundle position; green triangle, native posteromedial bundle position

DISCUSSION

The results of this study indicated that both the intraarticular graft orientation and tunnel position of this patient group with failed ACL reconstruction were nonanatomic, when compared to native ACL values from previous studies.[1, 2]

REFERENCES

1. Forsythe B, Kopf S, Wong AK, et al. The location of femoral and tibial tunnels in anatomic double-bundle anterior cruciate ligament reconstruction analyzed by three-dimensional computed tomography models. *J Bone Joint Surg Am.* 2010;92(6):1418-1426.

2. Jordan SS, DeFrate LE, Nha KW, Papannagari R, Gill TJ, Li G. The in vivo kinematics of the anteromedial and posterolateral bundles of the anterior cruciate ligament during weightbearing knee flexion. *Am J Sports Med.* 2007;35(4):547-554.

EFFECT OF GRAFT TENSIONING ON MECHANICAL RESTORATION IN A RAT MODEL OF ANTERIOR CRUCIATE LIGAMENT RECONSTRUCTION USING FREE TENDON GRAFT

Fu SC[1,2], Cheng WH[1,2], Cheuk YC[1,2], Mok TY[1,2], Yung SH[1,2], Rolf CG[3], Chan KM[1,2]
[1]The Chinese University of Hong Kong, Hong Kong SAR, China, [2]The Hong Kong Jockey Club Sports Medicine and Health Sciences Centre, Hong Kong SAR, China, [3]Department of Orthopaedic Surgery, Huddinge University Hospital, CLINTEC, Karolinska Institutet, Stockholm, Sweden

INTRODUCTION:

An optimal graft tensioning during fixation in Anterior Cruciate Ligament Reconstruction (ACLR) surgery is always of primary interest for orthopaedic surgeons, but there is disagreement on the effects of initial graft tension on the graft healing. Only a few animal studies (goat, dog, rabbit) investigated effects of graft tensioning, some detected improvements in healing outcomes with a higher initial tensioning but others didn't. All these studies mainly used bone-patellar tendon-bone (BPTB) grafts, while the information for free tendon graft are only available in an ex vivo study. In the present study, we established a rat model of ACLR using flexor tendon graft and evaluated the effect of initial graft tensioning on the healing outcomes.

MATERIALS AND METHODS:

Thirty-six Sprague-Dawley rats (male, 12 weeks old, 250-300g) were used. Under general anaesthesia, the rat was operated unilaterally on the right knee. The flexor digitorum longus tendon graft (20mm in length and 1mm in diameter) was harvested from a longitudinal medial incision. The intact ACL was excised and the successful transecton was confirmed by a positive Lachman test. Tibial and femoral tunnels, both with 1.2 mm diameter and 6 mm in length, were created from the footprint of the original ACL to the medial side of tibia and the lateral femoral condyle respectively. The graft was then inserted and routed through the bone tunnels, with a graft tensioning of either 2 or 4N tensioning during fixation. At 0, 2, 6 weeks post operation (n=6), the animals were euthanized to harvest knee specimens for static knee laxity test and graft pullout test (n=4). The remaining samples in each groups were processed for histological examination with H&E staining (n=2).

RESULTS:

Both 2N and 4N graft tensioning restored knee laxity to a similar level immediately after operation (week 0). 2N tensioning exhibited significant increase in knee laxity at week 2, then restored to the week 0 level at week 6; while 4N tensioning maintained the knee laxity at week 2 and dropped at week 6. At both week 2 and week 6, the knee laxity with 4N tensioning was significantly lower than that with 2N tensioning. 4N tensioning also led to a higher graft pullout force and graft stiffness as compared to 2N tensioning at week 2 post operation, but no significant difference was detected at week 6. Histological examination showed a better graft healing in samples with 4 N tensioning.

DISCUSSION AND CONCLUSION:

Our study suggests that higher initial graft tensioning will benefit graft healing in ACLR using free tendon graft. Higher initial graft tensioning prevented the increase in knee laxity and improved graft healing during early healing stage. At longer healing time points, higher initial graft tensioning further improved restoration of knee laxity, but its effect on graft healing became insignificant as revealed by pullout force. The beneficial effect of initial graft tensioning may reside on the preservation of graft integrity at early healing stage.

MECHANICAL AUGMENTATION USING SUTURES TO STIMULATE HEALING OF THE ACL IN THE GOAT MODEL

M.B. Fisher, K.E. Kim, H-J. Jung, P.J. McMahon, and S.L-Y. Woo
Musculoskeletal Research Center, Department of Bioengineering,
Swanson School of Engineering, University of Pittsburgh, Pittsburgh, PA

INTRODUCTION: In our research center, we have been pursuing functional tissue engineering (FTE) approaches including the use of extracellular matrix (ECM) bioscaffolds to improve the healing of injured ligaments and tendons [1-3]. Recently, we have used ECMs to treat a fully transected ACL in combination with suture repair in the goat model and have found that by 12 weeks, such biological augmentation led to an abundant amount of neo-tissue formation, with improved biomechanical properties of the healing femur-ACL-tibia complex (FATC) [3]. We have also found that the neo-tissue is weak during the early phase of healing, and additional mechanical augmentation to maintain initial joint stability may be needed [4, 5]. We hypothesize that mechanical augmentation using sutures could help to stabilize the joint, and thus, reduce excessive tension in the healing ACL and disruption of the healing process in order to allow neo-tissue to form and remodel. As a result, the biomechanical properties of the FATC would also be improved. Thus, the objective of this research was to examine the amount of positive impact of mechanical augmentation on ACL healing and to compare the results to those with biological augmentation.

METHODS: In five skeletally mature female goats, the ACL of the right stifle joint was transected and suture repaired [4]. Two additional sutures were passed from the femur to the tibia and fixed under tension (suture augmentation group). The left stifle joints served as a sham-operated control. After 12 weeks, the joint kinematics in response to a 67 N anterior-posterior (A-P) tibial load were measured using a robotic/universal force-moment sensor testing system [3]. After measuring the cross-sectional area (CSA) of the ACL, the FATCs were subjected to uniaxial tensile testing to obtain the stiffness and ultimate load. These data were compared to those previously obtained for ACL healing following ECM-treatment (n=7) at 12 weeks [3]. Data for the experimental groups were compared using an unpaired t-test. A paired t-test was used to compare the experimental groups to their respective sham-operated controls. Significance was set at $p<0.05$.

RESULTS: Preliminary results suggested that the amount of A-P tibial translation was similar between experimental groups ($p>0.05$). However, values for both groups were still 2-3 times higher than those for the sham-operated ACL ($p<0.05$). Gross observation of the healing ACL revealed that the suture augmentation group had continuous neo-tissue formation in all specimens, which was similar to the ECM-treated group. Quantitatively, statistical analyses of the CSA of the ACL could not detect significant differences between both experimental groups and their respective sham-operated controls ($p>0.05$) or between the experimental groups ($p>0.05$) (Fig. 1A). In terms of stiffness of the FATC, the suture augmentation and ECM-treatment groups also had comparable values (53±19 N/mm vs. 52±21 N/mm, respectively, $p>0.05$). When normalized by their respective sham-operated controls, their values reached 38±16% and 48±19%, respectively ($p>0.05$, Fig. 1B). The results on the ultimate load were also similar between the two groups (249±129 N and 209±122 N, respectively, $p>0.05$).

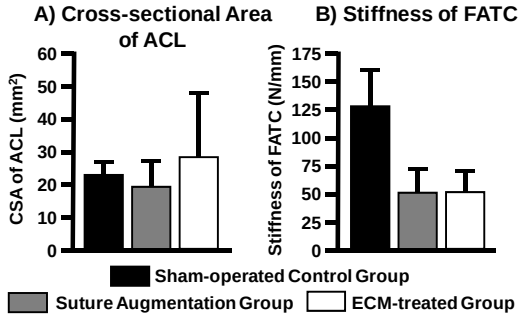

Figure 1. A) Cross-sectional area of the healing ACL and B) stiffness of the healing FATC (*$p<0.05$).

DISCUSSION: This report shows the potential of mechanical augmentation can indeed enhance ACL healing with sufficient tissue formation, in support of our hypothesis. The CSA of the healing ACL and the structural properties of the FATC compared well with those following biological augmentation (ECM-treatment). These biomechanical data were also consistent with those published in the literature for other FTE approaches used for ACL healing [6, 7]. The amount of A-P joint stability was still not near normal but the values were similar to those following ACL reconstruction at 12 weeks in the goat model – a well known limitation of animal models in part due to a lack of appropriate post-operative rehabilitation [8]. Nevertheless, we are encouraged by the current results and are taking the next step; that is, to examine the synergistic effects of using mechanical augmentation to stabilize the stifle joint and biological augmentation with ECM bioscaffolds to accelerate healing of the ACL to improve long-term outcome.

ACKNOWLEDGEMENTS: Financial support from Commonwealth of Pennsylvania and NSF Engineering Research Center Grant (#0812348). **REFERENCES:** 1. Liang, et al. JOR 2006; 24(4):811-9. 2. Karaoglu, et al. JOR 2008; 26(2):255-263. 3. Fisher, et al. ASME SBC. 2010. 4. Fisher, et al. ORS. 2010. 5. Fisher, et al. JOR 2010; 28(10):1373-9. 6. Joshi, et al. AJSM 2009; 37(12):2401-10. 7. Murray, et al. Arthroscopy 2010; 26(9 Suppl):S49-57. 8. Ng, et al. JOR 1995; 13(4):602-8.

NON-LINEAR MECHANICS OF TISSUE ENGINEERED LIGAMENT, ANTERIOR CRUCIATE LIGAMENT AND PATELLAR TENDON

Ma, J; Smietana, MJ; Wojtys, EM; Larkin, LM; Arruda, EM

University of Michigan, Ann Arbor, MI

INTRODUCTION: Anterior Cruciate Ligament (ACL) is the most commonly injured knee ligament and the leading cause of high school athletic injury. Due to the poor self healing ability of ACL, repair is required when it is ruptured. Tendon auto- and allo-grafts are common graft choices for ACL repair (about 300,000 repairs per year). Recent research has shown the patellar tendon (PT) has stiffer mechanical properties compared to those of the patient-matched ACL. The viscoelastic responses of these tissues are important when the tissue experiences a high strain rate or impact condition. Here we demonstrate the viscoelastic properties of ACL and PT are different. These unmatched biomechanics are believed an important reason limiting success of current ACL repairs. Our lab has tissue engineered 3-D scaffold-less bone-ligament-bone constructs (BLB) from bone marrow stromal cells and used them as allogenic grafts for ACL repairs in ovine model. The BLB is designed to have a compliant intra-articular region that accommodates knee motion, and stiffer bone ends that integrate well with native bone and rapidly remodel *in vivo*. The BLBs are explanted following 6 and 9 months of in vivo recovery. We have characterized the nonlinear mechanics of our tissue engineered BLBs, native ACL and PT from load-unload tensile tests and stress relaxation experiments and present the stiffnesses and viscoelastic responses of the three types of tissues.

METHODS: Engineered BLB constructs were fabricated as previously described [1]. After about 1 week of construct formation, the constructs were used in arthroscopic ACL repair in sheep. Following 6 and 9 months of in vivo recovery, BLBs, contralateral (CL) ACLs and patient-matched PT specimens were dissected for analysis. Uniaxial tension tests and stress relaxation experiments were conducted to obtain the tensile stiffness and viscoelastic properties of the in vivo BLB, CL ACL and patient-matched PT specimens using an MTS 810 servo hydraulic test system with a 25 kN load cell and a Dynamic Mechanics Analyzer with a 35 N load cell. ImageJ and Metamorph softwares were used for accurate strain determination via digital image correlation analysis.

RESULTS: Following 6 months in vivo recovery, the BLB explants have attained 52% of the tangent stiffness and 95% of the geometric stiffness of those of CL ACLs. As shown in **Figure 1**, stress relaxation response of PT (C) includes an initial rapid stress drop whereas the ACL (A) has a gradual stress drop. As the strain control increases, PT tends to relax faster whereas the ACL tends to relax slower. The stress relaxation result from the 6 months BLB explants (B) shows response that is virtually indistinguishable from that of the CL ACLs. The biomechanical testings of BLB explants at 9 months are ongoing and will also be discussed.

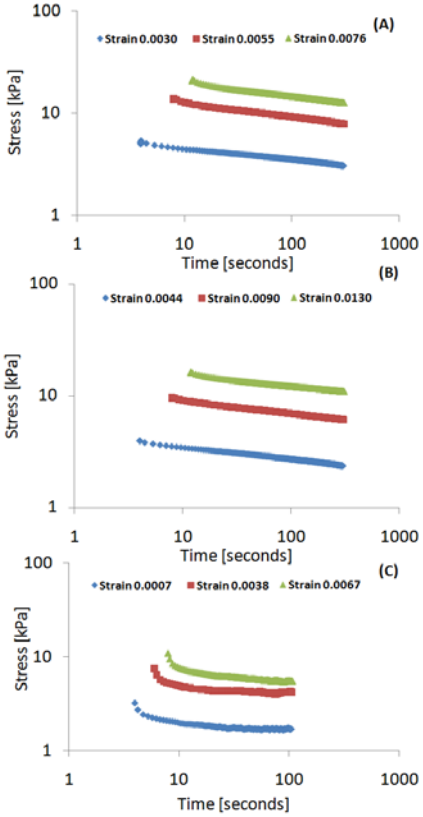

Figure 1. Comparison of viscoelastic behaviors of native ACL (A), patient-matched BLB explant (B) and PT (C).

DISCUSSION: Current PT grafts for ACL repair exceed the native ligament stiffness and strength. Our results have shown that an engineered ligament that is compliant upon implantation attains physiological stiffnesses and viscoelastic characteristics of native ACL after 6 month as an ACL repair. Native ACL has a characteristic viscoelastic relaxation response that is not shared by patellar tendon (PT) grafts; our multi-phasic BLB constructs did exhibit qualitatively and quantitatively similar stress relaxation responses to those of native ACL. These results indicate that the PT is not an ideal biomechanical replacement for the ACL, not only because it is too stiff, but also because its time dependent properties are very different at the time of implantation from those of native ACL.

REFERENCES: 1. Ma J, Goble K, Smietana MJ, Kostrominova T, Larkin LM and Arruda EM, "Morphological and Functional Characteristics of Three-Dimensional Engineered Bone-Ligament-Bone Constructs Following Implantation," *J Biomech Eng*, **131**(10): 101017-1 101017-9, 2009**.**

Effect of ACL Reconstruction on Primary and Secondary Restraints in the Porcine Knee for 6-DOF Motions

D.V. Boguszewski[1], J. T. Shearn[1], C. T. Wagner[2], D.L. Butler[1]
[1] Biomedical Engineering, University of Cincinnati, Cincinnati, OH and [2] LifeCell Corporation, Branchburg, NJ

INTRODUCTION. ACL reconstruction (ACL-R) attempts to restore normal knee kinematics. While bone-patellar tendon-bone (BPTB) grafts are successful and remain a gold standard, early onset OA still occurs [1]. Restoring normal function in all 6-DOF is vital to success. A previous study showed that ACL-R using a decellularized porcine regenerative tissue matrix (RTM) and RTM wrapped around a polymer core (Hybrid) both performed better than BPTB when looking at restoration of initial and cyclic fatigue intact knee force, with the Hybrid graft best matching normal [2,3]. In this study, we examine how each of these materials affects the primary and secondary soft tissue knee restraints. **METHODS.** Seventeen porcine knees were dissected free of all tissues except the four major knee ligaments, the menisci, and the joint capsule. The tibia was secured in a fixture to a 6-axis load cell on a 6-DOF Robot (KR210; KUKA), aligning the anatomical joint axes with the robot axes. ACL-R was performed using BPTB (n=5), RTM (n=5), and Hybrid (n=4). Tunnels were drilled within the tibial and femoral ACL footprint, and grafts tensioned to 88N at 60.5° flexion with the tibia translated 2mm posteriorly [2,3]. Intact (n=3) and ACL-R knees were cycled 2000 times using a modified 6-DOF ovine gait path [4] at 4mm of superimposed anterior tibial translation [5]. Selective cutting was performed in random order (MCL, LCL, PCL, medial meniscus, lateral meniscus, medial capsule, lateral capsule) with the motion path repeated for 10 cycles after each structure was removed (the ACL was always removed last). Changes in forces and moments represented the contribution of that structure to the overall intact knee force**. RESULTS. Stance Phase:** All contributions are listed in Table 1. The intact ACL is a primary restraint in 5 of the 6 DOF. The PCL, LCL, and MCL provide secondary contributions. All three ACL-R grafts performed similarly, matching the contribution of the intact ACL to the overall knee force in A-P, I-E, F-E, and Ab-Ad. However, each over constrained the joint in M-L and C-D, contributing over 80% of the intact knee force compared to 40% for the intact ACL. Relying almost exclusively on the graft, some structural contributions were altered after ACL-R (Fig. 1). **Swing Phase:** The intact ACL is a primary restraint in A-P, C-D, and F-E. The lateral meniscus and MCL are primary restraints in the remaining DOF, with secondary contributions from the ACL and PCL. The three ACL-R grafts alter the force distribution in A-P, C-D, F-E and Ab-Ad, showing a 50% or greater reduction in peak force and moment. ACL-R causes a shift of the primary restraint to the MCL, with the graft as a secondary contributor (Fig. 1). Overall the MCL is the primary restraint for 5 of the 6 DOF in the ACL-R knees, contrary to the intact ACL. **DISCUSSION.** ACL reconstruction, while restoring A-P force in stance, fails to replicate intact force in all 6-DOF and alters the load sharing between soft tissue structures. This altered load sharing could lead to altered joint kinematics and potentially cause the early onset of OA [1]. This study reveals the value of imposing a 6-DOF motion to study the functionality of different ACL reconstructions and their ability to restore normal force and moment restraints. Ultimately, this model will support the development of methods and materials to better restore knee function after ACL reconstruction.

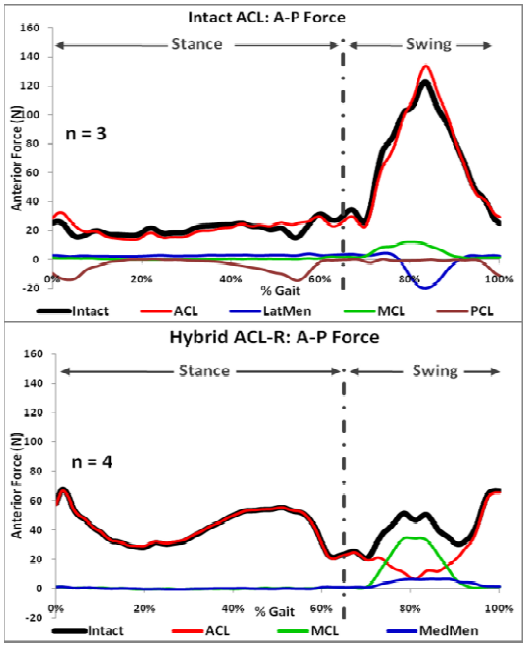

Fig. 1. A-P contributions (Intact ACL and Hybrid ACL-R)

Table 1. Primary (Secondary) restraints during stance and swing phase for the Intact ACL and 3 ACL-R grafts.

Stance Phase: Primary (Secondary) Restraints												
	Anterior	Posterior	Medial	Lateral	Compression	Distraction	Internal	External	Flexion	Extension	Adduction	Abduction
Intact	ACL	PCL	ACL,PCL	LCL	ACL,PCL (LCL,MCL)	-	-	-	ACL	PCL	LCL	ACL,PCL (MCL)
BPTB	ACL (MCL)	-	ACL	-	ACL,MCL (LCL)	-	-	MCL	ACL (MCL)	-	LCL	ACL (MCL)
RTM	ACL	-	ACL	-	ACL (LCL,MM)	-	-	-	ACL	-	LCL	ACL
Hybrid	ACL	-	ACL	MM	ACL (LCL,LM)	MM	-	LM	ACL	-	LCL,MM (MCL)	ACL
Swing Phase: Primary (Secondary) Restraints												
	Anterior	Posterior	Medial	Lateral	Compression	Distraction	Internal	External	Flexion	Extension	Adduction	Abduction
Intact	ACL (MCL)	LM	LM (ACL)	MCL (PCL)	MCL	ACL,LM	-	MCL (ACL,LM)	ACL (MCL)	LM	-	LM (ACL,MCL)
BPTB	MCL (ACL,MM)	LM	ACL	MCL (MM)	MCL	LM (MM)	-	MCL (LM)	MCL (ACL,MM)	LM	MM	ACL,MCL (LM)
RTM	MCL (ACL,MM)	LM	ACL	MCL	MCL (MM)	LM (ACL)	-	MCL (LM,MM)	MCL (ACL,MM)	LM	-	ACL (LM,MCL,MM)
Hybrid	MCL (ACL,MM)	-	ACL	MCL	MCL (LM)	ACL (MM)	-	MCL (ACL,LM)	MCL (ACL,MM)	-	MM	ACL (LM,MCL)

ACKNOWLEDGEMENTS. This study was supported by the LifeCell Corporation.

REFERENCES: 1. Von Porat et al, Ann Rheum Dis 2004. 2. Boguszewski et al, ORS 2010 Abstract. 3. Boguszewski, et al, SBC 2010 Abstract. 4. Tapper et al, JOR 2006. 5. Boguszewski et al, JOR 2010.

A Novel Robotic System Capable of Simulating Physiological Knee Motions Using a High-Speed Displacement/Force Control

Hiromichi Fujie, Ph.D.[1,2], Hitoshi Yagi, B.S.[1], and Yohei Matsuda, B.S.[1]

[1] Research Institute for Science and Technology, Kogakuin University, Japan
[2] Biomechanics Laboratory, Faculty of System Design, Tokyo Metropolitan University, Japan

INTRODUCTION: It has passed more than 20 years since the first report was made as regard with the application of robotic technology to the field of joint biomechanics[1)]. Since then, a variety of studies have employed commercially available articulated manipulators for the joint biomechanical studies[2-4)]. However, such articulated manipulators are generally poor at stiffness and precision although they were basically designed to achieve high speeds of motion while performing tasks in a large work space. To solve the problem, we have previously developed a robotic system consisting of a custom-made 6-degree of freedom (6-DOF) manipulator and a universal force-moment sensor (UFS)[5)]. Referring to the robotic system, the present study was aimed to develop a novel robotic system of rigid body/structure that allows a high-rate displacement/force control of the knee.

INSTRUMENTATION: A robotic system, consisting of a 6-DOF manipulator (custom-designed), servo-motor drivers (HA-800B-3A, Harmonic Drive Systems, Japan, and SGDS-01F12A, Yasukawa, Japan), a UFS (IFS40E15A100, JR^3, USA), a high-speed field bus (Mechatrolink-II, Yasukawa, Japan), and a control PC (Windows XP, Microsoft, USA), was developed (Figure 1). The manipulator consisted of 3 translational axes driven by 3 AC servo-motors (SGMAS-01A2A21, SGMAS-C2A2A2C, Yasukawa, Japan) and 3 rotational axes driven by 3 AC servo-motors (FHA-25C-160-S248-A, FHA-17C-160-S248-A, Harmonic Drive Systems, Japan). The novel system were designed, in partial analogy to the previous system[5,6)], so that 1) the manipulator had a material-test-machine-like unique arm configuration consisting of two mechanisms for allowing precise and easy control, 2) the arms and clamps of the mechanisms were consisted of highly stiff hollow-body structures, 3) the control PC and servo-motor controllers were serially connected using the high-speed field bus, and 4) system control was performed in a graphical language programming environment (LabView 8.1, National Instruments, USA) on the PC.

A displacement/force feedback control algorithm proposed for the previous system[6)] was employed in the novel system. Briefly, for displacement control of the knee, the manipulator moves at a 6x1 manipulator velocity $\boldsymbol{u}$ transformed from a 6x1 joint velocity $\boldsymbol{v}$ with respect to the joint coordinate system (KJCS)[7)]. For force/moment control of the knee, an error in force/moment at the KJCS between a prescribed one and actual one was transformed to a joint velocity $\boldsymbol{v}$, then the manipulator moves at a manipulator velocity $\boldsymbol{u}$ transformed from $\boldsymbol{v}$. The procedure that includes sensing of force/moment and displacement at the knee, calculation of $\boldsymbol{u}$, as well as manipulator motion was repeated at a rate of 100 Hz.

Figure 1: Novel robotic system for physiological knee motion paths

PRELIMINARY TEST: Porcine knee joints (n=3) were dissected down to the joint capsule and fixed to the developed system. Passive flexion-extension (FE) test and anterior-posterior (AP) drawer test were performed for the porcine knee joints. During the FE test, the FE DOF was rotated under the displacement control between 0 and 90 degree at a rate of 5 degrees/s while the other 5 DOFs were set under the force control with prescribed force/moment of zero. In the same way, during the AP test, the AP DOF was translated under the displacement control up to +-60 N at a rate of 1 mm/s while all the DOFs except the AP and EF DOFS were set under the force control with prescribed force/moment of zero. Six-DOF displacement and force/moment at the knee joint during the tests were determined.

RESULTS: As compared with previous tests performed using the previous robotic system[6)], joint motion was smoother in the present tests using the developed novel robotic system. Temporal changes in 6-DOF joint force/moment demonstrated that the actual force/moment was more precisely controlled at prescribed levels in the present system than in the previous system (Figure 2). Mean fluctuations of the P-D force during the FE test were 1.5 N, in the novel system, which were significantly smaller than 6.5 N in the previous system. Errors in other DOFs were also smaller in the novel system than in the previous system. A trend similar to the FE test was observed in the AP test.

DISCUSSION AND SUMMARY: To overcome the limitations in commercially available manipulators, we designed and developed a novel robotic system for joint biomechanics test. The system consisted of stiff body and structure, and allowed fast control and easy programming. Making use of these features, it was possible to simulate physiological knee motions such as FE rotation and AP translation. Note that these simulated motions were not consolidations of discontiguous knee postures but continuous paths of knee movements. We believe that it is possible to simulate physiological situations of the knee such as slow gait, ascending/descending of stairway, standing up from a chair, and so on. Currently, joint biomechanical tests are progressing using the system to assess ACL reconstruction techniques.

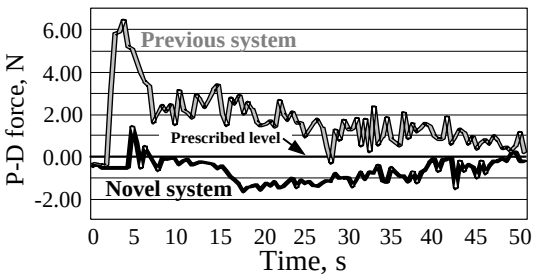

Figure 2: Temporal change in P-D force of a porcine knee joint during passive flexion

Reference: 1) Fujie et al (1989) Tissue Eng-BED (ASME), 2) Fujie, Woo, et al (1993) J Biomech Eng (ASME), 3) Rudy, Woo, et al (1996) J Biomech, 4) Woo, et al (1997) J Biomech, 5) Fujie et al (2004) J Biomech Eng (ASME), 6) Yagi, Fujie, et al (2010) ISLT, 7) Grood and Suntay (1983) J Biomech Eng.

Acknowledgment: The present study was financially supported by the Project-In-Aid for the Establishment of Strategic Research Centers (BERC, Kogakuin University) and Grant-In-Aid for Scientific Research (#20591766) both from the MEXT, Japan, and by Smith&Nephew.

NOVEL ALIGNED COLLAGEN-CARBON NANOTUBE FIBER FOR TENDON REPAIR

XingGuo Cheng, Sapna Desai
Department of Microencpasulation and Nanomaterials
Southwest Research Institute, 6220 Culebra Rd
San Antonio, TX, 78238

INTRODUCTION

Synthetic collagen fibers have been investigated extensively for tendon repair. However, due to the lack of alignment, hierarchical organization and optimal crosslinking density, the mechanical properties of synthetic collagen constructs are normally much inferior to those of natural tendon or xenografts[1]. In order to improve the mechanical properties of collagen fibers, we have invented a novel method to fabricate aligned collagen-carbon nanotube composite fibers with different CNT amount[2]. This novel material can be used as an advanced biomaterial for tendon/ligament repair and regeneration.

METHODS

Amine functionalized multi-walled carbon nanotubes (CNTs from NanoLab, Inc., outer diameter of 15±5 nm and length of 1-5 μm, 4 mg) were sonicated in 0.5 mL of ultrapure water and then further dispersed in 0.5 mL 2% glutaraldehyde overnight at 5°C. These CNTs were reacted with 3 mL dialyzed collagen (97% Type I, Davro Medical) overnight at 5 °C to allow chemical conjugation of CNTs with collagen. The CNT-collagen reaction mixture was fully dialyzed to remove any un-reacted reagents and ions. The above CNT-collagen conjugates then were subjected to an electrochemical process and aligned into a composite fiber.

RESULTS

Using linear electrodes at low voltage, the CNT-collagen conjugates were subjected to an electrochemical process. The isoelectric focusing process forces the CNT and collagen to be co-assembled into a highly-aligned dense collagen-CNT fiber. The incorporation of CNT inside collagen fiber make the fiber appear black (Figure 1a). Environmental SEM indicates that CNT is aligned along the fiber direction. The dimension of fiber is around 200 μm in diameter and 3 cm in length.

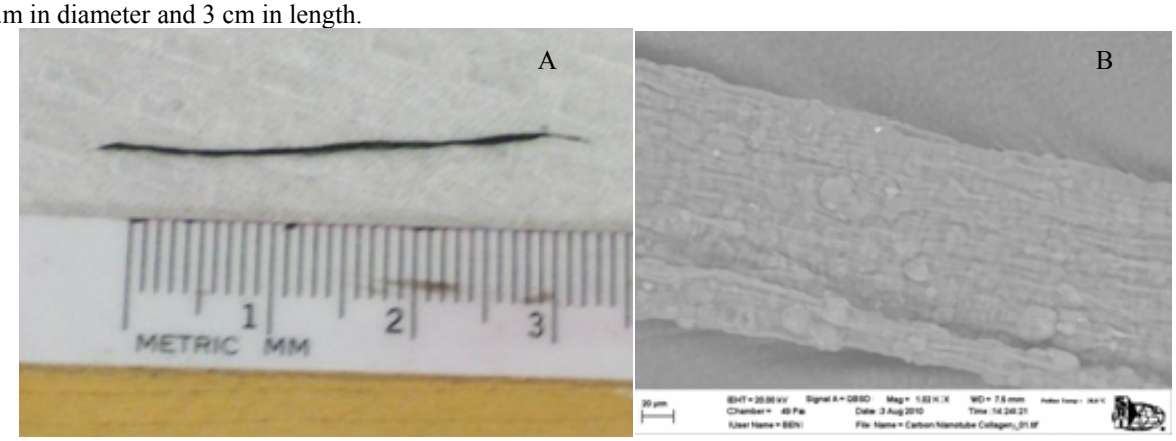

Figure 1 A) CNT-Collagen fiber. B) SEM image of aligned CNT-collagen fiber.

DISCUSSION

Our results indicate that it is feasible to co-assemble CNT with collagen to form composite fiber by the electrochemical process. CNT is one of the strongest materials on earth. The co-assembly of CNT with collagen not only can improve the mechanical properties of the fiber, but also offer new possibility to deliver therapeutic agents inside the nanotube as well. This novel biomaterial will be evaluated for cell and tissue response towards tendon repair.

ACKNOWLEDGEMENTS

Funding is supported by Southwest Research Institute Internal Research Program. Funding from USAMRAA (oppW81XWH-09-PRORP-IDA) is also acknowledged.

REFERENCES: 1. Cheng XG et al. Biomaterials 2008; 29(22):3278-3288. 2. Cheng XG, Poenitzsch V. US patent application, 12/813,834. 2010.

Tenomodulin Regulation in Equine Bioartificial Tendons *In Vitro*

[1]Banes, A.N.;[2,3] Qi, J.; [3]Tsuzaki, M; [2]Dmochowski, J.M; [1]Schramme, M.;[4]Nixon, Alan; [5]Roger Smith; [3]Yeung, N.;[3]Sumanasinghe, R; [+2,3] Banes, A.J. [1]North Carolina State University CVM, Raleigh, NC; [2]University of North Carolina, Chapel Hill, NC; [3]Flexcell Int. Corp., Hillsborough, NC; [4]Cornell School of Veterinary Medicine, Ithaca, NY; [5]Royal College of Veterinary Medicine, London, UK. +banes@flexcellint.com

Introduction: Tenomodulin (Tnmd) is a tendon marker gene with purported anti-angiogenic, and anti-proliferative properties. We found that the human and equine Tnmd gene has three isoforms with deduced molecular weights (MW) of 37.1, 28.2 and 22.3 kD. Tnmd proteins identified by Western blot have estimated MW of 48.5, 50, 70 and 80kD. We hypothesized that Tnmd isoforms would be down-regulated in cells adjacent to a wound to permit angiogenesis.

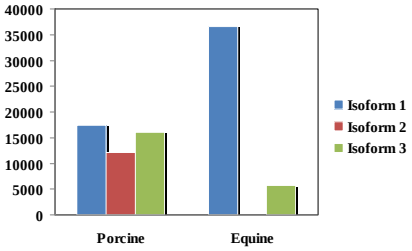

Figure 1. Expression of tenomodulin isoforms in equine.

Methods: Equine tenocytes from the superficial digital flexor tendons (SDFT) were isolated from 5 month-old, 2, 17 and 25 year-old horses during necropsy at the NCSU and Cornell Veterinary Schools. Tendon internal fibroblasts were cast as 3D bioartificial tendons (BATs). After 48h, a 2x4 mm full-thickness laceration was introduced to the wound group with a #10 scalpel blade. BATs subjected to strain received 3% uniaxial strain at 1Hz for 1 h. Wounded or strained BATs were collected and processed for quantitative PCR for Tnmd isoforms (n=4/group) and immunohistochemical localization of Tnmd (n=2/group). Cells were collected at 0, 1, 4, and 8 h post-wound and strain. 10% PAGE and Western blots were run on cells and supernatant fluids. Cells were also scratch-wounded on collagen-coated coverslips and assessed for Tnmd protein on days 1,2,3. Results were analyzed for statistical significance using a one-tailed t test.

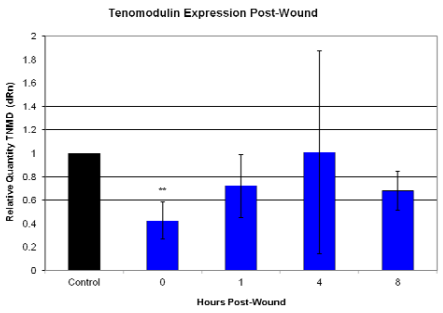

Figure 2. Tenomodulin expression was modulated by wound.

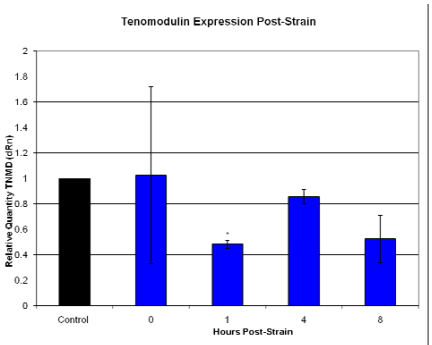

Figure 3. Tenomodulin expression was modulated by strain.

Results: Isoform 1 was the dominant Tnmd mRNA expressed in equine tissue and cells; I2 was slightly expressed and I3, the secreted form was about 20% of I1 (Figure 1). Tnmd expression diminished within 10 min between wounding a BAT and collection for the 0 h group suggesting an early response regulatory function (Figure 2). Tnmd was detected immunochemically in isolated cells and in BATs: Tnmd expression also decreased in samples taken from the wound region compared to the same region from nonwounded specimens. Likewise, expression decreased 1 hour after cessation of strain (Figure 3). Equine tenocytes expressed and secreted a high MW protein (Figure 4, Western blot).

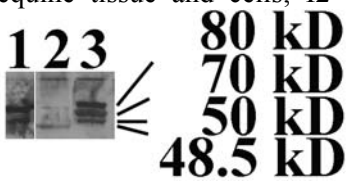

Figure 4. Western blot of equine tenomodulin. Lanes 1-3 are tendon tissue, cell lysate and conditioned medium, respectively.

Discussion: We observed that Tnmd was expressed and secreted in equine tenocytes but that wounding or straining a three-dimentional bioartificial tendon *in vitro* decreased both mRNA expression and protein localization at the wound site in 3D but not 2D. This is the first report of Tnmd modulation and secretion in a bioartificial tendon with wound and strain.

Acknowledgement: This work was supported by Flexcell Intl Corp. Dr. Banes is president of Flexcell and receives compensation as such.

TGFβ-mediated mechanical strain modulation of Metalloproteinases in human tenocytes

Jones E R; Jones G C; Riley G P
Soft Tissue Research Group, Cellular Protease Group, University of East Anglia, Norwich, United Kingdom.

INTRODUCTION

Tendinopathies are a range of diseases that involve pain and insidious degeneration and are a significant cause of morbidity. Relatively little is known about the underlying mechanisms; however onset is often associated with physical activity. Tendons most commonly affected are those exposed to higher levels of strain such as the supraspinatus and the Achilles. Matrix degrading enzymes such as metalloproteinases are regulated differentially in tendinopathy causing disruptions in the homeostasis of the extracellular matrix (ECM). An increase in the anti-inflammatory cytokine Transforming Growth Factor β (TGFβ) has also been documented. This project aims to investigate the effect of cyclic tensile strain loading and TGFβ stimulation on protease and ECM protein expression by human tenocytes in an established 3D culture system.

METHODS

Human tenocytes were derived by explant outgrowth from Achilles tendon specimens taken from patients with tendinopathy. The study was approved by the Cambridge Local Research Ethics Committee and the patients gave informed consent. Cells at early passage (<9) were seeded at $1.5x10^6$ cells/ml into collagen gels (rat tail type I at 1mg/ml) and stretched using a sinusoidal waveform of 0-5% at 1Hz using the Flexcell FX4000T™ system. Cultures were treated with or without 5ng/ml TGFβ1, TGFβ receptor I (TGFβRI) inhibitor (SB431542, 10μM) and a broad spectrum MMP inhibitor (GM6001, 25μM), as appropriate. Media and cells were harvested at a number of time points up to 48 hours. RNA was extracted from cells, reversed transcribed and analysed by qRT-PCR using the Applied Biosystems 7500 real time PCR system. Genes were normalized to TOP1 and 18s (n≥6). TGFβ was measured by incubating conditioned media with SW1353 cells transfected with a plasmid construct specific to SMAD2/3 and a luciferase reporter. TGFβ was measured using a luciferase assay and data was normalised to a values from a transfection control plasmid (n=5). Conditioned media was analysed by gelatin zymography to asses MMP2 activity (n=6). The Wilcoxon signed rank and students T test were used to analyze statistical significance, p=0.05 was chosen as the cut off.

RESULTS

We observed that mechanical strain regulated a plethora of protease and matrix genes using qRT-PCR techniques, these changes were largely anabolic. MMP1 (3-4 fold, p=0.021), MMP2 (1.5 fold, p=0.015), MMP3 (1.5 fold, p=0.010), MMP13 (2 fold, p=0.008) and Fibulin-1(2 fold, p=0.028) were significantly decreased with 48 hours mechanical loading. ADAM12 (2 fold, p=0.008) and COL1A1 (2 fold, p=0.028) were increased at 24 hours, and Elastin was increased at 8 (2 fold, p=0.018), 24 (4 fold, p=0.028) and 48 hours (10 fold, p=0.028) with mechanical loading. These affects were mirrored with TGFβ stimulation alone. We also demonstrated that the inhibition of the TGFβ signalling pathway (TGFβRI inhibition) abrogated the strain induced changes in mRNA. TGFβ activity was increased with 48 hours mechanical strain (21 fold, p=0.028) although there was no change in the total TGFβ mRNA was not significantly up-regulated with 0-48 hours strain. There was an increase in active MMP2 with 8 hours of strain (1.5 fold, p=0.028), however addition of a broad spectrum MMP inhibitor did not affect the level of TGFβ activation by mechanical loading.

DISCUSSION

The prolonged application of 5% cyclic mechanical strain in a 3D culture system induced an anabolic response in protease and matrix genes which indicates that a relatively-high level of cyclic strain does not induce catabolic effects upon the ECM. We have shown that it is not an increase in TGFβ synthesis, but TGFβ activation that plays a role in mechanotransduction. In addition we have shown that activation does not require MMP activity. In this system, activation of TGFβ may require other proteases (eg serine proteases) or a non-proteolytic mechanism. Previously we have reported a differential response in cultures seeded at lower verses higher cell densities, indicating that cell-cell contacts are important in the strain regulated response. Integrins are involved not only in cell-cell and cell-matrix communication, but in the activation of TGFβ via mechanical forces between the cell and the ECM that result in the separation of TGFβ and the latency associated peptide (Munger, Huang et al. 1999). Therefore mechanical forces may prove to be the mode of TGFβ activation in our study. Further research will reveal the mechanism of TGFβ activation by mechanical loading and give insight into how loading is linked to tendon disease.

REFERENES

Munger, J. S., X. Huang, et al. (1999). "The integrin alpha v beta 6 binds and activates latent TGF beta 1: a mechanism for regulating pulmonary inflammation and fibrosis." Cell **96**(3): 319-28.

Effects of Small Intestine Submucosa (SIS) Hydrogel on the Proliferation and Matrix Production of ACL Fibroblasts

K.E. Kim, R. Liang, G. Yang, S.L-Y. Woo
Musculoskeletal Research Center, Department of Bioengineering,
Swanson School of Engineering, University of Pittsburgh, Pittsburgh, PA

INTRODUCTION Porcine extracellular matrix (ECM) bioscaffolds, have been widely used in tissue engineering applications[1-4]. Studies have shown that these ECM bioscaffolds contain bioactive molecules, e.g. growth factors, fibronectin, and so on[5] that could stimulate fibroblast proliferation and DNA synthesis [5]. Recently, a hydrogel form of small intestine submucosa (SIS) ECM has been made from αGal-deficient pigs in our research center as this SIS hydrogel has immunological advantages over wild type ECM since the rejection-causing αGal epitope has been removed[6]. Therefore, the research questions are whether such a SIS hydrogel could still retain the positive effects on cell proliferation and matrix production, and, if so, whether these effects would be time dependent and/or could be influenced by the level of serum concentrations in culture. We hypothesized that since the genetic modification is targeted specifically to specific alleles of the α1,3-galactosyltransferase gene[7], the bioactive factors and their positive effects in the SIS would be unaffected, but their role can be limited by other biological agents present in the FBS used in cell culture.

METHODS Lyophilized powder of the porcine SIS was obtained from αGal-deficient SIS (Revivicor, Inc., Blacksburg, VA). The SIS powder was then dissolved through pepsin digestion, and western blot was performed for TGFβ, FGF-1, and Fibronectin. Then, the SIS hydrogel was made by adding PBS to the SIS digest to 6mg of dry SIS powder per ml, adjusting pH to 7.4, and incubating at 37°C for an hour. Pure collagen gel was formed through the similar procedure as the SIS hydrogel by using purified type-I collagen solution (3.2mg/ml) (Sigma Aldrich, St. Louis, MO). ACL fibroblasts were harvested from fresh hindlimbs of the Sprague Dawley rats by mincing the ACL tissue and digesting with collagenase for 2 hours. The fibroblasts (p3) were seeded on both gels in DMEM culture medium with 0, 1, and 10% FBS and cultured for 3 and 7 days. At the end of culture (N=3 for both time points), cell proliferation was measured using a BrdU assay kit (Calbiochem, Gibbstown, NJ). Also, mRNA expressions of collagen type-I and type-III (N=3 for 3 day and N=5 for 7 day) were measured using real time-PCR.

RESULTS The western blot results confirmed that the SIS hydrogel indeed contains TGFβ, FGF-1, and Fibronectin. The BrdU results showed that after 3 days of culture, the cell proliferation significantly increased with the SIS hydrogel when compared to those on the pure collagen gel at all three FBS concentrations (39% for 0% FBS, 31% for 1% FBS, and 22% for 10% FBS) ($p<0.05$); whereas by 7 day, a significant difference was found only at 0% FBS. At both time points, cell proliferation was significantly increased with 10% FBS over 0% and 1% ($p<0.05$). For collagen type-I, the SIS hydrogel had a significant effect on the mRNA expression at both time points ($p<0.05$). Individual comparisons showed that there were significant differences between the two gel types at all FBS concentration for 3 day, whereas differences were observed only for 1% and 10% FBS for 7 day. Conversely, we could not demonstrate significant effect on collagen type-III mRNA expressions at either time point ($p>0.05$).

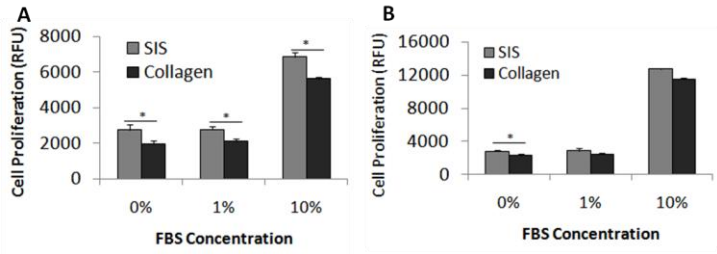

Figure 1. BrdU Resules on Cell proliferation **A:** at day 3; **B:** at day 7.
* significant difference between SIS hydrogel and pure collagen gel at a given FBS concentration

DISCUSSION The findings of this study indicate that the SIS hydrogel has the bioactive factors that can enhance cell proliferation as well as increase collagen type-I mRNA expression. However, the positive effects on cell proliferation was masked by higher concentrations of FBS and diminished over time but not in the case of collagen type-I. The data suggests that the initial availability of the GFs in the SIS significantly enhanced the cell proliferation, although this positive effect was limited by high serum concentration and time, which is in agreement with our initial hypothesis. Based on these results, the early use of SIS hydrogel as an injectable bioactive agent to aid the healing of ligament and tendon healing is suggested.

ACKNOWLEDGEMENTS Financial support from NIH T32 Biomechanics in Regenerative Medicine Predoctoral Training Fellowship (NIH/NIBIB EB003392-01) is gratefully acknowledged.

REFERENCES: 1. Sclamberg et al. J Shoulder Elbow Surg 2004. 2. Liyanage et al. Plast Reconstr Aesthet Surg 2006. 3. O'Connor et al. Urology 2002. 4. Bejjani and Zabramski J Neurosurg 2007. 5. Voytik-Harbin et al. J Cell Biochem 1997. 6. Phelps et al. Xenotransplantation 2007. 7. Phelps et al. Science 2003.

HUMAN MSCs PRODUCE COLLAGENOUS EXTRACELLULAR MATRIX IN MATRIX METALLOPROTEINASE-DEGRADABLE HYDROGELS

D.M. Doroski, and J.S. Temenoff
Coulter Department of Biomedical Engineering, Georgia Tech and Emory University, Atlanta, GA, USA

INTRODUCTION

Matrix metalloproteinases (MMPs) are a family of enzymes secreted by mesenchymal stem cells (MSCs) and fibroblasts to facilitate extracellular matrix (ECM) reorganization.[1] To establish parameters for design of future biomaterials for tendon/ligament tissue engineering, our laboratory has incorporated MMP-degradable peptides in a model synthetic hydrogel system in an effort to understand the relationship between remodeling of the biomaterial carrier and deposition of matrix molecules by embedded cells. Specifically, this study sought to determine whether human MSCs encapsulated in hydrogels containing MMP-cleavable motifs would produce more collagenous ECM than in non-degradable gels.

METHODS

Oligo(poly(ethylene glycol) fumarate with a poly(ethylene glycol) (PEG) chain of molecular weight 3KDa was combined (1:1 wt/wt) with PEG-diacrylate (nominal M_n 3,400) to form the non-degradable portion of the hydrogels. A GGGLGPAGGK peptide conjugated on each end to an acylated PEG chain (3kDa) served as the MMP-degrable portion of the hydrogels. The GRGDS adhesive peptide (1 µmol /g swollen hydrogel) was also used. Polymers were cross-linked (30µl, 15mm dia) in various ratios of non-degradable to degrable sequences (0%, 25%, 75%, or 100% MMP-degradable sequence by mass) using N,N,N',N-tetramethylethylenediamine and ammonium persulfate thermal radial initiators (0.018M, 10min, 37°C) with human MSCs (hMSCs, Lonza) encapsulated at 10 million cells/ml. At 1, 7, 14, and 21d real time RT-PCR and immunohistochemistry (IHC) were used to examine gene expression and protein production of tendon/ligament matrix proteins (collagen I – col I, collagen III – col III). Gene expression results were normalized to day 1 hydrogels without any MMP-cleavable sequences (0%). Significance was determined with a 2-way ANOVA followed by Tukey's Multiple Comparison Test ($p \leq 0.05$).

RESULTS

Col I expression was upregulated (Fig. 1) in 100% MMP-cleavable hydrogels compared to all other hydrogel types on days 7 and 14. Col III expression was upregulated (Fig. 2) in 100% MMP-cleavable hydrogels compared to 0% and 25% samples on day 21. Col I and col III were upregulated (Fig. 1&2) in all sample types by day 14 compared to d1. IHC staining indicated the presence of both col I and col III pericellularly in 100% MMP-cleavable hydrogels (Fig. 3). 0% hydrogels did not demonstrate any staining for col I or col III (not shown).

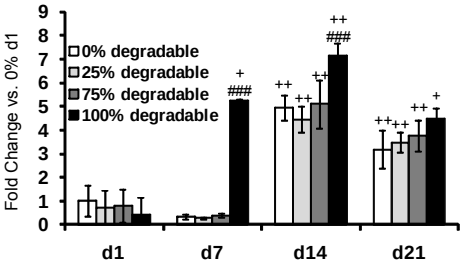

Fig. 1. Collagen I gene expression of hMSCs in hydrogels (n≥7 ±SD; p<0.05 compared to the 0%(#); 0% and 25%(##); or 0%, 25%, and 75%(###) hydrogels; respectively, for the given time point. p<0.05 compared to d1(+); d1 and d7(++); or d1, d7, and d14(+++); respectively, for the given hydrogel type).

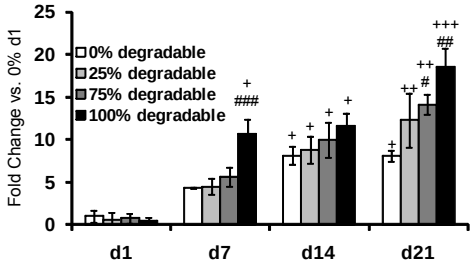

Fig. 2. Collagen III gene expression of hMSCs in hydrogels (n≥7 ±SD; p<0.05 compared to the 0%(#); 0% and 25%(##); or 0%, 25%, and 75%(###) hydrogels; respectively, for the given time point. p<0.05 compared to d1(+); d1 and d7(++); or d1, d7, and d14(+++); respectively, for the given hydrogel type).

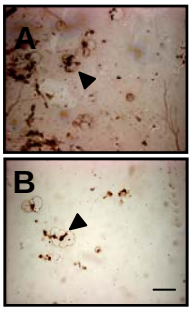

Fig. 3. IHC (100% hydrogels,d21) for collagen I (A) and collagen III (B). Arrow indicates pericellular staining. Scale bar = 20 µm.

DISCUSSION

The upregulation of col I and III expression seen in the 100% MMP-cleavable hydrogels compared to other hydrogel formulations, combined with the IHC results, indicates that localized degradation of the hydrogel matrix by encapsulated MSCs may facilitate production of tendon/ligament ECM components and suggests that the amount of the ECM produced can be controlled by the degradability of the material. Previous studies conducted in our laboratory with non-degradable gels demonstrated MSC differentiation toward a fibroblast phenotype under tensile strain.[2] Further work will employ this well-defined carrier material to better understand how local ECM deposition affects cellular responsiveness to tensile loading, thereby providing basic parameters for next-generation biomaterial/bioreactor combinations to be used in production of tissue-engineered ligament grafts.

ACKNOWLEDGEMENTS: Arthritis Foundation Investigator Award (JST); NIH R21 EB8918-1.

REFERENCES: 1) Fox, Stuart I. Human Physiology. 7th ed. p 127. 2) Doroski et al., Tissue Eng A, 2010. [Epub ahead of print].

Effects of cell freezing and thawing on the mechanical properties of a stem cell-based self-assembled tissue (scSAT)

Ryo Emura[1], Kei Oya[2], Hiroki Sudama[1], Kazunori Shimomura[3], Norimasa Nakamura[3], and Hiromichi Fujie[4,2]
[1] Division of Mechanical Engineering, Graduate School of Engineering, Kogakuin University, Tokyo, Japan
[2] Research Institute for Science and Technology, Kogakuin University, Tokyo, Japan
[3] Department of Orthopaedic Surgery, Osaka University Medical School, Osaka, Japan
[4] Faculty of System Design, Tokyo Metropolitan University, Tokyo, Japan

INTRODUCTION

The ligaments and tendons have superior functions, although their healing capacities are limited. It is one of potential options for the repair of such soft tissues to use cell-based therapies. We have been developing a novel tissue-engineering technique for the tissues which involves a stem cell-based self-assembled tissue (scSAT) bio-synthesized from synovium-derived stem cells[1)]. As the scSAT is a scaffold-free construct composed of mesenchymal stem cells (MSCs) with their native extracellular matrix, it is free from concern regarding long-term immunological effects. During the bio-synthetic process of the scSAT, it is occasionally required to cryogenically freeze the cells for presenvation. However, the effects of cell freezing and thawing on the mechanical properties of the scSAT has not been determined so far, although such data are important to set conditions for successful bio-synthesis of the scSAT. Therefore, the objective of the present study was to determine the effects of cell freezing and thawing on the mechanical properties of the scSAT cultured from human synovium-derived cells.

METHODS

Synovium-derived cells obtained from the synovial membrane of human knee joints were cultured in a monolayer in medium (DMEM, 10%FBS, 1%P/S). Cell proliferation was performed through 4 passages to increase the mesenchymal stem cells. The cells were cooled to -80 °C in a cell freezing medium (BLC-1P, Juji field Ins.) immediately after harvested, and were preserved at -80 °C for 24 hours, and then thawed by immersion in water at 37 °C (FT group). The rates of freezing and thawing were -3 °C/min and 60 °C/min, respectively, according to a manufacture-provided instruction. After the cells reached to a confluent condition on a culture plate, the cells were placed on the 6-well culture plate at the cell density of 6.0×10^5 cells/cm^2 in a medium containing 0.2 mM of ascorbic acid-2 phosphate to promote the bio-synthesis of extracellular matrix. At 28 days after culture started on the 6-well plate, synthesized matrices were carefully detached from the culture plate and allowed to undergo natural contraction for 1 hour to develop scSATs[2)]. For comparison, the scSAT specimens were subjected to the bio-synthetic process identical to that applied for FT group except the process of freezing and thawing (control group). The scSAT specimens (n=5 for FT group and n=8 for control group) were then subjected to tensile testing at a rate of 0.05 mm/s in PBS (-) at 37 °C using a custom-made micro tensile tester developed in our laboratory[3)]. Morphological observation of the surface structure of the scSAT was determined using a phase contrast microscope (IX71, Olympus, Japan). The real-time RT-PCR analysis was also performed for the scSAT specimens.

RESULTS & DISCUSSION

Stress-strain curves of the scSATs in the FT and control groups are shown in Fig 1. No significant difference was observed in terms of tensile modulus and strength between the two groups. However, 29% of the scSAT speciens in FT group were detached from culture plate during the bio-synthetic process for 28 days, while no specimen detached in the control group. Microscopic observation indicated that the surface structure was slightly more uneven in the FT group than in the control group. These results demonstrate that there is no effect of freezing and thawing process on the tensile modulus and strength as well as the surface structure of the scSAT, although the process deteriorates the cell-adhesion properties of the scSAT. The present study implies that the freezing and thawing process has no effect on the extracellular matrix production of human synovium-derived cells expect the production of adhesive materials such as fibronectin. We are performing both histological examination and real-time RT-PCR analysis to clarify this point.

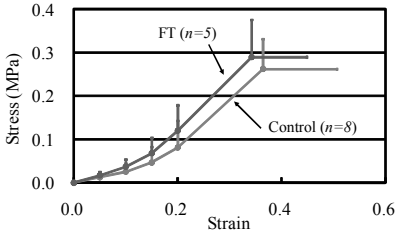

Fig 1: Stress-strain curves of scSATs in FT and control groups.

ACKNOWLEDGMENTS

The present study was financially supported in part by the Project-In-Aid for the Establishment of Strategic Research Centers from the MEXT, Japan (BERC, Kogakuin University)

REFERENCES: 1) Ando W. et al., Biomaterials, 28, 5462-5470, 2007, 2) Emura R. et al., Proceedings of the 6th WCB, 2010, 3) Fujie H. et al., Proceedings of the 53rd ORS, 2007.

EFFECTS OF MSC CELL SOURCE AND MEDIA SUPPLEMENTATION ON ALP EXPRESSION

A.P. Breidenbach, J.A. Turner, N.A. Dyment, and D.L. Butler
Biomedical Engineering Program, University of Cincinnati, Cincinnati, OH

INTRODUCTION. Tendon and ligament injuries account for nearly half the musculoskeletal injuries per year at a cost of $30 billion in the United States [1]. Mesenchymal stem progenitor cells (MSPCs) are one way to more effectively treat and repair acute soft tissue injuries [2]. Our lab has used MSPCs in tissue engineered constructs (TECs) to repair acute patellar tendon defect injuries in the rabbit to 150% of normal peak *in vivo* forces in 12 weeks [3]. However, to further improve these tissue-engineered repairs, we now seek to use murine genetics to investigate tendon development and natural healing and then apply this knowledge to repair in larger animal models.

The source of murine MSPCs for TECs can potentially influence tendon repair outcome. MSPCs reside in bone marrow and, to a greater extent, in the cortex of long bones [4,5]. However, we found that high densities of rabbit MSPCs from marrow frequently resulted in ectopic bone formation in the repair sites [6]. Controlling murine MSPC phenotype and minimizing osteogenic differentiation in cell culture will be critical to designing TECs that optimize repair outcome. As such, *we seek to develop isolation and culturing methods that produce a large, homogenous population of murine MSPCs with minimal osteogenic expression*. Thus, our objective is to characterize the effects of cell isolation and culture techniques (cell source, time in culture, type of media) on murine cell phenotype (homogeneity, alkaline phosphatase expression, proliferation rate).

METHODS. Cell Culture. MSPC cultures were harvested from marrow (flush) and cortical bone (chip) of tibia and femurs of four 15-20 week old mice (n=4) using previously published protocols [4,5] and allowed to proliferate to 80-90% confluency at P0. At P1 cells were cultured in either MesenCult mouse proliferation media (Stemcell Technologies; Vancouver, BC) or advanced DMEM (Gibco; Grand Island, NY) supplemented with 10% FBS. Cells were passed every 5 days and reseeded at 10,500 cells/cm^2. At P1, P3 and P6, cells were counted for proliferation rate and stained for alkaline phosphatase (ALP) (Takara; Madison, WI). ALP positive cells were counted and microscopic photographs were taken at each passage to assess changes in cell morphology. Statistics. Three-way ANOVA was used with cell source, time in culture and media supplementation as fixed factors ($p<0.05$).

RESULTS. Cell numbers for each cell source doubled every 3-4 days at P1, and progressively slowed for the remaining passages. Marrow flush cell proliferation stalled at P3, and chip cell proliferation stalled at P6. Chip cells had higher ALP expression than flush cells at P1, and ALP expression increased significantly across all time points for all treatments except flush cells cultured in MesenCult (Fig. 1). At P3 ALP was lowest in the flush cells cultured in MesenCult (3.95% ± 3.24%, mean ± SD). DMEM media significantly increased ALP expression in the flush cells at P3. DMEM did not significantly increase ALP expression in chip cells ($p>0.05$). Hematopoietic cells remained lowered and cell populations in all culture types became more homogenous at each passage (Fig. 2).

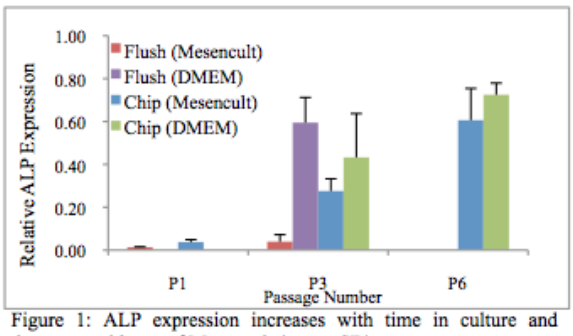

Figure 1: ALP expression increases with time in culture and decreases with use of Mesencult (mean±SD).

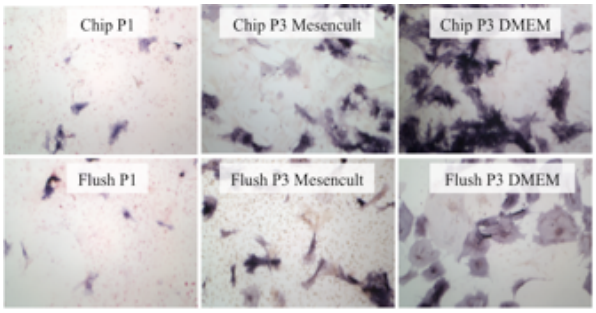

Figure 2: Homogeneity increases with time in culture (6.4x). Purple and red are indicative of ALP and TRACP expression, respectively.

DISCUSSION. The results of this study indicate that ALP expression in murine cells increases with time in culture and that rapid passage of cells from P1 to P3 results in more homogenous cell populations. Proliferation rate data indicates that cells should be used within three passages in order to maintain sufficient cell numbers. Lastly, flush cells cultured in MesenCult show decreased expression of ALP as desired, but these levels are still greater than levels seen in rabbit bMSCs (data not shown). Future studies will quantify expression of tenogenic and osteogenic markers using qRT-PCR. Minimizing osteogenic differentiation in these cell sources is essential prior to creating tissue-engineered constructs for tendon repair applications.

ACKNOWLEDGMENTS. Supported by NIH grant 56943-02 and student support by NSF IGERT 0333377.

REFERENCES: 1. Praemer et al. 1999; 2. Yin et al. Expert Opin Biol Ther, 2010; 3. Juncosa-Melvin et al. Tissue Eng, 2006; 4. Soleimani and Nadri. Nat Protoc, 2009; 5. Zhu et al. Nat Protoc, 2010.

Intramedullary and Extramedullary Free-Tissue Graft Reconstruction of the Acromioclavicular Joint Complex

[1]Adamson, GJ, [+2]Lee TQ
[+1]Congress Medical Foundation, Pasadena, CA,
[2]Orthopaedic Biomechanics Laboratory, Long Beach VA Healthcare System and University of California Irvine, Irvine, CA
tqlee@med.va.gov

INTRODUCTION

Several different surgical techniques have been described to address the coracoclavicular (CC) ligaments in acromioclavicular (AC) joint injuries. However, very few techniques focus on reconstructing the AC ligaments despite its importance in providing stability. The purpose of our study was to compare the biomechanical properties of two free-tissue graft techniques that reconstruct both the AC and CC ligaments in cadaveric shoulders, one with extramedullary AC reconstruction and the other with intramedullary AC reconstruction. We hypothesized that the intramedullary AC reconstruction will provide greater anteroposterior translational stability and improved load to failure characteristics than the extramedullary technique.

METHODS

Specimen and Testing System

Six matched pair cadaveric shoulders were used with a custom testing system. This custom testing system permits application of compressive loads across the AC joint (Figure 1).

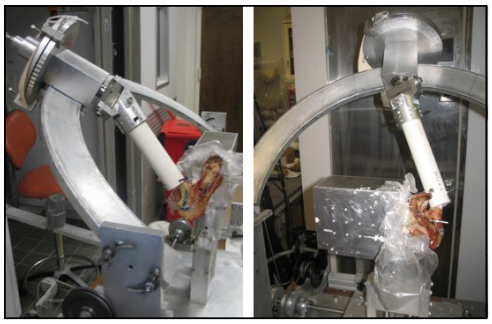

Figure 1: Custom Testing System. Permits motion with six degrees of freedom. The Potted scapula has three degrees of freedom of motion and is allowed to undergo motion in the AP and SI planes with predetermined forces. The clavicle is fixed in position based on anatomical position of the AC joint.

Reconstruction

Two reconstructions were performed on each AC joint. The first reconstruction was an extramedullary graft reconstruction, and it was performed as described by Grutter and Petersen in 2005.[1] In this reconstruction, 20 cm of allograft with a 4.5 mm diameter was used, and passed through 4.5mm drill holes in the clavicle and coracoid. Two 2.5 mm drill holes were also made in the acromion that allowed the two sutured ends of the graft to be passed through the acromion and tied tight on the lateral surface. The joint was then reduced and the remaining graft was pulled tight and tied to the lateral graft on the superior surface of the clavicle using a running #2 Fiberwire stitch (Arthrex Inc, Naples, FL). The second reconstruction was an anatomic reconstruction with an intramedullary free-tissue graft reconstruction of the CC and AC ligamentous complexes.[2] The CC reconstruction consisted of a tendon allograft looped under the coracoid and over the clavicle then sutured to it-self. The AC ligamentous complex was reconstructed with an intramedullary free-tissue graft and secured by Fibertape (Arthrex Inc, Naples, FL).

Translation and Load to Failure Testing

For each 10N, 20N and 30N of compressive load, anterior-posterior (AP) and superior-inferior (SI) translation testing was performed with 10N and 15N of translation loads. The translation of the AC joint in the AP and SI directions for the intact and reconstructed conditions was measured using a Microscribe 3DLX digitizing system (Immersion, San Jose, CA). Both reconstructed specimens then underwent load to failure testing via superior clavicle distraction at a rate of 50 mm/min.

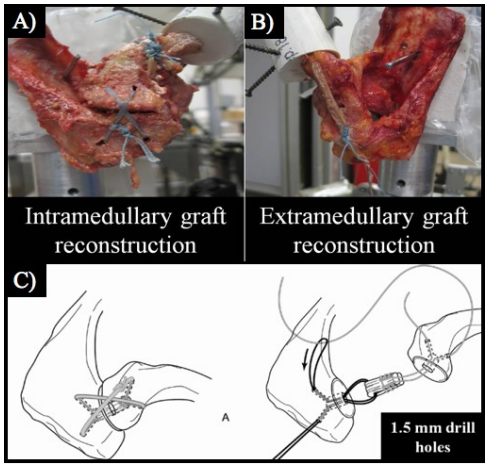

Figure 2: Reconstructions: A) The intramedullary graft reconstruction with Fiberwire limbs passed through 1.5mm osseous tunnels on the clavicle and acromion, Fibertabe crossed over the AC joint, and a 10cm free-tissue graft looped under the coracoid and over the clavicle and sutured onto itself, B) The Grutter extramedullary technique, with 20 cm of allograft passed through the clavicle and coracoid and tied at the acromion with #2 Fiberwire, C) A schematic of the intramedullary technique, showing a 5-cm piece of graft doubled over and placed into intramedullary holes in the acromion and clavicle.

RESULTS

Intramedullary reconstruction provided significantly greater translational stability in the anteroposterior direction than the extramedullary technique in all loading conditions except at 10 N of translation with 30 N of compression (Figure 3). There were no significant differences in translational stability in the superoinferior direction for any loading condition. The intramedullary reconstructed specimens demonstrated improved load to failure characteristics, however only ultimate load to failure and energy absorbed to clinical failure was significant.

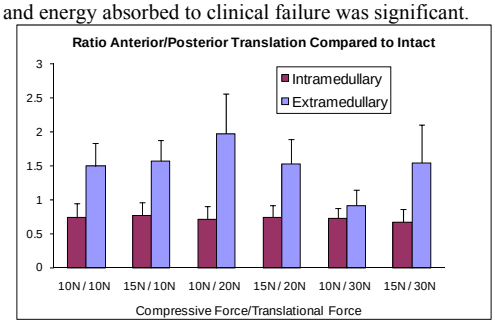

Figure 3. Ratio of each reconstruction relative to intact condition.

CONCLUSION

Intramedullary reconstruction of the AC joint provides greater stability in the anteroposterior direction and improved load to failure characteristics compared to the extramedullary technique. Reconstruction of the injured AC joint with an intramedullary free tissue graft may provide greater strength and stability than other currently used techniques, allowing patients to have improved clinical outcomes.

REFERENCES

1. Grutter PW, Petersen SA. Am J Sports Med. 2005; 33(11):1723-8.
2. Adamson GJ, Freedman JA, Lee TQ. Tech in Shoulder and Elbow Surg. 2008; 9(4):193-8.

ACKNOWLEGMENTS

VA Rehab R&D and Medical Research
California Orthopaedic Research Institute

QUANTITATIVE ANALYSIS OF THE HIP CAPSULAR LIGAMENTS AND THEIR FOOTPRINTS FOR ANATOMIC RECONSTRUCTION

[1]Telleria; J M; [2]Lindsey, D P; [1,2]Giori, N J; [1]Safran, M R
[1]Stanford University, Palo Alto, CA
[2]Veterains Affairs Palo Alto Health Care System, Palo Alto, CA

INTRODUCTION

Interest in the non-arthritic hip, including management of hip capsular laxity and functional instability, is rapidly increasing. Many hip procedures require capsulotomies and capsulectomies which may be left unrepaired, with unclear consequences. In the last few decades only two studies have specifically addressed the macroscopic anatomy of the hip capsular ligaments. Unfortunately, there are many inconsistencies in the reported macroscopic anatomy of the capsular ligaments and no study published to date addresses the ligamentous insertional footprints. This study quantitatively described the hip capsular ligaments and their insertional footprints to serve as a basis for anatomic repair and reconstructions of these structures.

METHODS

Anatomical measurements of the three main hip capsuloligamentous structures and their insertions were made using a three-dimensional digitalizing system (Revware Microscribe, Revware, Inc., Raleigh, NC) in 8 paired fresh-frozen cadaveric hips (mean age = 73.3±10.7 years {61-88}, two male specimens) without evidence of previous surgery. The three-dimensional coordinate points recorded by the Microscribe were imported into the modeling program Rhinoceros (McNeel North America, Seattle, WA) and computer models were generated to determine the mean areas and dimensions of the ligaments and footprints as well as their relative position to bony prominences about the hip. Three-dimensional models of the hip joint were also made to pictorially demonstrate the anatomic relationships. The mean, median, standard deviation and range were calculated for all ligament and insertional footprint areas, dimensions and distances between structures and osseous landmarks. This material is based upon work supported in part by the Office of Research and Development (Rehabilitation R&D Service), Department of Veterans Affairs.

RESULTS

The "Y" shaped iliofemoral ligament (ILFL) split distally into 2 distinct arms (mean area = 34.6cm^2). The pubofemoral ligament (PFL) was sling shaped (mean area = 13.0cm^2). The triangle shaped ischiofemoral ligament (ISFL) had a mean area of 18.4cm^2. The proximal ILFL was on the anterior and lateral supraacetabular region (mean area = 4.2cm^2), while the medial and lateral distal attachments are on the anterior and anteroinferior femoral neck just proximal to the intertrochanteric line (mean areas = 4.8cm^2; 3.1cm^2, respectively). The PFL proximal footprint was on the anteroinferior acetabulum (mean area = 1.4cm^2). The PFL blended with the medial ILFL anteriorly and the ISFL distally without a bony insertion. The proximal and distal ISFL insertional footprints were at the posteromedial acetabulum and anterior femoral neck (mean areas = 6.4cm^2; 1.2cm^2 respectively)

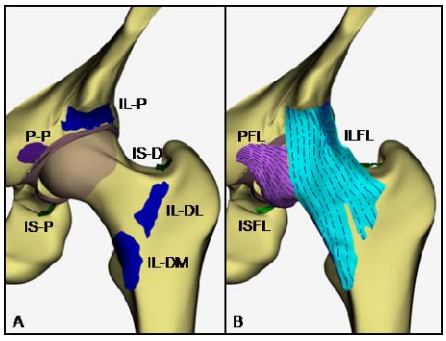

Figure 1. Computer model of the hip capsular ligament **(A)** insertional footprints **(B)** and whole ligaments demonstrating the ligamentous anatomy of the anterior hip. The PFL can be seen blending with the ILFL anteriorly. IL, iliofemoral; IS, ischiofemoral; P-P, pubofemoral-proximal; P, proximal; D, distal; DL, distal lateral; DM, distal medial.

DISCUSSION

In agreement with most other authors, the ILFL consists of two distinct bands and the ISFL is comprised of a single cohesive band. The PFL blends proximally with the medial border of the ILFL anteriorly and courses inferoposteriorly like a sling around the head of the femur – a finding reported only once before. Distally the PFL terminates by blending with the proximal aspect of the ISFL, near the acetabular rim, and does not have a femoral attachment. This is the first study to quantify the insertional footprints and whole ligament areas and dimensions. Quantification of these ligaments and their insertional footprints will help clinicians develop better techniques to clinically evaluate laxity of the hip, as well as develop open and/or arthroscopic procedures to address hip instability. Additionally, accurate quantitative descriptions of the ligaments may help with the design of biomechanical models and studies in the future.

SPINAL LIGAMENT TISSUE DEVELOPMENT *IN VIVO* AND CELL RESPONSE TO GROWTH FACTORS *IN VITRO*

[1]J.P. Brown, [1]R.M. Lind, and [1]C.K. Kuo
[1]Tufts University, Medford, MA

INTRODUCTION

Spinal ligaments are critical for joint stabilization between vertebrae. These tissues are susceptible to ossification, age-related hypertrophy, and iatrogenic damage during spine surgery, all of which have been associated with pain and aberrant function[1,2,3]. Our long term goal is to engineer these tissues for replacement. However, much is unknown, ranging from development to *in vitro* cell behavior. In this work, we report on our studies to characterize the development of spinal ligaments and the use of soluble cues to regulate gene expression of embryonic and postnatal axial T/L cells.

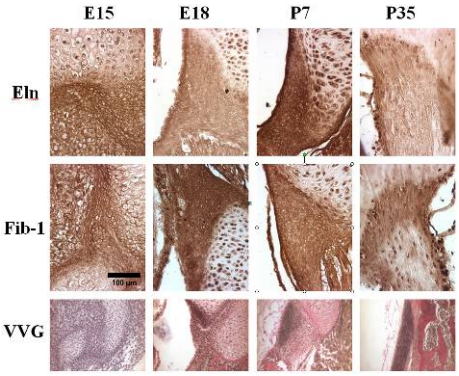

Figure 1. Immunostaining of LF for elastin (eln; top row) and fibrillin-1 (fib-1; center row). VVG staining of LF (bottom row).

METHODS

Spines of scleraxis-green fluorescent protein (ScxGFP) genetically engineered mice (a kind gift of R. Schweitzer) were harvested on embryonic days (E) 15 and 18 and postnatal days (P) up to 35 (Fig 2). Spine tissues were fixed, decalcified, and routinely embedded in paraffin. Spines were sectioned at 6 μm for histology (Verhoeff van Gieson stain; VVG) and immunohistochemisty (IHC; antibodies against tropoelastin (Eln), fibrillin-1 (Fib-1) and fibulin-4) and visualized. For *in vitro* cell studies, trunks and limbs from the same time points were digested and sorted via FACS on the basis of GFP expression to harvest scx-expressing axial and limb T/L cells, respectively. Cells were cultured in medium with 1% FBS +/- 1 ng/mL TGFβ2. Cells were imaged for GFP expression after 3 days.

RESULTS

Collagen (pink) and elastic fibers (black) of the LF were identified by VVG staining (Fig. 1 bottom row). Embryonic LF appeared highly cellular with a randomly oriented matrix. Elastic fibers became discernable by P7 and were thin and disorganized. At P35, fibers were thick and aligned cephalocaudally. IHC staining demonstrated that all three proteins were present at all time points, though intensity varied with age. Staining intensity for elastin peaked at P7 (Fig. 1 top row), as did fibulin-4 (not shown). Fibrillin-1 (fib-1) staining intensity peaked at E18 (Fig. 1 center row).

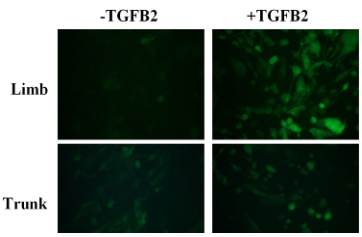

Figure 2. E15 limb and trunk T/L cells after 3 days of culture +/- TGFβ2.

By day 3 of cell culture, based on GFP intensity, axial T/L cells showed a moderately high level of scx expression, in contrast to weak expression by limb T/L cells (Fig. 2). When treated with TGFβ2, axial T/L cells maintained the same level of scx expression as without TGFβ2. However, scx expression of limb T/L cells increased significantly in the presence of TGFβ2 (Fig. 2).

DISCUSSION

Elastogenesis in the LF appears to follow a progression similar to that previously reported for other tissues[4,8]. During elastogenesis of aorta and lung, fibrillin-1 is the first to be expressed[4] and acts as a scaffold for tropoelastin alignment[5]. Fibulin-4 is required for elastic fiber formation[6] and is thought to chaperone tropoelastin crosslinking and its alignment onto microfibrils[5]. This study demonstrates, for the first time, a spatiotemporal characterization of key proteins involved in elastogenesis of the LF. Moreover, it shows a correlation between the production of these proteins and the appearance of elastic fibers.

In our *in vitro* study, TGFβ2 upregulated scleraxis (based on GFP intensity) in the limb T/L cells, while no significant effects on axial T/L cells were observed, demonstrating differential regulation of T/L cells *in vitro* as a function of anatomical location. TGFβ2 has been shown to be critical for T/L development during embryogenesis[7] and to upregulate scleraxis in mouse embryonic fibroblasts *in vitro*, but its ability to regulate other aspects of tendon development, such as elastogenesis, are unknown. We are continuing to investigate the potential role of TGFβ2 and other soluble factors on elastogenesis and T/L marker regulation of the axial T/L cells *in vitro*. Axial T/L cell differentiation will be characterized, in part, by the spinal ligament tissue markers identified in this work.

REFERENCES: 1. Okuda et al, Spine 2004. 2. Schrader et al, Eur Spine J 1999. 3. Genevay et al, Best Prac Res Clin Rheum 2010. 4. Kelleher et al, Cur Top Dev Bio 2004. 5. Wagenseil et al, Birth Def Res 2007. 6. McLaughlin et al, Mol Cel Biol 2006. 7. Pryce et al, Development 2009. 8. Mariani et al, Am J Respir Cell Mol Biol 2002.

A Novel Method to Quantify the Anatomy of the Anterior Cruciate Ligament: An Experimental study in Goats

[1]D. Tan Nguyen; [2, 3]Martijn van de Giessen; [3]Jeroen P. van den Wijngaard; [3]Pepijn van Horssen; [3]Geert J.Streekstra; [3]Jos A. Spaan; [1]C. Niek van Dijk; [1]Leendert Blankevoort

[1]Orthopaedic Research Center Amsterdam, Department of Orthopaedic Surgery, University of Amsterdam,
[2]Department of Applied Science, Quantitative Imaging group, Delft University of Technology
[3]Department of Bioengineering and Medical Physics, University of Amsterdam

INTRODUCTION: Knowledge of the 3-D collagen fiber architecture of the anterior cruciate ligament (ACL) is important because of its major influence on the biomechanical properties and function. Furthermore, the quantitative data can be utilized as baseline data for computational modeling and for the development of new treatments for cruciate ligament injuries. However, currently there is no objective method to quantify the collagen fiber architecture of ligaments. In this study we propose a novel method based on 3-D imaging to quantify the collagen fiber architecture of the goat ACL. Based on previous anatomic and morphologic studies, we hypothesize that within the goat ACL there exist at least three, distinct fiber orientation populations.

METHODS: To obtain the 3-D data images of the ACL, the imaging cryomicrotoom was used.[1] The automated microtome removed sections of 25µm from the embedded and frozen knee. And after each cut, the surface of the tissue block was illuminated with light with a bandwidth of 510/20nm to excite the autofluorescence of collagen molecules. By taking advantage of this autofluorescent property, collagen fibers can be visualized without the need for histologic processing and staining. Next, the autofluorescent light signals from the tissue block surface was photographed by a camera with an excitation filter (555/30 nm). The process of cutting and imaging is repeated for serial sectioning. And the stack of resulting images was used to form a 3-D reconstruction of the knee joint with the ligaments and other collagenous structures. With a custom fiber tracking software (based on structor tensor) the orientations of the fiber tracts were quantified and a tractography was done.[2] The 3-D orientation, bundle formation, connectivity and lengths of the tracts could be analyzed.

RESULTS: The structure tensor analysis method showed that the fiber tracts within the ACL differ in orientation. Grossly three different color-coded regions within the ACL which could correspondent with the AM bundle as depicted in green, the IM bundle as depicted in yellow, and the posterolateral bundle in red. When calculating the mean and standard deviation from multiple points at each color-coded region we can see that the vectors, defined by its elevation and deviation angle are significantly different from each other. With the tractography we could clearly visualize the twists within the ACL and the histogram of the tract lengths showed 3 peaks, indicative for 3 bundles. The connectivity maps also showed that there are 3 different principal attachments.

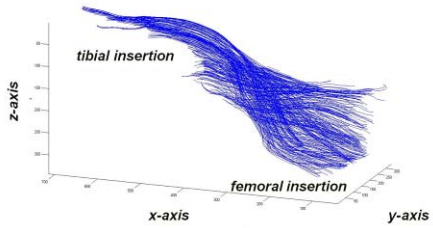

Fig.1A) Tractography of ACL

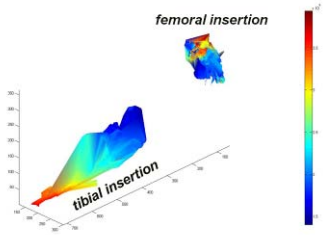

Fig. 1B) Fiber tract length of ACL

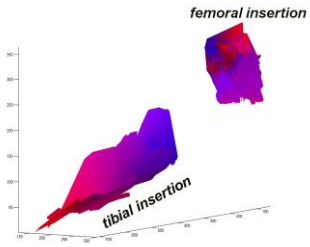

Fig. 1C) Connectivity map of fiber tracts

DISCUSSION: In this study we have quantified the 3-D collagen fiber orientation of the goat ACL. We quantitatively showed that there are three principal collagen fiber orientation populations within the ACL and visualized the fiber tracts, supporting our hypothesis. Additionally we have shown that the imaging cryomicrotome system in combination with fiber tracking and the data analysis is a useful tool to quantify the 3-D collagen fiber architecture.

ACKNOWLEDGEMENTS: The authors acknowledge the statistical expertise of Dr. Changfu Wu and the financial support of the Netherlands Organization for Scientific Research (Mozaiek grant).

REFERENCES: 1) Spaan JA et al., Med Biol Eng Comput. 2005; 2) van Kempen GMP et al., SCIA'99; 3) Fisher NI, Lewis T, Embleton BJJ. Statistical analysis of spherical data 1987

EFFECT OF CYCLE-DEPENDENT DAMAGE ON NORMAL AND HEALING LIGAMENTS

K.A. Fitzpatrick, S.J. Bailey, G.M. Thornton
McCaig Institute for Bone and Joint Health, University of Calgary, Calgary, Alberta

INTRODUCTION

Ligaments are subjected to sustained (creep) and repeated (fatigue) loading during daily activities. Because ligaments resist only tensile loads, fatigue loading has a non-zero mean stress or, rather, is a combination of cyclic and sustained loading. Thus, fatigue damage results from a combination of time-dependent damage from sustained loading and cycle-dependent damage from cyclic loading. The relative effect of time-dependent and cycle-dependent damage may differ between normal and healing ligaments. Our purpose was to examine the effect of time-dependent and cycle-dependent damage on normal and healing ligaments by comparing the time-to-rupture when exposed to continuous cyclic loading with non-zero mean stress (fatigue), sustained loading (non-interrupted creep) and sustained loading with occasional interruptions with unloading-loading cycles (interrupted creep). Our hypothesis was that the time-to-rupture of normal and healing ligaments would be greatest when exposed to non-interrupted creep followed by interrupted creep and then fatigue.

METHODS

Rabbit medial collateral ligaments (MCLs) were fatigue or creep tested at stresses relative to their ultimate tensile strengths (UTS): 60%UTS for normal MCLs [1] (n=11) and 45%UTS for healing MCLs that had healed for 14 weeks following MCL gap surgery [2] (n=10). After standardized preparation and mounting in an MTS system, the knee with isolated MCL underwent two compression-tension cycles from -5N to +2N which stopped at +1N to establish "ligament zero". After measuring MCL geometry and installing an environment chamber (37°C and 99% relative humidity), the MCL underwent 30 preconditioning cycles from +1N to a force corresponding to 5% of normal MCL UTS or healing MCL UTS. *Fatigue*: The MCL was cycled from +1N to a force corresponding to the desired stress level using a sine wave at 1Hz and cycling continued until rupture. *Non-interrupted Creep*: The MCL was loaded from +1N to a force corresponding to the desired stress level using a sine wave at 1Hz and constant force was maintained until rupture. *Interrupted Creep*: The MCL was loaded from +1N to a force corresponding to the desired stress level using a sine wave at 1Hz and constant force was maintained until rupture except when interrupted approximately every hour with one unloading-loading cycle using a sine wave at 1Hz. Time-to-rupture was defined as the last time the MCL supported 99% of the desired test force. Time-to-rupture during fatigue, interrupted creep and non-interrupted creep were compared using Wilcoxon signed-rank or Mann-Whitney U tests.

RESULTS

For normal MCLs tested at 60% of normal MCL UTS, time-to-rupture when exposed to sustained loading (non-interrupted creep) was significantly greater than when exposed to sustained loading that was occasionally interrupted with unloading-loading cycles (interrupted creep) ($p=0.06$; Table 1). For healing MCLs tested at 45% of healing MCL UTS, time-to-rupture during non-interrupted creep was not different than interrupted creep (Table 1). For normal MCLs tested at 60%UTS, time-to-rupture was 46-fold greater when comparing sustained loading (non-interrupted creep) to continuous cyclic loading (fatigue) ($p=0.05$). For healing MCLs tested at 45%UTS, time-to-rupture during non-interrupted creep was 7-fold greater than during fatigue ($p=0.06$).

DISCUSSION

At the different stress levels examined, normal ligaments appear to be more affected by cycle-dependent damage than healing ligaments. For normal MCLs tested at 60%UTS, time-to-rupture was 4-fold greater comparing non-interrupted creep to interrupted creep, and 46-fold greater comparing non-interrupted creep to fatigue. For healing MCLs tested at 45%UTS, time-to-rupture was not different comparing non-interrupted and interrupted creep but was 7-fold greater comparing non-interrupted creep to fatigue. For both normal and healing ligaments, combining cycle-dependent damage from cyclic loading and time-dependent damage from sustained loading expedited rupture.

ACKNOWLEDGEMENTS: NSERC, CIHR, McCaig Fund

REFERENCES: [1] Thornton GM et al. Clin Biomech 22:932, 2007 [2] Thornton GM, Bailey SJ. ISL&T-IX, 2009

Table 1: Time-to-rupture of normal MCLs or healing MCLs exposed to fatigue or creep loading until rupture.

Test Stress Level	Non-interrupted Creep Time-to-Rupture (hrs)	Interrupted Creep Time-to-Rupture (hrs)	Fatigue Time-to-Rupture (hrs)
60% of normal MCL UTS~57 MPa	23.6 [16.1-31.0] (n=2)	5.9 [2.8-11.3] (n=4)*	0.51 [0.09-1.01] (n=5)*^
45% of healing MCL UTS~8 MPa	40.4 [36.3-44.4] (n=2)	31.3 [20.7-40.4] (n=4)	6.0 [0.11-11.4] (n=4)*^

Data are shown as median [range] and normal MCL data are from Ref. [1].
** different than non-interrupted creep ($p<0.06$) and ^ different than interrupted creep ($p<0.07$).*

The effect of Platelet Rich Plasma (PRP) on Tendon Regeneration: an *in vitro* tissue culture study

Joseph Alsousou, Sarah Franklin, Philippa Hulley, Mark Thompson, Eugene McNally, Keith Willett

University of Oxford
Nuffield Department of Orthopaedic Rheumatology and Musculoskeletal Sciences
Oxford, UK

Purpose: The effect of PRP conditioned media on monolayer cell cultured has been studied by our group previously. However, PRP conditioned media effect on cell cultures may not represent PRP effect on tissues. There has been no published study of PRP effect on tendon tissue explants. This study aim is to investigate the response of tendon tissues explants to PRP application in regards to cell proliferation, migration and matrix production.

Methods: This is an *in-vitro* study on tendon explants obtained from Achilles tendon rupture patients. The samples were collected in sterile DMEM F12 solution. Samples were processed as soon as possible after collection. Using scissors or scalpel samples were diced into approximately 1-3mm^3 sections. Tendon pieces were transferred to wells of 6-well-plate and a small drop of media was added. Tendon pieces were spaced in wells, so no more than 50% of the well is used. Explants were incubated at 37c in CO_2 incubator for 48 hours. Tendon explants were cultured in three media types: 1. 100%PRP 2. 50% PRP 3. 50%FCS DMEM F12 media (standard culture medium).

Results:
Cells around each explant were counted using Olympus microscope (n=349). A semi-quantitative score was used to access cell numbers. Kruskal-Wallis statistical test showed that 100%PRP and 50%PRP cultures have significantly higher number of cells (p value 0.002 and 0.028 respectively). Ziva ultrasensetive prolifiration assay on cultured cells revealed that PRP significantly increased cell polifiration. PicoGreen assay confirmed an increase of DNA content in PRP treated explants. In addition, Col I and Col III gene expression increased remarkably with PRP application.

Conclusion: Our findings show that PRP have significant positive effect on Tendon cell rpolifiration and xollagen production. This indicates that PRP may have potential role as an orthobiological agent in Injuried tendon treatemen.

SUBSTANCE P ACCELERATES CELL PROLIFERATION AND ANGIOGENESIS IN AN ANIMAL MODEL OF ACHILLES TENDINOPATHY : EVIDENCE FAVOURING THE INVOLVEMENT OF NEUROPEPTIDES IN TENDINOSIS PATHOLOGY

G. Andersson (1) ✉, L. Backman (1,4), A. Scott (3,4), R. Lorentzon (2), S. Forsgren (1), and P. Danielson (1)
Dept of Integrative Medical Biology, Anatomy (1), and Dept of Surgical and Perioperative Sciences, Sports Medicine (2), Umeå University, Umeå, Sweden.
Centre for Hip Health and Mobility, Vancouver Coastal Health and Research Institute (3), and Dept of Physical Therapy, University of British Columbia (4), Vancouver, BC, Canada

INTRODUCTION

In previous studies we have found evidence favouring that human Achilles tendon cells (tenocytes) are capable of producing the neuropeptide substance P (SP). Furthermore, the preferred receptor for SP (the neurokinin-1 receptor, NK-1R) was widely expressed throughout the tendon, especially in patients suffering from chronic tendon pain (tendinopathy) with tissue changes (tendinosis) including hypercellularity and vascular proliferation. Considering known effects of SP, one might ask whether SP contributes to tendon cell proliferation and neovascularisation in tendinosis. We have an established animal (rabbit) model of Achilles tendinopathy based on overuse in the form of repetitive exercise. Recent studies with this model have shown that tendinosis-like changes are present after 3 weeks of exercise, but not after only 1 week. The current study aimed to test whether the development of tendinosis-like changes would be accelerated during a 1 week course of exercise with repetitive local administration of SP.

METHODS

In total four groups of animals (5-6 New Zealand white rabbits per group) were used. Three of these groups were subjected to the previously established protocol of Achilles tendon overuse for 1 week. One of these groups was not given any injections ('1 week controls'), whereas the second group was given repetitive SP injections in the paratendinous tissue of the Achilles tendon, and the third group ('NaCl controls') was given an equivalent schedule of saline injections. One additional control group existed in which the animals were neither subjected to the overuse protocol nor to any injections ('untrained controls'). Tendon cell number, vascular density, and the possible occurrence of paratendinous inflammation were evaluated. Immunohistochemistry and *in situ* hybridisation to detect NK-1R were also conducted.

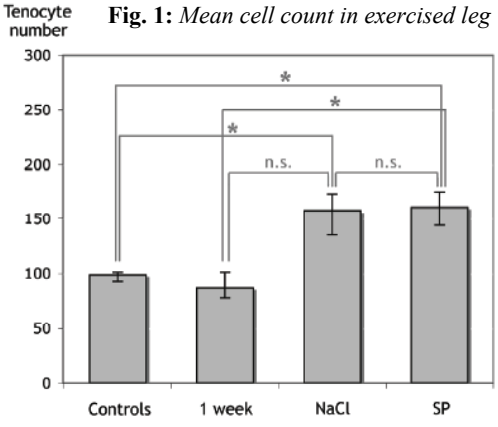

Fig. 1: *Mean cell count in exercised leg*

RESULTS

There was a significant increase in tendon cell number in the SP-injected group compared to both untrained controls and 1-week controls (**Fig. 1**). However, the same phenomenon was noticed for NaCl controls, i.e. tendon cell number was significantly increased in response to NaCl injections compared to untrained controls. There was an increase in the number of tendon blood vessels in the SP-injected group as compared to untrained controls, and this increase in vascularity was not seen for the NaCl controls or the 1-week controls. Paratendinous inflammation, as evidenced by invasion of inflammatory cells in the paratenon, was clearly more pronounced in the SP-injected group than in the NaCl controls. NK-1 R was detected in blood vessel walls (**Fig. 2**), on nerves, on inflammatory cells, and on tendon cells (**Fig. 3**).

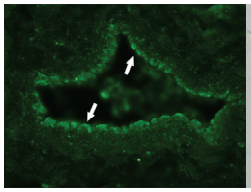

Fig. 2

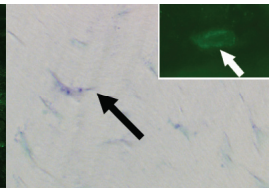

Fig. 3

DISCUSSION

The observations suggest that SP induces tenocyte proliferation and angiogenesis in the rabbit Achilles tendon, thus supporting a potential role of this neuropeptide in the processes that occur in tendinosis. The study corroborates findings in the human Achilles tendon in that NK-1 R was expressed on tenocytes and tendon blood vessel walls, thereby providing a potential anatomic basis for the observed effects of SP on the development of tendinosis. The hypercellularity observed in response to NaCl injections might be due to increased tissue pressure or to stimulation of endogenous SP-production, a phenomenon not unheard of. The angiogenic effect of SP-injections, on the other hand, appeared to be more specifically related to an induction of inflammation in the paratendon.

✉ gustav.andersson@anatomy.umu.se

TENDON CELLS PRODUCE SUBSTANCE P (SP) AND EXPRESS THE NEUROKININ-1 RECEPTOR *IN VITRO* : SP BEING INCREASED AFTER STRAIN AND CAUSING CELL PROLIFERATION

L. Backman (1,3,5) ✉, G. Fong (1), G. Andersson (1), P-A. Oldenborg (2), A. Scott (4,5), and P. Danielson (1)
Dept of Integrative Medical Biology, Anatomy (1) and Histology & Cell Biology (2),
and Dept of Surgical and Perioperative Sciences, Sports Medicine (3), Umeå University, Umeå Sweden.
Centre for Hip Health and Mobility, Vancouver Coastal Health and Research Institute (4), and Dept of Physical Therapy, University of British Columbia (5), Vancouver, BC, Canada

INTRODUCTION

In spite of scientific advances during recent years, the etiology and pathogenesis of tendinosis are yet not fully understood. It is, nevertheless, known that the tendon tissue in tendinosis patients exhibits pronounced changes such as cell proliferation and angiogenesis. Tendon cells in tendinosis tissue have been shown to produce an array of signal substances that was once thought to be confined to neurons. This includes the neuropeptide substance P (SP), but also catecholamines, glutamate, and acetylcholine. Furthermore, because the tendon cells also possess receptors for these signal substances, including the preferred receptor for SP (the neurokinin-1 receptor, NK-1 R), it is possible for the cells to act on themselves in an autocrine/paracrine fashion.

It is previously known that SP has prominent effects on connective tissue, such as cell proliferation, angiogenesis, apoptosis, and neuroinflammation. Experimentally we have furthermore shown that the endogenous production of SP in animal tendons precedes tendinosis-like changes *in vivo*, and that exogenously administrated SP accelerates the occurrence of tendinosis-like changes in the tendon tissue. If this also applies to human tendon tissue, is not known.

In this study, we have established a human tendon cell culture model to study the endogenous production of SP, with and without loading, the expression of the SP receptor NK-1 R, and the effect on the tendon cells *in vitro* by exogenously administered SP.

METHODS

Achilles tendon biopsies from healthy controls were grown as primary cultures. Cells from passage 3 to 6 were used to investigate endogenous SP production with different biochemical methods on protein- and mRNA-level, and the expression of NK-1 R was studied using the same techniques. The FlexCell system was used for 2D *in vitro* loading on collagen I treated plates.

RESULTS

Immunocytochemistry (ICC) and flow cytometry (FACs) demonstrated the presence of NK-1 R in some of the tendon cells. Real-time PCR (RT-PCR) also showed mRNA for NK-1 R in these cells. Presence of SP in the tendon cells was showed with ICC and ELISA, whereas the presence of SP mRNA was confirmed with RT-PCR. The mRNA levels of SP were significantly elevated after loading (Fig. 1). Exogenously distributed SP was found to be proliferative to the tendon cells in a dose-dependent manner up to a plateau phase, after which SP seemed cytotoxic. ICC also illustrated how cells that were positive for SP interacted with cells positive for NK-1 R, suggesting a communication of paracrine attribute also in the *in vitro* culture plates.

Fig. 1: *SP mRNA expression*

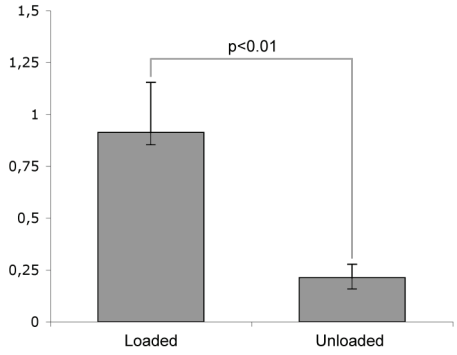

DISCUSSION

The presence of SP and NK-1 R in human tendon cells *in vitro*, confirms previous *in vivo* results, making the theories of an autocrine/paracrine SP loop in human tendon tissue more plausible. The production of SP in human tendon cells is here furthermore for the first time shown on protein level; previous studies on human tendon tissue only having displayed the presence of SP mRNA in these cells.

Overuse is the most frequently accepted extrinsic factor for tendinosis development. In light of that, it is interesting that our *in vitro* loading result show increased SP mRNA as an early response to strain. The increased expression makes it reasonable to consider that SP is involved in mechanistic aspects of overload in tendinosis, and this also confirms *in vivo* results in an animal model. In addition, characteristic of tendinosis are angiogenesis, hypercellularity, and apoptosis, changes that SP has been proven to be associated with in earlier studies. The presence of NK-1 R on the tendon cells provides a morphological correlate for SP to have effects on the cells, and the proliferative effect of SP on human tendon cells is confirmed in this study.

✉ ludvig.backman@anatomy.umu.se

EVIDENCE FOR PRODUCTION OF AND EFFECTS OF TNF-ALPHA IN THE HUMAN ACHILLES TENDON -STUDIES AT PROTEIN AND mRNA LEVELS

J. Bagge[1], J. Gaida[2], H. Alfredson[3], C. Purdam[4], J. Cook[2], S. Forsgren[1]

1. Department of Integrative Medical Biology, Section for Anatomy, Umeå University, Umeå, Sweden
2. Physiotherapy Department, Faculty of Medicine, Monash University, Victoria, Australia
3. Department of Surgical and Perioperative Sciences, Umeå University, Umeå, Sweden
4. Department of Physical Therapies, Australian Institute of Sport, Belconnen, ACT, Australia

INTRODUCTION

Tendinosis is a common, and often disabling condition, particularly among recreational and sports active persons. It is unclear why tissue changes such as collagen disorganization, cell proliferation and (in the late stage of the disease) apoptosis, occur in tendinosis. Furthermore, it is unclear where the pain is coming from. Recent studies have shown that tenocytes, especially in tendinosis tendons, unexpectedly produce several signal substances. TNF-alpha is a substance related to effects such as tissue derangement, apoptosis and pain, and plays an important role in inflammation. It is unclear how TNF-alpha is expressed in human tendon tissue and if TNF-alpha is involved in tendinosis. Therefore, the purpose of the present study was to evaluate the expression patterns of TNF-alpha and its receptor TNF-receptor 1 (TNFR1) in tendinosis and non-tendinosis human Achilles tendons.

METHODS

Biopsies from Achilles tendinosis tendons and pain free normal Achilles tendons were analyzed. Immunohistochemistry was used to evaluate TNF-alpha and TNFR1 at the protein level. In-situ hybridization was used to evaluate TNF-alpha and TNFR1 mRNA expression. Ratings of the immunoreactions were made. Immunostainings for control purpose were performed using two different methods: preabsorbtion with blocking peptide and omission of the primary antibody. Sense probes and stainings for beta actin were performed for control purpose of the in situ hybridazation. For both methods, the expression patterns in control tissues were also evaluated in parallel.

RESULTS

The tenocytes in both tendinosis tendons and normal tendons were immunoreactive for TNF-alpha and for TNFR1. The rating of the intensity of the immunoreactions revealed that TNF-alpha was equally expressed in tendinosis tendons compared to normal tendons. However, interestingly, in the tendinosis tendons, the tenocytes showed clearly stronger immunoreactions of TNFR1 compared to the situation in normal tendons.

Marked TNF-alpha mRNA expression was found in the tenocytes in both tendinosis tendons and normal tendons. Although less clear than for TNF-alpha, TNFR1 mRNA was also found to exist in tendinosis and normal Achilles tendon tenocytes.

DISCUSSION

For the first time, TNF-alpha and TNFR1 were detected at the tissue level in human Achilles tendons. This was evident both at the protein level (i.e. via immunoflourescense) and mRNA-level (i.e. via in-situ hybridization). Thus, the study shows that TNF-alpha and TNFR1 exist and can be produced in the human Achilles tendon. It can be hypothesized that a local production of TNF-alpha can have autocrine/paracrine effects on the tendon tissue. Interestingly, the levels of TNFR1 were stronger in tendinosis tendons than in normal tendons. This implies that tendinosis tendons might be more sensitive to the effects of TNF-alpha, suggesting that tissue changes seen in tendinosis tendons might be related to effects of TNF-alpha. The findings are of great interest as TNF-alpha has well-known effects during tissue reorganization in various tissues, and treatments that interfere with TNF-alpha are used with great success for several conditions. The effects of TNF-alpha on tenocytes will be further explored in our lab.

ACKNOWLEDGEMENTS

The authors want to thank Ulla Hedlund for excellent technical support.

Characterization and Expression of Tenomodulin Isoforms in Human Tendon

[1]Dmochowski, J.M.; [1,2]Qi, J.; [2]Tsuzaki, M; [2,3]Banes, A.N.; [1]Bynum, D.; [1]Patterson, M.; [1]Gomez, S.+[1,2]Banes, A.J., +[1]University of North Carolina, Chapel Hill, NC, [2]Flexcell Int. Corp., Hillsborough, NC, [3]North Carolina State University CVM, Raleigh, NC. banes@flexcellint.com

Introduction: The tendon marker gene, tenomodulin (Tnmd) is a type II transmembrane protein with 7 exons, and 34% homology to chondromodulin-1,a C-terminal, putative anti-angiogenic sequence and furin cleavage site, proliferative sequence and membrane spanning domain. We hypothesized that human tendon would express different amounts of the three isoforms, and be regulated by strain and wounding.

Figure 1. Isoforms of human tenomodulin

Methods: The human genome was data mined for Tnmd sequences, revealing three isoforms. Human flexor digitorum profundus and flexor carpi radialis tendons, tibial bone, medial collateral ligament and soft tissues liver, kidney and brain were collected at surgery or purchased, then cDNAs prepared for quantitative polymerase chain reaction for amplification of Tnmd isoforms 1,2,3. Cells were cultured from human tendons and porcine Achilles tendon (AT) for immunochemical analysis. Samples were analyzed by PAGE and Western blot for protein isoforms and secreted protein. Cells were stretched using a Flexcell strain unit at 1Hz, 3% strain for 1h/d 4 days.

Results: We discovered three reported but unpublished Tnmd isoforms using the Genecards database and I-TASSER molecular modeling program to predict 3D structures and functions (three isoforms (I1: 37.1; I2 28.7, I3 22.1 kDa) (Fig. 1). Modeling program predicted that I1 is a cytosine methyl transferase, I2 a SUMO-2 class protein preventing Ikb degradation in the inflammatory pathway and I3 is a plextrin homology domain protein with a potential structural role. Stretched cells showed Tnmd nuclear localization in response to applied strain (not shown). Western blots showed 4 bands (48.2, 53.7, 62.7, 89.2 kDa). Strain application to cultured cells up then down-regulated expression of I1, as well as causing nuclear translocation of a C-terminal fragment.

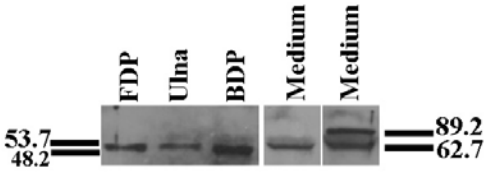

Figure 2. Western blot of human tenomodulin

Discussion: Tnmd is a tendon biomarker with a purported but unvalidated anti-angiogenic function. qPCR and Western blot data demonstrated that Tnmd has three isoforms and at least 4 IC positive bands concordant with multiple isoform expression, glycosylation variants and possible dimerization. The sequence is highly conserved but modeling does not suggest an anti-angiogenic function, rather a regulatory role. Tnmd was readily detectable at the inner PM leaflet or near the nucleus depending on the growth substrate, and showed nuclear translocation post-strain. Tnmd is secreted and may play a role in the matrix. Given the robust growth of tenocytes in vitro from three species, we conclude that Tnmd is not inhibitory to cell proliferation, migration or matrix compaction. Preliminary data indicate that tenocytes do not block angiogenesis in a CAM assay. Taken together, the data indicate a regulatory role for Tnmd underscoring the nuclear translocation. RNAi and reporter construct studies underway will clarify the functions of each isoform in tendon homeostasis.

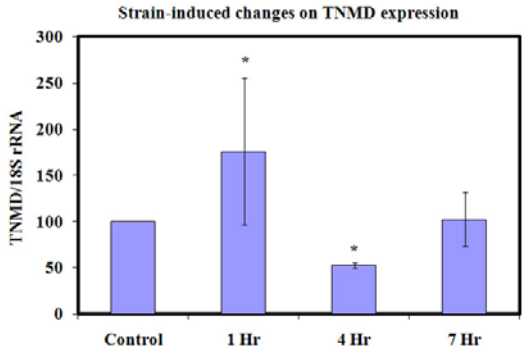

Figure 3. Tenomodulin expression is modulated by strain

References: 1.Brandau et al. 2001 2. Shukunami et al. 2001

Acknowledgements: Supported by a grant from Flexcell Intl Corp.

Resident's Ridge Formation Is Explained by Stress/Strain-Induced Bone Remodeling

Hiromichi Fujie, Ph.D.

Biomechanics Laboratory, Faculty of System Design, Tokyo Metropolitan University, Japan
Research Institute for Science and Technology, Kogakuin University, Japan

INTRODUCTION: The reconstruction technique of the human anterior cruciate ligament (ACL) has been improved in the last decade. Since the ACL attaches to the posterior-superior border of the lateral wall of the intercondylar notch of the femur[1,2], current ACL reconstruction surgery aims to make a femoral bone tunnel for graft fixation as close to the anatomical site of the ACL attachment. Such a surgical technique is called "anatomical ACL reconstruction". Biomechanical studies indicated that joint stability is highly restored in the anatomical ACL reconstruction as compared with the conventional ACL reconstruction[3]. In addition, the cortical bone beneath the ACL attachment site is thicker[4], therefore it is beneficial for graft fixation. In order to succeed the anatomical ACL reconstruction, it is the most crucial to microscopically identify the anatomical site of the ACL attachment. Previous studies indicated that the resident's ridge is located just anterior to the ACL femoral attachment[4-6] and, therefore, can be used as a reference landmark for the anatomical ACL reconstruction. Although the resident's ridge seems to win endorsements of the role in the ACL reconstruction, no explanation was proposed so far as regard with the reason for ridge formation. The author believes that the formation of the resident's ridge can be biomechanically explained. Therefore, the objective of the present study was to propose a biomechanical hypothesis as regard with the resident's ridge formation, and to validate the hypothesis through a finite element method (FEM) analysis of stress/strain-induced bone remodeling.

HYPOTHESIS AND ASSUMPTION: The author proposed a hypothesis that the resident's ridge formation occurs due to stress/strain-induced cortical bone remodeling near the femoral ACL attachment. Since the minimum effective strain (MES) for bone remodeling was reported to range between 800 and 2,000 με by Frost[7], it was assumed that compressive strains above the range evoke adaptive bone remodeling in the present, preliminary study.

FEM ANALYSIS: A computational 2-dimensional model of a cortical bone near the femoral insertion site of the ACL was created using 5x40 pixel-based finite elements in ABAQUS (version 6.4), as shown in Figure 1. The bone was assumed to be homogeneous and isotropic material with Young's modulus of E=30 GPa and Poisson's ratio of ν=0.3 using CPS4R elements. To simulate the ACL force application, while the right and left edges of the model were rigidly fixed, anterior force of 100 N was applied to the centered 9 nodes of the surface with an oblique angle of 10 degree. Strain distribution within the cortical bone was analyzed under the plane stress condition. Using compressive strain as a scalar function, bone surface movement was performed by adding a new pixel on a surface if the local strain exceeded the above-indicated MES. The procedure including the strain analysis and bone surface movement was repeated until equilibrium state was attained.

Results revealed that a ridge-like bone formation occurred in the area anterior to the ACL attachment (grey and black elements), where the resident's ridge is observed in normal knee (Figure 2). The ridge-like bone included a summit of a single element, just anterior to the ACL attachment, and spread not only in anterior area but also beneath the ACL attachment. In addition, the cortical bone exhibited hypertrophy on the reverse side of the ACL attachment (grey elements).

DISCUSSION AND SUMMARY: The present study was performed using a stress/strain-induced bone remodeling theory to explain the formation mechanism of the resident's ridge. It was considered that the ACL force was directly transmitted as a compressive stress to the cortical bone site anterior to the ACL attachment and transmitted as a bending-induced compressive stress to the reverse side of the cortical bone. These stresses caused compressive strains in the cortical bone. We also found that the cortical bone beneath the ACL attachment behind the ridge became thicker, which agrees well with the anatomical observation[4]. Thus, the remodeled bone structure obtained in the analysis corresponded well with the anatomical feature of the bone structure near the ACL femoral attachment (Figure 2). These results suggest that the formation of the resident's ridge and adjacent bone structure is explained by the proposed hypothesis of bone remodeling. Note that the quantitative results were dependent on the analytical condition, however, the trend of obtained results as to ridge formation was identical regardless of the analytical condition. Moreover, the author believes that the hypothesis proposed explains not only the resident's ridge formation but also the formation of other ridges near the bone attachments of the ACL tibial side, Popliteus tendon, Achilles tendon, and so on. More detailed analysis is progressing using a more precise FEM model.

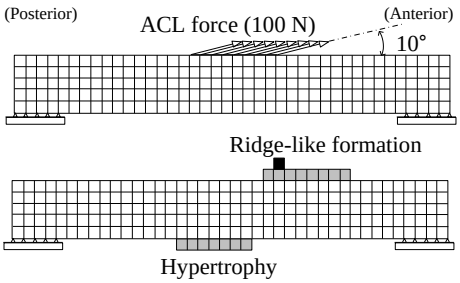

Figure 1: 2-D FEM model of cortical bone subjected to ACL force of 100 N (upper) and a ridge-like bone formation and hypertrophy at the reverse side at 4th step (lower)

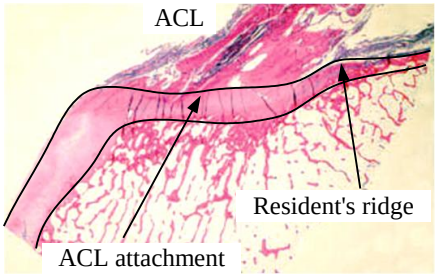

Figure 2: ACL attachment on the femur with the resident's ridge

Reference: 1) Amis and Jacob (1998) *KSSTA*, 2) Shino et al (2009) *KSSTA*, 3) Fujie et al (2011) *ORS*, 4) Hutchinson and Ash (2003) *Arthroscopy*, 5) Shino et al (2008) *Arthroscopy*, 6) Purnell et al (2008) *AJSM*, 7) Frost (1983) *CORR*.

Acknowledgment: The present study was financially supported by the Project-In-Aid for the Establishment of Strategic Research Centers (BERC, Kogakuin University) and Grant-In-Aid for Scientific Research (#20591766) both from the MEXT, Japan, and by Smith&Nephew.

EFFECTS OF LOW-INTENSITY RESISTANCE TRAINING WITH RESTRICTED MUSCLE BLOOD FLOW (KAATSU) ON TENDON REGENERATION AFTER ACL RECONSTRUCTION

Hung chen-chu. [1], Katsumata S. [1], Itakura H. [2], Kuramochi R. [3], Kudo M.[4], and Fukubayashi T. [5]
1: Graduated School of Sport Sciences, Waseda University, Tokorozawa, Saitama, Japan
2:physical therapist of Health Care and Rehabilitation Center, Japan Women's College of Physical Education, Tokyo, Japan
3: Faculty of school of health and sport sciences, Chukyo University, Toyoda, Nagoya, Japan
4: The University of Tokyo Graduate School of Arts and Science, Meguro, Tokyo, Japan
5: Faculty of Sport Sciences, Waseda University, Tokorozawa, Saitama, Japan

【INTRODUCTION】

Some previous studies have already shown that KAATSU training can enhance the skeletal muscle volume (ref. 1). Last year we presented that the regenerated ST tendon showed larger cross sectional area (CSA) in the KAATSU group (ref 2). So, we presumed KAATSU training not only induce the muscle volume hypertrophy but also promote the ST tendon regeneration.

【METHODS】

36 athletes (age: 19-24), who received ACL reconstruction with ST tendon, were separated into KAATSU group and non-KAATSU (control) group. There were 11 males and 7 females in KAATSU group, and 9 males and 9 females in control group. Both groups were applied the same rehabilitation protocol except KAATSU training. KAATSU training usually applied twice a week from one month after the operation up to four month. We evaluated the morphological changes of ST tendon (CSA and T2 relaxation time) with magnetic resonance imaging (MRI) every month after the reconstruction. We also measured the volume of ST muscle. MRI conditions were as follows: repetition time, 3000 ms; echo time, 10, 20, and 30 msec.

【RESULTS】

After starting of KAATSU training, CSA of ST tendon was increased considerably comparing with control group in male athletes (fig 1.), but no difference was found in female athletes.
ST muscle volume slightly increased after six months compared with the control group.
T2 relaxation time was slightly higher in KAATSU group in 1st and 2nd month, but it became the same after 3rd month (fig.2).

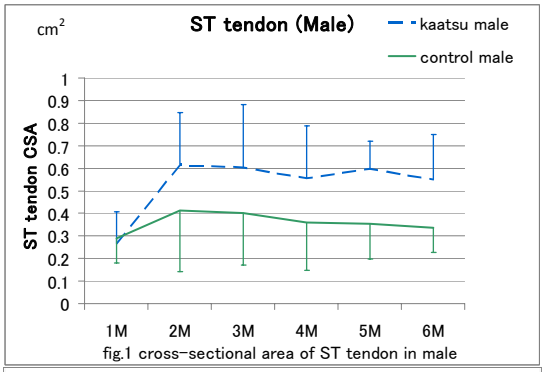

fig.1 cross-sectional area of ST tendon in male

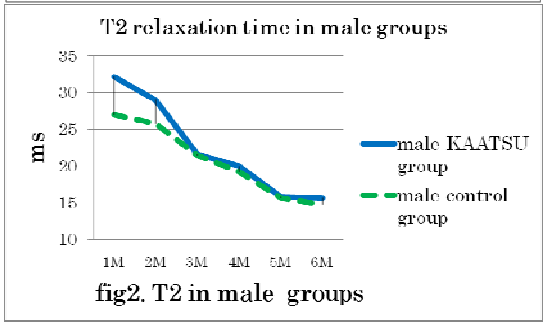

fig2. T2 in male groups

【CONCLUSION】

From our results, KAATSU training may be effective only for the male athletes as far as the tendon regeneration.

【REFERENCES】

1. Kuramochi R. et al: effects of low-intensity resistance training with restricted muscle blood flow on tendon and ligament maturation-study of after ACL reconstruction Hong Kong, ISL&T-X, 2010
2. Yudai Takarada et al: Effects of resistance exercise combined with vascular occlusion on muscle function in athletes, European Journal of Applied Physiology; 86(4): 308-314, Feb 2002

ACTIVATION OF WNT SIGNALING PATHWAY IN AN OSSIFIED FAILED TENDON HEALING ANIMAL MODEL

[1,2]Yuk Wa LEE, [1,2,3]Pauline Po Yee LUI, [1,2]Yin Mei WONG, [1,2]Yun Feng RUI, Xialing ZHANG, Kerong DAI, [1,2]Qi TAN, [1,2]Yuk Wai LEE, [1,2]Ming NI, [1,2]Kai Ming CHAN

1 Department of Orthopaedics and Traumatology, Faculty of Medicine, The Chinese University of Hong Kong, Hong Kong SAR, China.
2 The Hong Kong Jockey Club Sports Medicine and Health Sciences Centre, Faculty of Medicine, The Chinese University of Hong Kong, Hong Kong SAR, China.
3 Program of Stem Cell and Regeneration, School of Biomedical Science, The Chinese University of Hong Kong, Hong Kong SAR, China

INTRODUCTION

Osteo-chondrogenic BMPs were reported to contribute to ectopic chondro-osteogenesis and failed healing in tendinopathy. The Wnt signaling plays a vital role in stem cell proliferation and differentiation, bone homeostasis, pathological calcification and was shown to cross-talk with the BMP signaling pathway. This study aimed to examine the activation and spatial-temporal expression of Wnt pathway mediators in an ossified failed tendon healing animal model.

METHODS

0.3mg of collagenase was injected into the patellar tendon of 30 rats to induce ossified failed tendon healing (Lui et al., 2009). Equal volume of saline solution was injected into the patellar tendon of 5 rats to serve as controls. Patellar tendons of collagenase group were harvested at week 2, 4, 8, 12 and 16 (n=5 for each group). Patellar tendons of saline group were harvested at week 16. The spatial and temporal expression of Wnt3A (a member of Wnt protein family responsible for activating the canonical Wnt pathway), Lrp5 (a Wnt co-receptor) and beta-catenin (key transcription factor mediating the functions of the canonical Wnt pathway) were examined by immunohistochemistry.

RESULTS

There was activation of Wnt pathway in the ossified failed tendon healing animal model. The spatial and temporal expression pattern of Wnt3A, Lrp5 and beta-catenin were similar. There was no expression of Wnt3A, Lrp5 and beta-catenin in the saline group. At week 2, strong expression of Wnt3A was observed in the healing tendon cells while mild expression of Lrp5 and beta-catenin were observed in those cells. Increased expression of Wnt3A, Lrp5 and beta-catenin in healing tendon cells were observed at week 4. The expression levels of Wnt3A, Lrp5 and beta-catenin decreased in the healing tendon cells, but increased in the chondrocyte-like cells at week 8. High expression level of Wnt3A, Lrp5 and beta-catenin were found in the ossified deposits and chondrocyte-like cells at week 12 and remained high thereafter.

DISCUSSION

There was increased expression of Wnt3A, Lrp5 and beta-catenin in the healing tendon cells, chondrocyte-like cells and ossified deposits in the animal model, which showed similar spatial-temporal expression pattern to osteo-chondrogenic BMPs reported in our previous studies (Lui et al., accepted). Activation of the Wnt signaling pathway and its interaction with osteo-chondrogenic BMPs might contribute to ectopic chondro-osteogenesis and failed healing in tendinopathy.

ACKNOWLEDGEMENTS

This work was supported by equipment / resources donated by the Hong Kong Jockey Club Charities Trust

REFERENCES:

1. Lui PPY, Fu SC, Chan LS, Hung LK, Chan KM. Chondrocyte phenotype and ectopic ossification in collagenase-induced tendon degeneration. J Histochem Cytochem 2009; 57, 91-100.
2 Lui PPY, Wong YM, Rui YF, Lee YW, Chan LS, Chan KM. Expression of Chondro-osteogenic BMPs in Ossified Failed Tendon Healing Model of Tendinopathy. J Orthop Res, accepted.

TRIGGER FINGER IS A FORM OF TENDINOSIS

A-C Lundin (1), P Eliasson (2) and P Aspenberg (2)

Department of Hand and Plastic surgery (1), Department of Orthopaedics (2), IKE, Faculty of Health Science, Linköping University, Linköping, Sweden

INTRODUCTION

At surgery for trigger finger, the tendons often appear swollen, with loss of natural colour and lustre. It is widely considered that the major pathology lies in the A1-pulley. There are many publications concerning pulley pathology and histology, but all papers about tendon histology in trigger fingers that we have found were written before the tendinosis concept became accepted.

We hypothesized that trigger fingers would show similar histopathology as tendinosis in the Achilles tendon.

METHODS

We took 39 Biopsies from FDS and FPL tendons during surgery for trigger finger and 10 control biopsies during surgery for carpal tunnel syndrome and amputations. They were given a random number, sectioned parallel to the longitudinal axis of the tendon, and stained. Ten H&E- and Acian blue (Abl) slides were excluded (6 trigger fingers, 4 controls) and eleven Van Gieson slides (VG) (7 trigger fingers, 4 controls), all because of poor slide quality.

Two investigators independently analyzed the material under light microscope in a blinded fashion.

The VG glasses were classified as normal or abnormal.

The H&E and Abl glasses were analyzed using a modification of the Movine score, a semi quantitative grading scale used in achillodynia, with separate assessment of fibre structure, fibre arrangement, rounding of the nuclei, regional variations in cellularity, decreased collagen stainability, hyalinization and glucosaminoglycan content. The total histological score for a given slide could vary between 0 (normal) and 18 (the most severe abnormality).

RESULTS

The two investigators came to identical results analysing the VG slides, all 6 control biopsies were rated as normal, and 31 of the 33 trigger finger biopsies as abnormal.

Then we scored the 38 H&E and Alb slides. The mean score for the trigger finger material was 13.9 (SD 3.2) and for the normal material 2.5 (SD 1.9) with an inter investigator variability of 3.6.

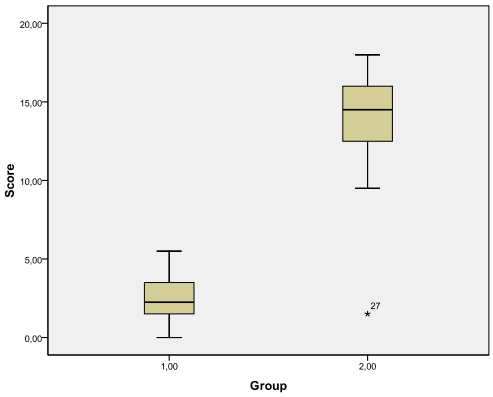

DISCUSSION

We saw a histological picture resembling Achilles tendinosis in the analyzed trigger finger biopsies, but not in the control material.
We also showed that it is possible to discriminate control biopsies from trigger finger biopsies.
But we can´t be sure that this is true of course.
One weakness of the study is that the material is small, Another weakness is that only two of the biopsies in the control material were taken from under the first annular ligament. The other control biopsies had to be taken from a slightly more distal site due to surgical access. But still we can describe tendinosis-like changes in the trigger finger biopsies.
We are not sure of the clincal implications but it is intriguing with a description of tendon pathology in a disease until now described as a pathology in the annular ligament
And as we se it, this means that we have one more tendon to use in the field of tendinopathy research.

REFERENCES

1. Movin, T. et al. (1997). "Tendon pathology in long-standing achillodynia. Biopsy findings in 40 patients." Acta Orthop Scand **68**(2): 170-175.
2. Maffulli, N., V. Barrass, et al. (2000). "Light microscopic histology of achilles tendon ruptures. A comparison with unruptured tendons." Am J Sports Med **28**(6): 857-863.
3. Moore, J. S. (2000). "Flexor tendon entrapment of the digits (trigger finger and trigger thumb)." J Occup Environ Med **42**(5): 526-545.
4. Xu, Y. and G. A. Murrell (2008). "The basic science of tendinopathy." Clin Orthop Relat Res **466**(7): 1528-1538.

PROBING BIOCHEMICAL CONTRIBUTIONS TO MECHANICAL PROPERTIES OF DEVELOPING TENDON

J.E. Marturano, Z.A. Schiller, and C.K. Kuo
Department of Biomedical Engineering, Tufts University, Medford, MA, USA

INTRODUCTION

The mechanical properties of adult tendon have been extensively studied with macro-scale tensile tests. In contrast, those of small embryonic tissues and relationships between localized mechanical properties and tissue composition have not been characterized. Localized tendon mechanical properties on the nano- and micro-scale and their correlation to tissue composition may be particularly relevant to developing cells. Using force-volume atomic force microscopy (FV-AFM), we previously characterized changes in small-scale embryonic chick tendon elastic modulus and found that average modulus increases by 3- or 10-fold depending on probe size[1]. However, a defined correlation between mechanical and compositional changes in developing tendon has yet to be established. While GAGs[2] and collagen crosslinking density[3] have been strongly correlated with mechanical properties in adult tendon, little is known about their mechanical contributions to embryonic tendon during development. In this study, we investigated trends in DNA and glycosaminoglycan (GAG) content and also the effects of crosslinking inhibition via β-aminopropionitrile (BAPN) treatment on mechanical properties during tendon development.

METHODS

Tendon composition: Chick embryos were sacrificed between Hamburger-Hamilton (HH)[4] stages 28 to 43 (ca. 5.5-18.5 days). Tendon dry-to-wet mass ratio was obtained by weight pre- and post-lyophilization. DNA mass was isolated with PCI-ethanol[5] and assayed at 260 nm absorbance. GAG mass was quantified using a DMMB absorbance assay[6] with DNA interference deducted. *FV-AFM*: An AFM probe with 20 nm radius and 0.06 N/m stiffness was employed. Indentation arrays (16x16) were captured over a 10x10 μm area on tissue that had been cryosectioned (20 μm) and immersed in PBS.

RESULTS

We found that tendon dry-to-wet mass ratio varies considerably during development, and DNA-to-dry mass progressively decreases by 3-fold (Fig. 1a). Interestingly, GAG-to-dry mass ratio remained nearly constant (Fig. 1b), and GAG-to-DNA mass ratio increased beginning at HH 38 (Fig. 1c). When treated with BAPN, no significant differences in fiber morphology were observed using second harmonic generation imaging, as compared to saline treated controls[7]. However, BAPN treatment reduced average tendon elastic modulus by 30% when measured via FV-AFM (Fig. 2).

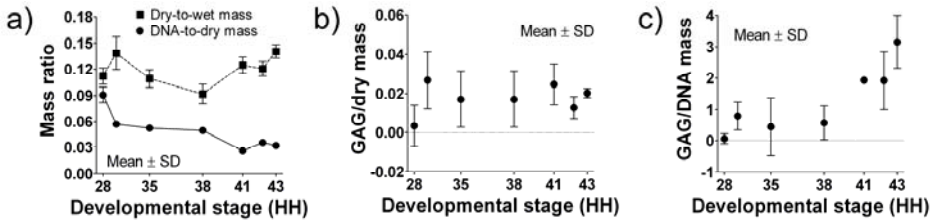

Figure 1: Changes in tendon composition during embryonic tendon development between HH 28, 30, 35, 38, 41, 42 & 43. a) Tendon dry-to-wet mass (top curve) and DNA-to-dry mass (bottom curve), b) GAG-to-dry mass, and c) GAG-to-DNA mass.

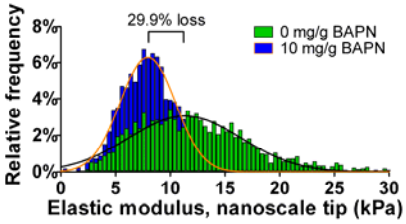

Figure 2: Preliminary FV-AFM elastic modulus histograms of HH 40 tendon with 0 or 10 mg/g BAPN treatment. A 29.9% average decrease was found.

DISCUSSION

During the rapid increase in apparent modulus in late tendon development (HH 38-43)[1], dry-to-wet mass and DNA-to-dry mass ratios were inversely related with time (Fig. 1a), suggesting that cellular contributions to elastic modulus are highest in early development. While GAG/DNA ratios increased with time, and at later stages were in the range of those found in 14 wk. murine tail tendon[8], constant GAG-to-dry mass ratios (Fig. 1b) suggested limited contribution to increasing modulus. Given this, we examined collagen crosslinking as an influential contributor to increasing tendon elastic modulus. Interestingly, BAPN treatment had minimal effect on collagen morphology yet reduced elastic modulus by 30% (Fig. 2), suggesting that collagen crosslinking contributes significantly to tendon elastic modulus. We are currently investigating these and other elements that may contribute to embryonic tendon mechanical properties.

REFERENCES: 1. Marturano et al. ORS Transactions 2010. 2. Robinson et al. J Biomech Eng 2005. 3. Couppé et al. J Appl Physiol 2009. 4. Hamburger & Hamilton J Morphol 1951. 5. Chomczynski & Sacchi Nat Protoc 2006. 6. Barbosa et al. Glyobiology 2003. 7. Marturano et al. ORS Transactions 2011. 8. Mikic J Orthop Res 2008.

Tendon-derived Stem Cell (TDSC): A Better Stem Cell Source Compared to Bone Marrow-derived Mesenchymal Stem Cell (BMSC) for Tendon Regeneration?

Ming Ni, MDa,1,2,5; Pauline Po Yee Lui, PhD§,a,1,2,3; Yun Feng Rui, MDb,1,2; Yuk Wa Lee, MPhil b,1,2;Tsui Yu Mok, MScb,1,2; Yuk Wai Lee, PhD b,1,2; Qi Tan, MPhil b,1,2; Yin Mei Wong, MPhil b,1,2; Siu Kai Kong, PhD4; Pui Man Lau, MPhil4; Gang Li, PhD1,2,3; Kai Ming Chan, MD1,2

1 Department of Orthopaedics and Traumatology, Faculty of Medicine, The Chinese University of Hong Kong, Hong Kong SAR, China.

2 The Hong Kong Jockey Club Sports Medicine and Health Sciences Centre, Faculty of Medicine, The Chinese University of Hong Kong, Hong Kong SAR, China.

3 Program of Stem Cell and Regeneration, School of Biomedical Science, The Chinese University of Hong Kong, Hong Kong SAR, China.

4 Department of Biochemistry, The Chinese University of Hong Kong, Hong Kong SAR, China.

5 The Department of Orthopaedics, The General Hospital of Chinese PLA, Beijing, China, 100853.

a Ni M and Lui PPY have equal contribution in this work.

b Rui YF, Lee YW, Lee YW, Tan Q, Wong YM have equal contribution in this work.

INTRODUCTION

Adult stem cells hold great promise to be used for tendon repair and regeneration. This study aimed to compare the effect of allogeneic TDSCs and BMSCs for tendon repair as well as to investigate their repair mechanisms.

METHODS

Sprague Dawley rats with patellar tendon window injury were divided into 3 groups: Fibrin glue constructs with or without tendon-derived stem cells (TDSCs) and bone marrow-derived stem cells (BMSCs) from GFP rats were transplanted into the window defect. At various times, one batch of animals were killed and the patellar tendon was harvested for ex vivo imaging of GFP signal, followed by routine histology, polarization microscopy, while another batch of animals was killed for biomechanical test. Data was presented as mean ± SD and shown in boxplots. Comparison of biomechanical parameters of the 3 groups was done using Kruskal-Wallis test, and then the comparison of biomechanical parameters of any two groups was done using Mann-Whitney U test as the data was not normally-distributed. All the data analysis was done using SPSS (SPSS Inc, Chicago, IL, version 16.0). $p<0.050$ was regarded as statistically significant.

RESULTS

Patellar tendon healing in the TDSCs and BMSCs groups was significantly better compared to that in the control group, as indicated by higher cellularity at week 1 and more extracellular matrix production at week 2 and week 4. Higher vascularity was noted in the BMSCs group at week 1 compared to those in the TDSCs and control groups. The window gap has more fibrillar tissues in the TDSCs and BMSCs groups compared to that in the control group at week 2. At week 4, the TDSCs group showed more extracellular matrix production as well as better cell and fiber alignment than that in the control group and BMSCs group. The transplanted TDSCs, as indicated by the GFP signal they carried, were localized in the wound gap at week 1 and 2 and became undetectable at week 4, whereas the transplanted BMSCs were only seen at week 1 and became undetectable at week 2 afterwards. Both the ultimate stress and Young's modulus were significantly higher in the TDSCs and BMSCs groups compared to those in the control group at week 4 (all $p<0.050$), but there was no significant difference between the TDSCs and BMSCs groups. No obvious immuno-rejection with the transplantation of allogeneic TDSCs and BMSCs was observed.

DISCUSSION

Preliminary data supported that histologically slightly better outcome with the use of TDSCs compared to BMSCs. TDSCs can be an alternative cell source for tendon tissue engineering. Further experiments are required to confirm whether allogeneic TDSCs is a better alternative source compared to BMSCs for tendon repair

ACKNOWLEDGEMENTS

This work was supported by equipment/resources donated by the Hong Kong Jockey Club Charities Trust.

REFERENCES:

1. Rui YF et al. Tissue Engineering Part A 2010.
2. Chong AKS et al. J Bone Joint Surg Am 2007.
3. Juncosa-Melvin N et al. Tissue Eng 2006.
4. Harris MT et al. J Orthop Res 2004
5. Ryan JM et al. J Inflamm (Lond) 2005
6. Van EF et al. Tissue Eng 2004

Location Specific Role according to the Degree of Repair Completion of Massive Cuff Tear on Glenohumeral Joint Biomechanics

Joo Han Oh[†*], Michelle H. McGarry[†], Bong Jae Jun[†],
Akash Gupta[†], Kyung Chil Chung[†], James Hwang, Thay Q Lee[†]
[†]*Orthopaedic Biomechanics Laboratory, VA Healthcare System and UC Irvine, Long Beach, CA*
[*]*Department of Orthopedic Surgery, Seoul National University College of Medicine, Korea*

INTRODUCTION: The development of new instruments and surgical techniques has improved the outcome of rotator cuff repair even in massive tears; however, based on cuff integrity or amount of retraction with massive cuff tears a complete repair may not be possible allowing for only partial repair. The cuff integrity or amount of retraction in massive cuff tear affects the degree to which the repair can be completed. The effect of degree of repair completion of massive cuff tears on glenohumeral joint biomechanics has not been evaluated. Therefore, the purpose of this study was to compare the rotational range of motion, glenohumeral kinematics and gap formation following massive rotator cuff tear and repair according to the degree of repair completion.

METHODS: Eight fresh frozen cadaveric shoulders were tested with a custom testing system (Figure 1). All soft tissues were removed except the glenohumeral joint capsule, insertion of rotator cuff muscles, deltoid, pectoralis major and latissimus dorsi. Muscle loading was applied based on the ratio of the physiological muscle cross-sectional areas: 20N for supraspinatus, 30N for subscapularis, infraspinatus/teres minor, pectoralis major, and latissimus dorsi, and 60N for deltoid. Testing was performed in the scapular plane with 0°, 30°, and 60° shoulder abduction with a 2:1 ratio of glenohumeral to scapular abduction. Maximum internal rotation (Max IR) and external rotation (MaxER) were measured with 3.4 Nm of torque. The position of the humeral head apex (HHA) with respect to the glenoid was measured using a MicroScribe 3DLX from Max IR to Max ER in 30º increments. Gap formation was measured at 4 points from anterior to posterior using the MicroScribe at every rotation in 0º abduction. Following testing of the intact rotator cuff, a massive rotator cuff tear was created by incision of the supraspinatus and infraspinatus tendon from their insertions on the greater tuberosity. A complete repair consisting of a posterior transosseous equivalent repair (TOE) with anterior single row repair and two anterior margin convergence sutures was performed. Testing was then repeated for four different partial repairs (Figure 2). For partial repair 1, the anterior single row repair was released. For partial repair 2, the margin convergence sutures were released. For partial repair 3, the posterior TOE was released and a posterior single row repair with two anterior margin convergence sutures was performed. Finally, for partial repair 4, the margin convergence sutures were removed. Range of motion, humeral head apex position and gap formation at each condition were compared using a repeated measures ANOVA with a Tukey post hoc test was used for statistical analysis with a significance level of 0.05.

RESULTS: Massive tear increased total ROM and shifted the humeral head apex superiorly in maximum internal rotation compared to the intact condition ($p < 0.05$). The complete repair (posterior TOE, anterior single row, and margin convergence) restored rotational ROM to intact, while all partial repairs did not. Abnormal humeral head apex elevation due to massive cuff tear was restored by all repairs to the intact condition at all abduction angles ($p<0.05$). Release of the anterior single row significantly increased the anterior gap formation in all humeral rotation positions ($p<0.05$). Release of the marginal convergence sutures also significantly increased the anterior gap formation at all humeral rotation positions with posterior TOE and for maximum external rotation with posterior single row ($p<0.05$).

DISCUSSION: Only complete repair of both the supraspinatus and infraspinatus tendons restored both the rotational range of motion and glenohumeral kinematics to the intact state. Infraspinatus repair was necessary to maintain normal glenohumeral joint kinematics even with anterior partial repair. Margin convergence was effective to decrease anterior gap formation. This study demonstrates the location specific role according to the degree of repair completion in restoring abnormal shoulder biomechanics due to massive cuff tear.

ACKNOWLEDGEMENTS
VA Rehab R&D and Medical Research
California Orthopaedic Research Institute

REFERENCES: 1. Burkhart SS et al., Arthroscopy. 10(4): 363-370, 1994. 2. Duralde XA and Bair B. J Shoulder Elbow Surg.14: 121-127, 2005. 3. Moser M et al., Orthopedics. 30(6): 479-482, 2007

Morphological changes of human-derived mesenchymal stem cells in response to freezing preservation

Kei Oya[1], Ryo Emura[2], Hiroki Sudama[2], Kazunori Shimomura[3], Norimasa Nakamura[3], and Hiromichi Fujie[4,1]

[1] Research Institute for Science and Technology, Kogakuin University, Tokyo, Japan
[2] Graduate School of Engineering, Kogakuin University, Tokyo, Japan
[3] Department of Orthopaedic Surgery, Osaka University Medical School, Osaka, Japan
[4] Faculty of System Design, Tokyo Metropolitan University, Tokyo, Japan

INTRODUCTION

Stem cell-based therapies have great potentials for the regeneration of tissues or organs injured in accidents or diseases. The mesenchymal stem cells (MSCs), which are one of the somatic stem cells, have various differentiation potentials not only to osteocytes, chondrocytes, and adipocytes, but also to ligament/tendon fibroblasts. Therefore, one expectation of regenerative therapies for ligaments and tendons is the use of MSCs. For this purpose, we have developed a novel tissue-engineering technique which involves a stem cell-based self-assembled tissue (scSAT) bio-synthesized from synovium-derived MSCs[1)]. The MSCs are generally used without cell freezing preservation after isolating from body tissues. However, it is often difficult to obtain a sufficient amount of MSCs from the tissues. Therefore, it may be required to establish a freezing preservation technique of the MSCs. However, the changes in biological properties of MSCs due to freezing preservation have not been sufficiently clarified. Therefore, the aim of this study was to determine the properties of human synovium-derived MSCs subjected to cell freezing preservation. In addition, the properties of scSAT bio-synthesized from the preserved MSCs were also investigated.

METHODS

Synovium-derived MSCs obtained from the synovial membrane of human knee joints were grown in a cultivation medium (Dulbecco's modified Eagle medium (DMEM) supplemented with 10% fetal bovine serum (FBS), 100 U mL^{-1} penicillin and 100 μg mL^{-1} streptomycin). The cells were incubated at 37°C in a fully humidified atmosphere of 5% CO_2 in air. The cells were passaged 4 times after primary culturing. The cells were frozen at a rate of −3°C min^{-1} and preserved in a cell-freezing medium (BLC-1P, Juji field Ins.) at −80°C for 24 h after harvesting by trypsinization. Then they were thawed in hot water at a rate of 60°C min^{-1} up to 37°C and cultured for 14 days in the conditions identical to that before freezing (freezing group). The proliferation rate and morphologies of the MSCs were observed: The proliferation rate was measured with cell counting and the morphologies were observed using a phase contrast microscope and a scanning electron microscope (SEM). Moreover, the cells were seeded on the tissue culture treated dishes at 6.0 x 10^5 cells cm^{-2} in a cultivation medium supplemented with 0.2 mmol L^{-1} ascorbic acid-2 phosphate to promote the bio-synthesis of extracellular matrix (ECM). After ECM maturation, synthesized matrices were detached from the culturing dishes and allowed to undergo natural construction for 1 h to develop scSATs[2)]. The thicknesses of the scSATs were determined. In addition, the morphologies of the scSATs were observed. As a control, non-frozen MSCs cultured in the conditions identical to that for the freezing group were prepared.

RESULTS and DISCUSSION

The MSCs in both freezing and control groups were adhered, extended, and proliferated well on the cell culturing dishes. However, the numbers of the MSCs in freezing group were less than those in control group. Moreover, the proliferation rate of the MSCs in freezing group was also less than that in control group. Although no significant morphological difference was observed between two groups, the scSATs was thinner in freezing group than in control group. The obtained results suggest that the freezing preservation has a negative effect on the cell adhesion and ECM production. This may be attributable to the changes in intra/extracellular events such as gene expressions and protein productions due to the freezing preservation.

ACKNOWLEDGEMENTS

The present study was financially supported in part by the Project-In-Aid for the Establishment of Strategic Research Centers from the MEXT, Japan (BERC, Kogakuin University).

REFERENCES: 1) Ando W. *et al*., Biomaterials, 28, 5462-70, 2) Emura R. *et al*., Proceedings of the 6th World Congress on Biomehanics, 2010.

EXPRESSION OF CHONDRO-OSTEOGENIC BMPs IN CLINICAL SAMPLES OF CALCIFYING AND UNCALCIFYING PATELLAR TENDINOPATHY - A HISTOPATHOLOGICAL STUDY

Yun Feng Rui, MD[1,2,5]; Pauline Po Yee Lui, PhD[1,2,3]; Christer Gustav Rolf, MD[4]; Yin Mei Wong, MPhil[1,2]; Yuk Wa Lee, MPhil[1,2]; Kai Ming Chan, MD[1,2]

1 Department of Orthopaedics and Traumatology, Faculty of Medicine, The Chinese University of Hong Kong, Hong Kong SAR, China. 2 The Hong Kong Jockey Club Sports Medicine and Health Sciences Centre, Faculty of Medicine, The Chinese University of Hong Kong, Hong Kong SAR, China. 3 Program of Stem Cell and Regeneration, School of Biomedical Science, The Chinese University of Hong Kong, Hong Kong SAR, China. 4 Department of Orthopaedics, Clintec, Karolinska Institutet, Stockholm, Sweden. 5 Department of Orthopaedics, Ninth People's Hospital, Shanghai Jiaotong University School of Medicine, Shanghai, P.R. China.

Introduction: The pathogenesis of chronic tendinopathy is unclear. Expression of BMP-2/-4/-7 was reported in ectopic chondro-ossification sites in an ossified failed tendon healing animal model of tendinopathy. This study aimed to investigate the expression of these chondro-osteogenic BMPs in clinical samples of patellar calcifying and un-calcifying tendinopathy.

Methods: Patellar tendon samples were collected from 15 patients with patellar tendinopathy and 15 controls undergoing anterior cruciate ligament (ACL) reconstruction with patellar-patellar tendon-bone autograft. Ossification observed in one tendinopathy sample was characterized by histology, alizarin red S staining, alcian blue staining, TRAP staining and immunohistochemical staining of Sox9, OPN and OCN. The expression of BMP-2/-4/-7 was examined in all samples using immunohistochemistry.

Results: Regions of hypo- and hyper- cellularity and vascularity, with loss of crimp structure of collagen matrix, were observed in tendinopathy samples. Round cells and in some cases, cells with typical chondrocyte phenotype were observed. For the sample with ectopic ossification with positive alizarin red S staining, OPN- and Sox9-positive chondrocyte-like cells with alcian blue stained extracellular matrix, OCN-positive osteoblast-like cells and TRAP-positive multi-nucleated cells were observed surrounding the ossified deposits. No expression of BMP-2/-4/-7 was observed in healthy tendons while moderate and strong expression of BMP-2 and BMP-4/7, respectively, were observed in the un-calcifying tendinopathy samples. The calcifying tendinopathy sample showed the strongest and weakest expression of BMP-2 and BMP-7, respectively, among all the tendinopathy samples.

Discussion: Ectopic expression of BMP-2/-4/-7 was observed in calcifying and un-calcifying tendinopathy and these chondro-osteogenic BMPs may play roles in their pathogenesis. A clearer understanding of the pathogenesis of tendinopathy may lead to new treatment strategies aiming at inhibiting the activities of these chondro-osteogenic BMPs.

Acknowledgements:

This work was supported by equipment / resources donated by the Hong Kong Jockey Club Charities Trust.

METHOD FOR STATIC AND DYNAMIC MECHANICAL STIMULATION OF SCAFFOLD-FREE ENGINEERED SINGLE FIBERS FOR TENDON CONSTRUCTS

N.R. Schiele, D.B. Chrisey, and D.T. Corr
Department of Biomedical Engineering, Rensselaer Polytechnic Institute, Troy, NY

INTRODUCTION

In an effort to mimic embryonic tendon development, we have developed a cell-based and scaffold-free method to direct fibroblast cell growth to form single fibers [1,2]. A scaffold-free approach toward tendon engineering presents a unique challenge, as there is no initial structure to apply the necessary external mechanical stimulus. Early application of mechanical cues (within hours of cell attachment) is essential to achieve the desired cell and fiber alignment, tissue maturation, and most significantly, mechanical properties. As an important step towards scaffold-free tendon constructs, the objective of this study was to establish a method to provide the necessary static and dynamic mechanical cues to the growing fibers, to ultimately achieve the desired structure and mechanical properties.

METHODS

To create growth channels, an UV laser (TeoSys, Crofton MD) was used to micromachine 3D features in 2% agarose gel, creating linear channels of 1.6-cm length, ~250-μm width, and ~100-μm depth. Collagen type I sponge disks (4-mm diameter, Kensey Nash, Exton, PA), with a 1-mm diameter centered through-hole, were placed into 4-mm cut-outs in the agarose at both ends of the linear channels. FlexCell® Tissue Train® plates were modified to include loading pins affixed to each tab on the plate. The growth channel assemblies were then mounted on the pins of the modified Tissue Train® plate, to allow application of uniaxial tension (**Fig1**). Human fibronectin (BD Bioscience, Bedford, MA) was pipetted (30 μl of 0.3 mg/ml) into each collagen sponge disk, allowed to wick into the growth channel, and then dried in a laminar flow hood for one hour. Human dermal fibroblast cells (1.0 ml of ~5 x 10^5 cells/ml) in culture media (89.5% DMEM, 10% FBS, 0.5% penicillin-streptomycin, 50 μg/ml L-ascorbic acid) were introduced to the growth channels using a pipette. Following fibroblast-seeding, the growth channels were incubated for 24 hrs (37 °C, 5% $C0_2$, 95% RH) under static tension. Static tension was verified by transecting the formed fibers after 20 hrs of incubation (n=2). The modified Tissue Train® assemblies were mounted into the FlexCell® system and dynamically strained (0.75% strain at 0.5 Hz for 8 hrs, 8 hrs of static tension, and 1.0% strain at 0.5 Hz for the final 8 hrs). Identical construct assemblies not subjected to dynamic strain in the FlexCell® system served as static tension controls. Following mechanical loading (static tension and dynamic cyclic strain), fibers were removed from the growth channels, placed on glass slides, and imaged with polarized light microscopy (20X).

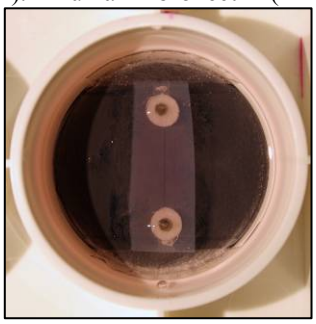

Fig1. Tissue Train® plate with mounted growth channel

RESULTS

Fibroblasts-derived fibers integrated into the collagen disks at the ends of the linear channels and provided the initial growth cue of static tension. Generation of axial tension within 20 hours of seeding the channels with cells was verified, as the transected fibers retracted toward the collagen disks. This retraction was most pronounced when transected within close proximity (~1 mm) to the disks. Dynamically strained fibers formed collagen structures, clearly visible with polarized light microscopy within 48 hrs (**Fig2**).

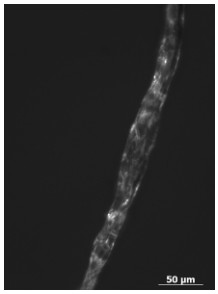

Fig2. Polarized light image of a cyclically strained fiber

DISCUSSION

We have developed a method to provide early application of the mechanical cues necessary for tissue maturation of a scaffold-free engineered construct. The collagen disks provide the structure necessary for both static and dynamic mechanical stimulation of the fiber. Furthermore, the collagen disks allows cellular and fiber integration into a rigid structure at each end of the growth channel within the first few hours (4-6 hrs) of cell growth, to provide the initial cue of static tension. At 24 hours, the cell-based constructs are sufficiently stable to allow application of dynamic (cyclical) strain using the collagen disks as points of attachment to a modified FlexCell Tissue Train® system. This method represents the first step toward replicating the high-cellularity of embryonic tendon and the necessary mechanical cues during development.

REFERENCES

1. Schiele N.R. et. al., 2008, Proceeding, ASME 2008 Summer Bioengineering Conference, B.B. Lieber et al., eds.
2. Schiele N.R. et. al., 2009, Proceeding, ISLT-IX, S.L-Y. Woo et al., eds.

Long-term survival of concurrent meniscus allograft transplantation and repair of the articular cartilage: A prospective two- to 12-year follow-up report

+[1,2]Stone, K R; [1] Walgenbach, A W; [2]Adelson, W S; [2]Pelsis, J R; [2]Turek, T J
+[1]The Stone Clinic, San Francisco, CA [2]Stone Research Foundation, San Francisco, CA
kstonemd@stoneclinic.com

INTRODUCTION:

Loss of the meniscus generates increased forces on the knee cartilage and other joint structures and increases the risk of articular cartilage degeneration and development of arthritis [4,9]. The appropriate treatment for loss of the meniscus with unicompatmental knee arthrosis remains controversial[3,5]: with common treatment being osteotomy, unicompartmental (UNI) or total knee arthroplasty (TKA). Biologic treatment options, including meniscus allograft transplantation and articular cartilage repair, can potentially slow the progression of arthritis without limiting a patient's option for joint arthroplasty in the future.

METHODS:

One hundred nineteen meniscus allograft transplantations were performed in 115 patients with severe articular cartilage damage. All patients underwent an informed consent process as approved by an independent Institutional Review Board. Study inclusion criteria consisted of irreparable injury of the meniscus or loss of the meniscus with pain and Outerbridge (OB) Grade III or IV changes in the respective compartment and knee range-of-motion of at least 90°. Microfracture was used to treat articular cartilage damage if the defect area was small (≤25 mm^2), if it was located far posterior, or if it was directly under the meniscus allograft transplant on the tibial side. Articular cartilage paste grafting[7] was used to treat accessible defects > 25 mm^2. Patients consented to clinical examinations with subjective patient evaluations pre-operatively and at 2-, 3-, 5-, 7-, and 10-year post-operative intervals. IKDC, WOMAC, and Tegner Index scoring methods were used to follow pain, activity, and function. Tegner Index represents the ratio of current Tegner score as compared with highest pre-injury Tegner score[6]. Procedure failure was defined as removal of allograft without revision, or progression to knee arthroplasty (TKA or UNI)[2,8]. Analysis of overall patient survival was achieved by the Kaplan-Meier (KM) survival analysis method. Multivariate analysis using the Cox proportional hazards model was carried out to assess the effect of confounding variables on allograft survival. Secondary analysis of patient reported subjective outcomes data was accomplished using the Wilcoxon rank-sum test for 2 independent non-parametric samples. Significance level was set at $\alpha < 0.05$. Results are presented as mean ± standard deviation. Ninety-five percent confidence intervals, where given, are presented in brackets. Subjective patient outcomes were evaluated in cases with a minimum 2-year follow-up[1] (N = 101).

RESULTS:

Eighty-three (69.7%) patients were male and 32 (30.3%) female. Eighty-five (71.4%) cases were medial and 34 (28.6%) cases were lateral. Mean age at time of surgery was 46.9 years (range, 14.1-73.2 years). Twenty-two cases were classified intraoperatively as OB grade III (18.5%) and 97 cases were classified as OB grade IV (81.5%).Patients underwent an average of 5 concomitant procedures (range, 1-9 procedures). Average follow-up was 5.8 years (range, 2.1 months – 12.3 years). Forty-seven percent of cases required at least one subsequent non-failure related surgery. Kaplan-Meier estimated mean survival time was 9.9 ± 0.4 years (Figure 1). Twenty-five of the original 119 procedures failed (20.1%) with a mean failure time of 4.7 years (range, 2.1 months -10.4 years); 18 of these cases progressed to knee arthroplasty. There was no significant difference in the number of concomitant procedures between those cases that failed (5.3 ± 1.6 procedures) and those that did not (4.9 ± 1.7 procedures), ($p = 0.333$). Patients experienced significant improvements from baseline in subjective outcome measures of pain, activity, and function over the course of follow-up ($p < 0.05$), with exception the 7-year Tegner Index score* (Figure 2). Procedure survival was not affected by sex, severity of cartilage damage, axial alignment, degree of joint space narrowing, or medial vs lateral allograft.

Figure 1. Mean Survival Distribution

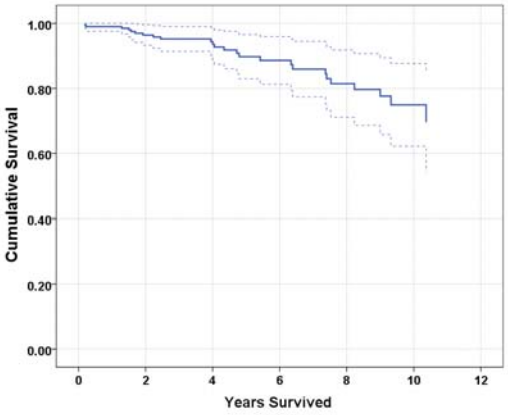

Figure 2. Subjective Outcome Measures

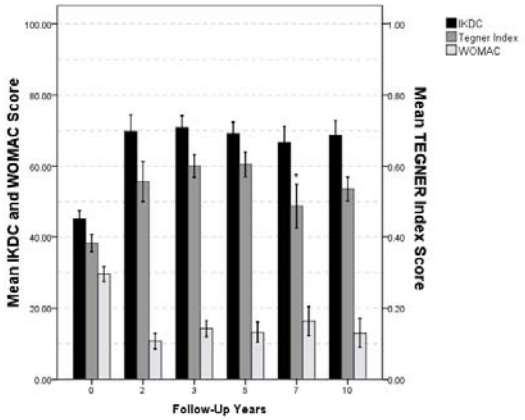

DISCUSSION:

Severe arthritis is often considered a contraindication for meniscus allograft transplantation. However, in this study of meniscus replacement combined with an articular cartilage repair in a heterogeneous patient population, improvements in pain, activity, and function occurred independent of the classic contraindications of age, severity of arthritis, joint space narrowing, and axial alignment. Due to concomitant procedures performed, it is difficult to narrow in on the isolated effect of the meniscus allograft. We speculate that these combined procedures may produce a soft-tissue interpositional arthroplasty, which accounts for some of the improvement. Meniscus allograft transplantation, when performed with articular cartilage repair, need not be limited to young patients with minimal articular cartilage damage as demonstrated by the results of this study, which representing the longest and largest evaluation of its kind. Biologic joint reconstruction, rather than bionic (artificial) replacement, may be an appropriate first step for many people with knee joint arthritis.

REFERENCES:

1. Cole (2006); 2. Farr (2007); 3. Gioe (2007); 4. Lohmander (2007); 5. Pennington (2003); 6. Rodkey (2008);7. Stone (2006); 8. Verdonk (2006); 9. Zielinska (2006)

TENSILE PROPERTY OF STEM CELL-BASED SELF-ASSEMBLED TISSUES (scSAT) CULTURED ON MICRO-PATTERN PROCESSED GLASS PLATES WITH VARIOUS MICROGROOVE DEPTH

Hiroki Sudama[1], Yoshihide Sato[1], Ryo Emura[1], Kazunori Shimomura[2], Norimasa Nakamura[2], and Hiromichi Fujie[3, 1]
[1]Biomechanics Laboratory, Department of Mechanical Engineering, Kogakuin University, Tokyo, Japan
[2]Department of Orthopaedic Surgery, Osaka University Graduate Medical School, Osaka, Japan
[3]Faculty of System Design, Tokyo Metropolitan University, Tokyo, Japan

INTRODUCTION

We have been performing a study on the stem cell-based self-assembled tissues (scSAT) as a candidate material for the repair of damaged soft tissues[1)]. As the scSAT is composed of cells with their native extracellular matrix, it is free from concern regarding long-term immunological effects. For biological reconstruction of the microstructure of the ligaments and tendons, it is required for the scSAT to have anisotropic properties. Previous studies indicated that, when the scSAT was cultured on a glass plate having microgroove structure on the surface, cells and collagen matrix were aligned parallel to the direction of the microgroove[2)]. However, the effect of microgroove depth on the tensile properties of the cultured scSAT is unknown. Therefore, the effect was determined in the present study.

MATERIALS AND METHODS

Micro pattern-processed glass plates having an array of parallel grooves (100 μm in width and 10 or 30 μm in depth) were developed through lithographic and isotropic wet etching. Mesenchymal stem cells were obtained from the synovial membranes of human knee joint by means of collagenase treatment. After subculture of seven times, the cells were plated on the 6 well-plates (control group) or micro pattern-processed glass plates (10 or 30 μm microgroove (MG) groups) at a density of 6.0 x 10^5 cells/cm^2 in DMEM (10% FBS, 1% P/S, 0.2 mM ascorbic acid 2-phosphate). After 14 days, synthesized matrices were carefully detached from those plates and allowed to undergo active contraction for 1 hour to develop scSATs. The scSAT was, then, subjected to tensile testing at a rate of 0.05 mm/s in PBS at 37 °C using a custom-made micro tensile tester developed in our laboratory[2)]. The tensile load was applied parallel or perpendicular to the oriented direction. Histological observation was performed for the surface structure of the scSAT using a digital microscope. Structural anisotropy was evaluated through FiberOri8single03 (computer software)[3)].

RESULTS AND DISCUSSION

Historical observation indicates that no orientation was observed in the control group, while cells and tissues were oriented along the direction of the grooves in the MG groups (Fig.1). The control scSAT exhibited roughly isotropic structure with the orientation intensity of 1.10 ± 0.06 and with the angle of 25 ± 49°. In contrast, the scSATs of the MG groups exhibited anisotropic structure with the orientation intensity of 1.36 ± 0.03 and 1.26 ± 0.09 and with the angle of -5 ± 4° and -4 ± 4° in the MG10 and MG30 groups, respectively. Note that the orientation angle of 0° means parallel to the microgroove direction. The tensile strength was shown in Fig. 2. As compared with the control group (0.11 ± 0.02 MPa), the strength was significantly higher in the MG groups. Moreover, the tensile strength of the MG30 group (0.34 ± 0.10 MPa) was significantly higher than MG10 group (0.15 ± 0.02 MPa). We also found that the tensile strength was significantly higher in the direction to parallel the groove (0.16 ± 0.06 MPa) than in the direction perpendicular (0.04 ± 0.02 MPa). These results suggest that the developed micro pattern-processed glass plate provides scSAT with higher strength, and anisotropic structure and properties as compared with normal culture glass plate. Moreover, the strength of the scSAT depends on the depth of the microgroove; the strength is higher in the scSATs cultured on the glass plate having deeper microgroove.

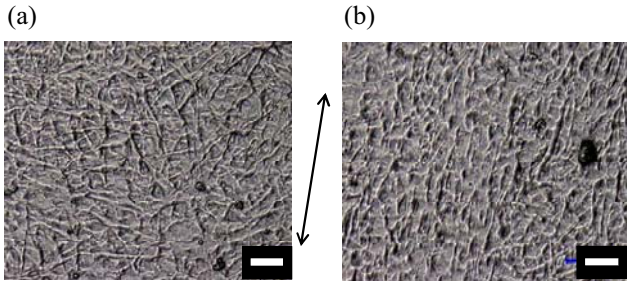

Fig.1 Digital microscopic observation of the control (a) and the MG groups (b). The scales indicate 30 μm, while the arrow indicates the direction of the microgrooves.

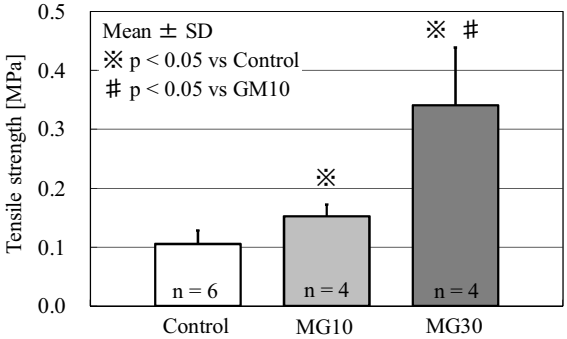

Fig.2 Tensile strength of the control and MG groups in tensile test

REFERENCE

1) Ando W, Fujie H et al. Biomaterials, 28, 5462-5470, 2007.
2) Sudama H, Fujie H et al. ISL&T – X, 59, 2010.
3) Emae T. et al. Nordic Pulp and Paper Research Journal 21(2), 253-259, 2006.

ACKNOWLEDGMENT

The present study was financially supported in part by the Project-In-Aid for the Establishment of Strategic Research Centers from the MEXT, Japan (BERC, Kogakuin University).

Effect of In Vitro Passages on the Biological Properties of Tendon-Derived Stem Cells (TDSCs) – Implication in Musculoskeletal Tissue Engineering

Q Tan[1, 2], YF Rui[1, 2, 4], YW Lee[1, 2], PPY Lui[1, 2, 3]

1 Department of Orthopaedics and Traumatology, Faculty of Medicine, The Chinese University of Hong Kong, Hong Kong SAR, China. 2 The Hong Kong Jockey Club Sports Medicine and Health Sciences Centre, Faculty of Medicine, The Chinese University of Hong Kong, Hong Kong SAR, China. 3 Program of Stem Cell and Regeneration, School of Biomedical Science, The Chinese University of Hong Kong, Hong Kong SAR, China. 4. Department of Orthopaedics, Ninth People's Hospital, Shanghai Jiaotong University School of Medicine, Shanghai, P.R. China.

INTRODUCTION

Tissue engineering has received strong attention recently for the development of functional replacement tissue. Recently, our laboratory has successfully identified a new stem cell source in rat tendons termed tendon-derived stem cells (TDSCs) (Rui et al., 2010), which promoted early and better recovery after tendon injury. An efficient, high yield process to obtain enough cells in vitro for transplantation underpins cost-effective clinical application of adult mesenchymal stem cells (MSCs) for tissue engineering. It is not clear if the biological properties of TDSCs can be maintained and how long that they can be preserved during in vitro expansion (Izadpanah R et al., 2008). This study therefore aimed to compare the self-renewal and multi-lineage differentiation potentials of TDSCs at early (P5), mid (P10) and late (P20, P30) passages.

METHODS

Tendon-Derived Stem Cells (TDSCs) were isolated from GFP rat patellar tendon and sub-cultured up to passage 30. The clonogenicity of the cells were assessed by colony forming assay (CFA) while their proliferative potential was assessed by Brdu cell proliferation assay. The osteogenic, and adipogenic differentiation potential of TDSCs were assessed by Alizarin Red Staining assay and Oil Red Staining assay, respectively, as well as mRNA expression of lineage-specific markers, upon induction (Sethe S et al., 2006). The mRNA of tendo- related markers, *Scx* and *Tnmd*, were also accessed to test the tenogenic differentiation potential (Zhou Z et al., 2010).

RESULTS

Our results showed that the colony numbers increased with passaging ($p=0.004$). The mid and late passages of TDSCs proliferated faster than the early (P5) passage ($p=0.001$). Under normal culture condition, there was no significant differences in *alp* and *Runx2* mRNA expression of different passages of TDSCs, but the mRNA expression of *Spp1* (osteopontin) ($p=0.001$) and *BMP2R1A* ($p=0.019$) decreased with passaging. The Alizarin red S staining assay showed that the Alizarin-red-positive calcium nodules increased with passaging after osteogenic induction. Under normal culture condition, the mRNA expression of *C/EBP α* ($p=0.001$) and *PPARγ2*($p=0.001$) in the late passage was lower than that in the early and mid passages of TDSCs. Lipid droplets formed after incubating the cells in the complete medium with adipogenic supplements for 21days in the early and mid passages of TDSCs, but this adipogenic differentiation potential was not seen in the late passages (P20, P30) of TDSCs. The potential of TDSCs to differentiate into tenocytes was also diminished in the long-term culture. The expression of two tendon - related markers, *Scx* ($p=0.013$) and *Tnmd* ($p=0.001$), was lower in the late passage, compared to those in the early and mid passages of TDSCs.

DISCUSSION

In conclusion, the early and mid passages of TDSCs can maintain the biological properties. The increase in colony numbers with passaging might be due to enrichment of stem cells during sub-culture. There is a loss of multi-lineage differentiation potential in late passages. Considering the time needed for in vitro cell expansion and differentiation potential of these cells, the use of mid passages of TDSCs may be more appropriate for musculoskeletal tissue engineering.

ACKNOWLEDGEMENTS

This work was supported by equipment/resources donated by the Hong Kong Jockey Club Charities Trust.

REFERENCES:

1. Rui YF, Lui PP, Li G, Fu SC, Lee YW, Chan KM. Isolation and characterization of multipotent rat tendon-derived stem cells. Tissue Eng Part A. 2010 May; 16(5):1549-58.
2. Izadpanah R, Kaushal D, Kriedt C, Tsien F, Patel B, Dufour J, Bunnell BA. Long-term in vitro expansion alters the biology of adult mesenchymal stem cells. Cancer Res. 2008 Jun 1; 68(11):4229-38.
3. Sethe S, Scutt A, Stolzing A. Aging of mesenchymal stem cells. Ageing Res Rev. 2006 Feb; 5(1):91-116. Epub 2005 Nov 28.
4. Zhou Z, Akinbiyi T, Xu L, Ramcharan M, Leong DJ, Ros SJ, Colvin AC, Schaffler MB, Majeska RJ, Flatow EL, Sun HB. Tendon-derived stem/progenitor cell aging: defective self-renewal and altered fate. Aging Cell. 2010 Oct; 9(5):911-5.

THE PRECISE HIP ARTHROSCOPIC CAPSULOLIGAMENTOUS ANATOMY

[1]Telleria; J M; [2]Lindsey, D P; [1,2]Giori, N J; [1]Safran, M R
[1]Stanford University, Palo Alto, CA
[2]Veterains Affairs Palo Alto Health Care System, Palo Alto, CA

INTRODUCTION

Hip instability and capsular laxity are being increasingly recognized as sources of disability and damage to the hip joint. Notably, in addition to capsular injury associated with traumatic dislocation and subluxation, atraumatic hip instability and capsular laxity are being increasingly recognized as significant sources of disability. To date no study has described the precise arthroscopic anatomy of the hip capsular ligaments or their relationships to instrumentation or other pertinent soft tissue and osseous landmarks in the hip. Knowledge of arthroscopic capsuloligamentous anatomy may prove helpful in planning surgical procedures, including identifying safe zones for capsulotomies and partial capsulectomies; this information may also aid in biomechanical modeling studies in the future. This study describes the normal arthroscopic locations of the hip capsular ligaments in the central and peripheral compartments.

METHODS

Eight paired fresh-frozen cadaveric hips (mean age = 73.3±10.7 years {61-88}, 2 male specimens) were dissected to expose the hip capsule. Transcapsular needles were placed at the borders of the hip capsular ligaments. Arthroscopy was performed (with video capture) and the relationship of the needles, and thus the ligaments, to the portals and other landmarks in the hip were recorded using a clockface reference system (12 o'clock = lateral; 3 o'clock = anterior) and a laser-etched probe. This material is based upon work supported in part by the Office of Research and Development (Rehabilitation R&D Service), Department of Veterans Affairs.

RESULTS

The iliofemoral ligament (ILFL) ran from 12:45 – 3:00 o'clock. The ILFL was pierced by the anterolateral (ALP) and anterior (AP) portals just within its lateral and medial borders, respectively (Table 1). The pubofemoral ligament (PFL) was located from 3:30 – 5:30 o'clock; the lateral border was at the psoas-U perimeter and the medial border was at the junction of the anteroinferior acetabulum and the cotyloid fossa. The ischiofemoral ligament (ISFL) ran from 7:45 - 10:30 o'clock. The posterolateral portal (PLP) pierced the ISFL just inside its superior/lateral border and the inferior/lateral border was located at the posteroinferior acetabulum. In the peripheral compartment the lateral ILFL and superior/lateral ISFL borders were in proximity to the lateral synovial fold. The medial ILFL and lateral PFL borders were closely approximated to the medial synovial fold.

Arthroscopic Location of the Hip Capsular Ligaments in the Central Compartment

Ligament	Landmark	Landmark Distance Mean ± SD
Lateral ILFL	Just lateral to the ALP	1.1 ± 1.6 mm
Medial ILFL	Just medial to the AP	1.5 ± 1.8 mm
Lateral PFL	Adjacent to the psoas-U	0.4 ± 1.1 mm
Medial PFL	Anteroinferior acetabulum junction with cotyloid fossa	1.0 ± 1.9 mm
Inferior/ medial ISFL	Near posteroinferior acetabulum	5.5 ± 4.2 mm
Superior/ lateral ISFL	Just anterolateral to PLP	5.3 ± 5.8 mm

Table 1. Arthroscopic location of the hip capsular ligaments in the central compartment.

DISCUSSION

Based on these findings just over 60% of the hip capsule that can be addressed arthroscopically is reinforced by the hip capsular ligaments. The inferior/posteroinferior aspect of the capsule from approximately 5:30 – 7:45 o'clock, and the lateral aspect from approximately 10:30 – 12:45 o'clock were not reinforced by the capsular ligaments. Given their large size these areas could potentially have implications for procedures affecting the capsule. During hip arthroscopy capsulotomies and capsular windows are often made by connecting the AP and ALP; based on our findings an incision between these points would almost completely transect the ILFL. Our results also indicate that ALP capsulotomies extended anteriorly will likely incise the ILFL, AP capsulotomies extended laterally or inferiorly could incise the ILFL or PFL, respectively, and PLP capsulotomies extended posteriorly may incise the ISFL. The hip capsular ligaments have consistent arthroscopic locations, are associated with distinct landmarks in the central and peripheral compartments and are closely related to the standard hip arthroscopy portals. These findings will help identify which structures are addressed during surgery, potentially reduce iatrogenic hip instability, and may help in the development of future hip procedures.

Comparison Between Outcomes Of Male And Female Subjects
After Anatomic Double-Bundle Anterior Cruciate Ligament Reconstruction Using Hamstring Tendon Graft

H. Tohyama, E. Kondo, R. Hayashi, N. Kitamura, K. Yasuda
Department of Sports Medicine, Hokkaido University School of Medicine, Sapporo, Hokkaido, Japan

INTRODUCTION

Recently, clinical trials have shown that their anatomic double-bundle reconstruction procedures are significantly superior to their single-bundle procedures concerning the knee stability (1), although a few studies reported that there were no significant differences between the two procedures (2). However, no studies to examine gender-based differences in clinical outcome after anatomic double-bundle ACL reconstruction have been conducted to date, while it has been known that gender-based differences exist in clinical outcome after single-bundle ACL reconstruction (3). Therefore, we hypothesized that in clinical outcome after anatomical double-bundle ACL reconstruction using hamstring tendons, knee stability is significantly worse in female patients than in male patients. The purpose of the present prospective comparative study is to test this hypothesis.

METHODS

A prospective comparative study was conducted in patients who underwent anatomical double-bundle ACL reconstruction using hamstring tendons, performed by a single senior surgeon between 2002 and 2004. 174 patients were enrolled in this study; 52 patients were lost to 2-year follow-up, resulting in 122 patients (70%) that were evaluated in this study. Patients were prospectively evaluated using objective and subjective criteria both preoperatively and postoperatively. At two years after surgery, each patient underwent clinical examinations on the Lachman test, the pivot-shift test, a KT-2000 arthrometer (MEDmetric, San Diego, CA, USA), the Lysholm score, IKDC. We then compared the clinical outcomes of 49 female subjects with those of 73 male subjects. We identified no statistical differences between two groups with regard to the age at the time of surgery, the time from the injury to the surgery, or the follow-up period.

RESULTS

At the time of surgery, the height and the body weight of female patients were significantly smaller than those of male patients (both $p<0.0001$). Regarding the graft diameters of the anteromedial (AM) and posterolateral (PL) bundle grafts for ACL reconstruction, the graft diameters in the female group were significantly smaller than those in the male group (AM: $p<0.0001$, PL: $p=0.0002$). On Lachman testing, 98% of the female group and 97% of the male group were rated as negative. Regarding the pivot-shift test, 80% of the female group and 85% of the male group were rated as negative. The $\chi 2$ test did not show a significant difference in these manual tests between the female and male groups. The average side-to-side differences of the KT-2000 arthrometer values were 1.3 +/- 1.7 mm in the female group and 1.4 +/- 1.7 mm in the male group. We could not show a significant difference in side-to-side differences of the KT-2000 arthrometer values between the female and male groups ($p=0.731$). There were no significant differences in Lysholm score or IKDC evaluation between the female and male groups (Lysholm score: $p=0.4957$; the IKDC: $p=0.4616$).

DISCUSSION

The present study demonstrated that the height, body weight, and graft diameter of each bundle were significantly less in the female patients than in the male patients at the time of surgery. However, the results of assessment for ligament laxity in the female group were almost identical to those of the male group at the 2-year postoperative evaluation after anatomical double-bundle ACL reconstruction using hamstring tendons. Huston and Wojtys (4) reported that both female athletes and non-athletes have greater anterior laxity than their male counterparts. Biomechanical studies showed that the contribution of the ACL graft to anterior knee stability is greater in the double-bundle ACL reconstruction than in the single-bundle procedure (5). The lower contribution of the ACL graft to anterior knee stability in the female patients likely induces greater anterior laxity after single-bundle ACL reconstruction with hamstring graft. Therefore, there is a possibility that the greater contribution of the ACL graft to anterior knee stability reduces the gender-based difference in anterior laxity after double-bundle ACL reconstruction.

REFERENCES: 1. Yasuda K, et al. Arthroscopy. 2004. 2. Meredick RB, et al. Am J Sports Med, 2008. 3. Noojin FK, et al. Am J Sports Med. 2000. 4. Huston LJ, Wojtys EM. Am J Sports Med. 1996. 5. Yagi M, et al. Am J Sports Med. 2002.

HIGH-ACCURATE ANALYSIS OF THE POINT OF APPLICATION OF LIGAMENT FORCE: A NOVEL CALIBRATION METHOD OF THE UNIVERSAL FORCE-MOMENT SENSOR

Hitoshi Yagi[1)], BS and Hiromichi Fujie[2,1)], Ph.D.
1 Biomedical Engineering Research Center, Research Institute for Science and Technology, Kogakuin University, Japan
2 Biomechanics Laboratory, Faculty of System Design, Tokyo Metropolitan University, Japan

INTRODUCTION: To determine the force applied in ligaments, a unique methodology was developed using a universal force moment sensor (UFS) by Fujie, Woo, et al.[1)]. The feature of the methodology is that it is possible to determine not only the magnitude but also the direction and point of application of ligament force through a force transformation scheme. The methodology allowed to determine the point of application of the force in the anterior cruciate ligament (ACL) at the tibial insertion site[1,2)]. However, it was problematic that the error in the point of application increased in the analysis for femoral insertion site of the ACL. Two reasons were considered; 1) the ACL tilts close to the insertion surface, and 2) the error of the UFS output increases with the increase of distance from the UFS to the insertion site. The second reason is attributable to that the UFS accuracy becomes worse when the load application point locates at a further distance from the UFS. Therefore, the present study was performed to develop a new calibration method of the UFS so that load measurement accuracy at the insertion site can be improved. In addition, the technique developed was applied to determine the ACL force at the femoral insertion site.

THEORY AND DEVELOPMENT: A force-moment vector, $\boldsymbol{F}$, is defined as a 6x1 row vector consisting of 3 forces and 3 moments. It is assumed that the relationship between the input force-moment vector ($\boldsymbol{F_{in}}$) and output force-moment vector ($\boldsymbol{F_{out}}$), both with respect to the UFS, is described in a linear fashion using a 6x6 conversion matrix, $\boldsymbol{A}$, as shown in equation 1.

$$\boldsymbol{F_{out}} = \boldsymbol{A}\,\boldsymbol{F_{in}} = \begin{bmatrix} a_{1,1} & \cdots & a_{1,6} \\ \vdots & \ddots & \vdots \\ a_{6,1} & \cdots & a_{6,6} \end{bmatrix} \boldsymbol{F_{in}} \qquad (1),$$

$$\boldsymbol{F_{1out}}-\boldsymbol{F_{2out}}=\boldsymbol{A}\,(\boldsymbol{F_{1in}}-\boldsymbol{F_{2in}}) = \begin{bmatrix} a_{1,1} & \cdots & a_{1,6} \\ \vdots & \ddots & \vdots \\ a_{6,1} & \cdots & a_{6,6} \end{bmatrix} \begin{bmatrix} 0 \\ 0 \\ 0 \\ kf \\ 0 \\ 0 \end{bmatrix} = \begin{bmatrix} a_{1,4} \\ a_{2,4} \\ a_{3,4} \\ a_{4,4} \\ a_{5,4} \\ a_{6,4} \end{bmatrix} kf \qquad (2)$$

Consider a rigid body fixed to the UFS as shown in Figure 1. A force $\boldsymbol{f}$ is externally applied to ($-z$) direction to a point P_1 $(x, y, z)^T$ on the rigid body, where the superscript T denotes the transpose of the vector. The external force $\boldsymbol{f}$ is mechanically equivalent to the input vector, $\boldsymbol{F_{1in}}=(0, 0, -f, -yf, xf, 0)^T$, with respect to the UFS coordinate system. At this moment, the output vector, $\boldsymbol{F_{1out}}$, measured with respect to the UFS coordinate system is not identical to $\boldsymbol{F_{1in}}$ because of a cross-coupling phenomenon due to structural errors of the UFS. When the point of application of the external force $\boldsymbol{F}$ is translated by k parallel with y-direction to another point P_2 $(x, y+k, z)^T$, the external force is equivalent to the input vector, $\boldsymbol{F_{2in}}=(0, 0, -f, -(y+k)f, xf, 0)^T$. Again, the output vector $\boldsymbol{F_{2out}}$ is not identical to $\boldsymbol{F_{2in}}$ with the same reason. These input and output vectors are substituted into equation (1), and then we obtain the relationship between the output vector difference and 4th row ($a_{i,4}$) of the matrix $\boldsymbol{A}$, as shown in equation(2). By obtaining the relationship with various k, the 4th row of the matrix $\boldsymbol{A}$ can be determined through a linear least square method. In the same way, the 5th and 6th rows of the matrix $\boldsymbol{A}$ can be determined.

To determine the 3rd rows of the matrix $\boldsymbol{A}$, the external force $\boldsymbol{f}$ is applied to the point P_1 again, as shown in Figure 1. The relationship between the input and output force-moment vectors is described as shown in equation (3).

$$\boldsymbol{F_{1out}}=\boldsymbol{A}\,\boldsymbol{F_{1in}}= \begin{bmatrix} a_{1,1} & \cdots & a_{1,6} \\ \vdots & \ddots & \vdots \\ a_{6,1} & \cdots & a_{6,6} \end{bmatrix} \begin{bmatrix} 0 \\ 0 \\ -f \\ -yf \\ xf \\ 0 \end{bmatrix} = \begin{bmatrix} -a_{1,3} - a_{1,4}y + a_{1,5}x \\ -a_{2,3} - a_{1,4}y + a_{1,5}x \\ -a_{3,3} - a_{1,4}y + a_{1,5}x \\ -a_{4,3} - a_{1,4}y + a_{1,5}x \\ -a_{5,3} - a_{1,4}y + a_{1,5}x \\ -a_{6,3} - a_{1,4}y + a_{1,5}x \end{bmatrix} f \qquad (3)$$

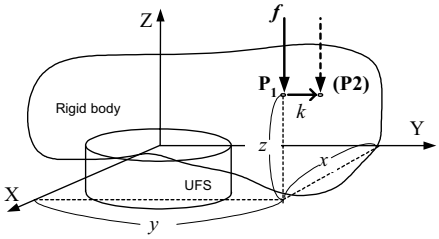

Figure 1: An external force $\boldsymbol{f}$ is applied to a rigid body fixed to a UFS

By obtaining the relationship with various f, the 3rd row ($a_{i,3}$) of the matrix $\boldsymbol{A}$ can be determined through a linear least square method. In the same way, the 1st and 2nd rows of the matrix $\boldsymbol{A}$ can be determined. Finally, the inverse matrix $\boldsymbol{A^{-1}}$ is calculated which allows to determine the input force-moment $\boldsymbol{F_{in}}$, equivalent to the external force $\boldsymbol{f}$, from the UFS output $\boldsymbol{F_{out}}$.

VALIDATION: A metal frame was fixed to the UFS (IFS40E15A100, JR^3, USA), and the proposed calibration was performed by applying external force of 100 N around a point P $(50, 143, 190)^T$ on the frame. After the calibration, external forces were applied to a point P' close to the P, the point of application was determined using the obtained $\boldsymbol{A^{-1}}$. The distance between the calculated and actual coordinates of the P' was determined. Result revealed that the error in position was only 0.79 mm under the proposed method, which was significantly lower than that (10.2 mm) when the calibration method was not used.

SUMMARY: We developed a novel calibration method of the UFS which allows for high-accurate analysis of the point of application of ligament forces. Currently, we are determining the point of application of ACL force at the femoral insertion site, which is one of the major topics in the field of ACL biomechanics.

Reference: 1) Fujie, Livesay, Woo, et al. J Biomech Eng (1995), 2) Livesay, Fujie, Woo, et al. Annal of Biomech. (1995)
Acknowledgment: The present study was financially supported by the Project-In-Aid for the Establishment of Strategic Research Centers (BERC, Kogakuin University) and Grant-In-Aid for Scientific Research (#20591766) both from the MEXT, Japan, and by Smith&Nephew.

The Influence of ACL Graft on Knee Joint Axial Rotation during Level Walking

+[1]Zheng, N; [1]Wang, H; [2]Fleischli, JE
+[1]University of North Carolina at Charlotte, [2]OrthoCarolina, Charlotte, NC nzheng@uncc.edu

INTRODUCTION

ACL reconstruction is often performed in order to restore knee joint stability [1]. However, reports in the literature suggest that reconstruction of an injured ACL does not significantly reduce the risk of knee OA [2]. Previously reported motion pattern differences between ACL-reconstructed (ACL-R) knees and healthy knees indicate that current ACL reconstruction surgeries may not fully restore the joint stability, especially the knee axial rotation [3]. Higher radiographic OA were reported in knees with patella tendon autograft and in those with hamstring tendon autograft [4]. In this study, the knee joint axial rotation during walking was examined in subjects with unilateral ACL-R knees. We hypothesized that there were no significant influence of ACL graft on knee joint axial rotation following ACL reconstructive surgery and rehabilitation.

METHODS

Forty-five subjects with unilateral ACL-R knee were recruited and signed consent forms before being tested using an IRB approved protocol. All patients went through aggressive rehabilitation programs and were permitted for full daily activities. Fifteen of them had gracilis and semitendinosus autograft (GSAuto), 12 of them had hamstring tendon autograft (HTAuto), 3 of them had patellar tendon autograft (PTAuto), 5 of them had gracilis and semitendinosus autograft enhanced by semitendinosus allograft (GSBoth), 5 of them had patellar tendon allograft (PTAllo), 3 of them had hamstring tendon allograft (HTAllo), and 2 of them had Achilles tendon allograft (ATAllo).

Ninety-one 10 mm retro-reflective markers were attached to major joint landmarks and lower extremity segments [3]. An 11-camera motion analysis system (MAC, CA) was used to record the motion data at 60 Hz while the subject walked through a calibrated volume in normal speed. Ten walking trials of each subject were recorded. Three good walking trials were processed from each subject and the average was used for data analysis. The knee joint axial rotation was determined based on a previously reported method [3]. Maximum and minimum values and ranges of motion during both the stance and swing phase, and values at 7 key frames during a gait cycle were determined. Multivariate tests using general linear model were performed to test differences between groups with different ACL grafts (SPSS, IL).

RESULTS

Figure 1 shows the means of knee joint axial rotation during walking for subjects with different ACL grafts. There was a significant difference ($p<0.05$) in knee joint axial rotation among subjects with different ACL grafts. At the mid stance when the knee joint had maximum flexion, the knee joint axial rotation in subjects with GSAuto graft was significantly greater than those in subjects with HTAuto (4.9 ± 1.4^{o}, $p=0.023$). There were no significant differences in the maximum internal and external rotation between graft groups ($p>0.05$) although the Achilles tendon allograft had greater external rotation and less internal rotation during the stance phase (Fig. 2). When combined autografts with allografts, subjects with the gracilis and semitendinosus grafts had greater internal rotation than those with hamstring tendon grafts (4.2 ± 1.2^{o}, $p=0.011$).

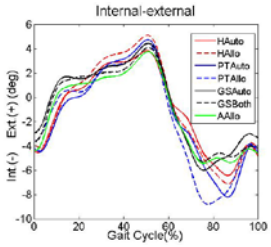

Fig. 1 Mean Knee Aixal Rotation for different grafts.

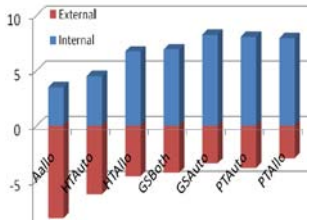

Fig. 2 Means of the maximum internal and external rotation of the knee during stance phase for each graft group.

DISCUSSION

In this study we examined the knee axial rotation during walking between subjects with different ACL grafts. Significant differences in knee axial rotation were found between subjects with different ACL grafts, specifically between the GSAuto and HTAuto. Although greater differences in means were found between other groups there was no statistical significance due to their small sample sizes. There were significant differences in knee axial rotation between difference graft sources (i.e., patellar tendon, hamstring tendon and Achilles tendon), but not between autograft and allograft. Achilles tendon, patella tendon and hamstring tendon grafts have different mechanical properties, such as stiffness, which may have caused the significant differences in knee axial rotation during walking. Altered axial rotation of the knee during daily activity is believed to be one of mechanical risk factors of knee OA. Further researches with larger sample sizes are needed to confirm the effects of ACL graft types on knee joint axial rotation and their contribution to knee OA.

REFERENCES: 1. Daniel DM. et al, *Am J Sports Med* 1994; 2. Lohmander LS et al, *Arthritis Rheum* 2004; 3. Gao B et al *Clin. Biomech* 25(3):222-229, 2010; 4. Pinczewski, *L. A. Am J Sports Med 35(4):* 564-74, 2007

Notes

International Symposium on Ligaments & Tendons - XI
January 12, 2011
University of California, Irvine

7:30 am - 8:15 am	**Registration & Check-In**
8:15 am - 8:30 am	**Opening Ceremony, Welcome & Announcements** Dr. Savio L-Y. Woo and Dr. Ranjan Gupta
8:30 am – 10:15 am	**Podium Session 1** Tendon Session Chairs: Michael Lavagnino, DVM and Joo Han Oh, MD, PhD
10:15 am - 10:45 am	**Break and Poster Session 1**
10:45 am - 11:45 am	**Podium Session 2** Rotator Cuff Session Chairs: Orr Limpisvasti, MD and Sang-Jin Shin, MD, PhD
11:45 am – 12:45 pm	**Lunch and Poster Viewing**
12:45 pm - 2:25 pm	**Podium Session 3** Knee ACL Session Chairs: Braden Fleming, PhD and Masataka Sakane, MD, PhD
2:25 pm – 2:45 pm	**Break and Poster Session 2**
2:45 pm - 4:13 pm	**Podium Session 4** Tissue Engineering Session Chairs: Catherine Kuo, PhD and Pauline Lui, PhD
4:15 pm - 5:15 pm	**Podium Session 5** Ligament Session Chair: Martha Murray, MD and Nicola Mafulli, PhD
5:15 pm	**Closing Remarks**
5:30 pm – 6:30 pm	**Reception and Cocktail Hour (Cash Bar)**
6:30 pm	**Dinner and Award Ceremony**